PHARMACOLOGICAL COSTIMULATION OF ENGINEERED T CELLS

PHARMACOLOGICAL COSTIMULATION OF ENGINEERED T CELLS

By ZOYA ADEEL, B.SC.

A thesis submitted to the School of Graduate Studies in
Partial Fulfilment of the Requirements for the Degree of Master of Science

McMaster University

McMaster University MASTER OF SCIENCE (2024) Hamilton, Ontario (Biochemistry and Biomedical Sciences)

TITLE: Delivering Pharmacological Costimulation to Augment the Anti-tumour Activity of Engineered T cells

AUTHOR: Zoya Adeel, B.Sc. (McMaster University)

SUPERVISOR: Jonathan L. Bramson

NUMBER OF PAGES: xii, 76

Lay Abstract

T cells protect the human body by surveilling and removing harmful cells. Scientific advancements have allowed us to re-target T cells to better eliminate cancer; this approach has demonstrated great clinical success for the treatment of blood cancers. Genetic modification strategies to enhance the clinical efficacy of existing re-targeted T cell products have been effective but are associated with toxicities. We propose using a chemical biology approach to enhance the function of modified T cells with small molecules, while potentially mitigating toxicities during treatment. We investigated over 15,000 chemicals compounds to identify candidate(s) that may improve genetically modified T cell function.

Abstract

Background: Chimeric antigen receptor (CAR) T cell therapy enlists genetic engineering to express a tumour targeting synthetic receptor on a patient's T cells. While endogenous T cells rely on costimulatory signals for their development but not their effector function, CAR T cells are completely reliant on costimulatory domains incorporated within the CAR structure to promote T cell expansion and persistence *in vivo*, resulting in enhanced anti-tumour activity. Toxicities following CAR T cell infusion are linked to the magnitude and speed of the CAR T cell expansion, which is a function of signaling mediated through the costimulatory domain. Having a "druggable" method to provide costimulatory signals could be a strategy to: (i) tune *in vivo* T cell expansion, (ii) allow the physician to toggle costimulation during periods where it is advantageous to the therapeutic strategy, and (iii) enhance endogenous immune cell anti-tumour activity. A high throughput screen assessing 4000 biologically active compounds for their effect on engineered T cell proliferation identified Ferutinin, a natural small molecule with no known immunomodulatory activity. A small library of Ferutinin analogues (N=25) were synthesized to predict and optimize its biologically active molecular structure(s).

Methods: We first assessed the impact of Ferutinin analogues on multiple classes of tumour re-targeting receptors TAC and DAP12 synthetic antigen receptor (SAR) engineered T cell function. We chose the TAC and DAP12 SAR receptor because they mediate T cell activation via natural signalling pathways and include no costimulatory domains. We then developed a high throughput screen (HTS) using luciferase as an indirect measure of TAC T cell number and screened >15,000 compounds with known biological activity at McMaster University's Centre for Microbial and Chemical Biology. Finally, we validated the outcomes of the HTS.

Results: Our studies did not find evidence of improved TAC or DAP12 SAR T cell function in the presence of Ferutinin analogues. The HTS did find classes of compounds with characterized costimulatory activity, including immunomodulatory drugs, phorbol esters and SMAC mimetics. 8-Geranyloxypsoralen and BAY 60 6583 demonstrated on-target enhancement of TAC T cell proliferation independent of T cell donor.

Conclusions: These findings demonstrate the utility of small molecules as a method to enhance proliferation of engineered T cell products, recapitulating the effects of a costimulatory signal.

Dedication

To my late grandfather, Abdul Ghafoor Mian, who taught me the importance of education and hard work. Your wisdom continues to inspire me every day. This thesis is a testament to your influence in my life.

Acknowledgements

This thesis would not have been possible without the guidance and encouragement of many people who have been part of my journey.

To my supervisor, Dr. Jonathan Bramson, I am so grateful for your mentorship. You conduct science with rigour, communicate conscientiously and lead with humour and compassion. Your Mr. Miyagi-like emphasis on repetition and mastering the fundamentals will stay with me throughout my career. Thank you for introducing me to the ‘hopeless’ world of wet lab science.

To my committee members, Dr. Eric Brown, Dr. Jakob Magolan and Dr. Carl Richards, your feedback and expertise have been crucial in refining my work and challenging me to think more critically.

I would also like to acknowledge Derek Cummings, Dr. Joni Hammill, Dr. Bonnie Bojovic, Chris Baker and the HITS team for their unwavering support. Thank you for being available to us, patient with us and keeping the lab afloat. It should be mandatory for every lab to have their own Derek, Joni, Bonnie and Chris. To my mentor and friend, Dr. Duane Moogk, I will miss our morning life chats in TC. Thank you for the advice and laughs. On this note, it would be remiss of me not to acknowledge Dr. Katie Moisse, for whom I would not be in research without. I am so fortunate to have worked with the best two humans.

To CMCB wizards, Cecilia Murphy and Susan McCusker, thank you for taking such meticulous care of my molecules. The centre is lucky have you. I would also like to acknowledge my peers and members of the Bramson Lab, the McMaster Immunology Research Centre, Centre for Discovery in Cancer Research and Department of Biochemistry and Biomedical Sciences, who have helped me along the way.

This would not have been possible without the support of my family. To my parents and grandparents, who have taken it upon themselves to alleviate each and every barrier to my personal and professional success, it goes without saying, but I appreciate you dearly. I hope this thesis makes your proud.

To my fiancé, Ayhaan, even though you studied accounting and practice finance, you are an honorary Master of Science in my books. I could not have done this without you, and I am so lucky to have you by my side.

Table of Contents

Lay Abstract .... **iv**

Abstract .... **v**

Acknowledgements .... **vii**

List of Abbreviations and Symbols .... **xi**

Declaration of Academic Achievement .... **xiii**

1.0 Introduction **1**

1.1 Cancer *1*

1.3 An Overview of T cell biology *3*

An Introduction to T cells 3
TCR: MHC – Signal 1 4
Costimulation – Signal 2 5
T cell function 7

1.4 Engineered T cells for cancer *8*

T cell engineering and synthetic receptors 8
Transgenic TCR 9
The antigen specificity of T cells depends on the TCRα and TCRβ chain (Janeway et al., 2001). A transgenic TCR with modified TCRα and TCRβ chains can recognize selected tumour antigens through pMHC presentation (Chandran & Klebanoff, 2019). Adoptive transfer of TCR modified T cells are advantageous because it allows for the infusion of large numbers of antigen-specific T cells (Leung & Heslop, 2019). Additional benefits to using transgenic TCRs include: (i) canonical signalling pathways to active the T cell; (ii) target antigens that are not limited to membrane proteins, both of which are barriers for some synthetic receptors (Baulu et al., 2023). However, transgenic TCRs are MHC-restricted and can be ineffective due to a loss of MHC expressing tumour cells due to immune evasion (Cornel et al., 2020). 9
Chimeric antigen receptor (CAR) 9
Challenges with CAR T cells 11
The KIR CAR 12
The T cell antigen coupler 14
1.5 Research Context 16

2.0 OBJECTIVES **19**

2.1 Assess the functional changes to DAP12 SAR and TAC T cells when treated with Ferutinin and Ferutinin analogue(s). *19*

2.2 Develop an automated reporter-based proliferation assay *19*

2.3 High throughput screening of biologically active compounds *19*

3.0 RESULTS **20**

3.1 Validation of Ferutinin and analogues on enhancing engineered T cell performance *20*

Commercial Ferutinin provides greater functional benefit than Ferutinin synthesized at McMaster 20

Ferutinin analogues intermittently augment DAP12 SAR and TAC T cell function 24

3.2 Developing an automated reporter-based proliferation assay *26*

Luciferase possesses distinct advantages from fluorescence 26

DAP12 SAR T cells are amenable to a Luciferase reporter system 28

Engineering TAC T cells with Luciferase 34

3.3 Screening the Ferutinin analogue library 43

3.4 High throughput screening bioactive compound libraries *45*

Screening 11,428 molecules from the Bioactive 2 Library *45*

Screening 3840 molecules from the Bioactive A Library *49*

Secondary Assay - Stage I: Validating Compound Specificity *51*

Secondary Assay - Stage II: Determining the Dose Response *53*

Secondary Assay - Stage III: Multi-donor CellTraceTM Violet Proliferation and Survival *55*

4.0 DISCUSSION **58**

Commercial Ferutinin provides greater functional benefit than Ferutinin synthesized at McMaster *58*

Ferutinin analogues intermittently augment DAP12 SAR and TAC T cell function *58*

Luciferase possesses distinct advantages from fluorescence *59*

DAP12 SAR T cells are amenable to a Luciferase reporter system *59*

Engineering TAC T cells with Luciferase *60*

Screening the Ferutinin analogue library *62*

High throughput screening bioactive compound libraries *62*

Future Directions *68*

5.0 MATERIALS & METHODS **71**

Lentivirus production *71*

Gamma retrovirus production *71*

Generation of engineered human T cell products with lentivirus *71*

Phenotyping *72*

Generation of engineered human T cell products with gammaretrovirus *72*

Flow cytometry *73*

Microbead antigen loading *73*
Cell Maintenance *73*
In Vitro Cytotoxicity Assay *73*
CellTrace™ Violet Proliferation Assay *74*
Luminescence Proliferation Assay *74*
High Throughput Screen *74*
Z-Factor *74*

6.0 BIBLIOGRAPHY **77**

Appendix **88**

List of Abbreviations and Symbols

Abbreviations

ACT	Adoptive cell transfer
APC	Antigen presenting cell
ATP	Adenosine 5’-tiphosphate
AUC	Area under the curve
BMCA	B cell maturation antigen
C-SMAC	Central supramolecular activation complex
CAR	Chimeric antigen receptor
CD	Cluster of differentiation
CMCB	Centre of Microbial Chemical Biology
CRS	Cytokine release syndrome
CTLA-4	Cytotoxic T-lymphocyte antigen 4
CTV	CellTrace Violet
DAG	Diacylglycerol
DAP12	DNAX-activating protein of 12
DARPin	Designed ankyrin repeat protein
DMSO	Dimethyl sulfoxide
E:T	Effector-to-target ratio
gRV	Gammaretrovirus
H NMR	Hydrogen nuclear magnetic resonance
HER2	Human epidermal growth factor receptor 2
HTS	High throughput screen
IAP	Inhibitor of apoptosis
ICOS	Inducible costimulatory
IFN	Interferon
IgSF	Immunoglobulin superfamilies
IL-	Interleukin-
IMiD	Immunomodulatory drugs
IQM	Interquartile mean
ITAM	Immunoreceptor tyrosine-based activation motif
KIR	Killer immunoglobulin-like receptor
KIR2DS2	Killer Cell Immunoglobulin Like Receptor, Two Ig Domains And Short Cytoplasmic Tail 2
LAT	Linker for activation of T cells
LFA-1	Lymphocyte function-associated antigen 1
LFA-3	Lymphocyte function-associated antigen 3

MAPK	Mitogen-activated protein kinase
MHC	Major histocompatibility complex
MOI	Mutliplicity of infection
NFAT	Nuclear factor of activated T cells
NGFR	Nerve growth factor receptor
NK	Natural killer
NK-κB	Nuclear factor kappa B
NKG2D	Natural killer group 2, member D
p-SMAC	Peripheral supramolecular activation complex
PBMC	Peripheral blood mononuclear cells
PD-1	Programmed death 1
PI3K	Phosphoinositide 3-kinases
PKC	Protein Kinase C
pMHC	Peptide-MHC complex
PROTAC	Proteolysis targeting chimera
rsLuc	Red shifted Luciferase
scFv	Single-chain variable fragment
SMAC	Supramolecular activation complex
TAC	T cell antigen coupler
TCR	T cell receptor
TGF	Transforming growth factor
TH1	T helper 1
TNFRSF	Tumour necrosis factor receptor family
TREM1	Triggering receptor expressed on myeloid cells 1
VLA-4	Very late activated antigen-4

Symbols

α	alpha
β	beta
°C	degrees Celsius
δ	delta
ε	epsilon
γ	gamma
κ	kappa
μ	micro
ζ	zeta

Declaration of Academic Achievement

This document was independently authored by Zoya Adeel with editorial support from Dr. Jonathan Bramson. The studies and experiments described were conceptualized, conducted and analyzed by Zoya Adeel in collaboration with Dr. Jonathan Bramson, with contributions from colleagues listed below.

- Princeton Luong developed and synthesized Ferutinin, Ferutinin analogues and Ferutinin degradation products.
- Ariya Shiwram prepared gamma retrovirus, cultured human T cells, and completed secondary assessments.
- Cecilia Murphy and Susan McCusker provided technical support with operating high throughput screening instruments.
- All schematics were generated using BioRender unless otherwise noted.

1.0 Introduction

1.1 Cancer

Cancer is a disease of abnormal cellular division. Neoplastic cells may arise from random genomic mutations, environmental exposures (e.g. carcinogens), endogenous factors (e.g. reactive oxygen species) or genetic predisposition to DNA damage that disrupt the balance between cellular proliferation and programmed cell death (Loeb & Loeb, 2000). It may take years to accumulate genetic mutations that result in uncontrolled proliferation and cancer development (Weinberg, 1996). Some of these transformed cells will eventually multiply, recruit and reprogram non-cancerous stromal and immune cells to establish a pro-tumorigenic microenvironment. With the aid of accessory cells, cancer cells can orchestrate the remodelling of vasculature and the extracellular matrix, allowing for their metastasis to distal tissue sites (De Visser & Joyce, 2023).

Although cancers vary considerably both genotypically and phenotypically, in 2000, Hanahan and Weinberg stated the fundamental hallmarks of cancer that define malignancy: i) sustained proliferative signalling; ii) resisting cell death; iii) inducing angiogenesis; iv) enabling replicative immortality; v) activation invasion and metastasis; vi) evading growth suppressors (Hanahan & Weinberg, 2000). Progress in our understanding of the mechanistic underpinnings of carcinogenesis led to the addition of two more hallmarks in 2011: metabolic reprogramming and evading the immune system (Hanahan & Weinberg, 2011). Cancer and the immune system are inextricably linked, where the latter plays a role in the suppression and progression of cancer.

1.2 Cancer and the immune system

Indeed, cancer development has been attributed to a failure of the immune system, which is a network of organs, tissues and proteins that protect against malignancies and external pathogens (Shurin, 2012; Cooper & Hausman, 2000). The cancer immunosurveillance hypothesis, initially proposed by Burnet and Thomas in the late 1950s, suggests that somatic genetic changes transform cells toward malignancy, provoking recognition by the immune system and subsequent elimination of nascent cancer cells (Burnet, 1957). Seminal research by Schreiber's group in murine models supporting this theory found more spontaneous tumours formed in $RAG2^{-/-}$ knockout (immunocompromised) mice than in wild type mice (Dunn et al., 2004). Evidence from human organ transplantation studies in the early 21st century also linked cancer and immune function, where immunosuppressed organ transplant patients had higher rates of cancer than non-immunosuppressed patients receiving matched organs (which would not be expected to trigger an immune response) (Adami et al., 2003; Vajdic & Van Leeuwen, 2009; Lindelöf et al., 2000). Moreover, greater infiltration of effector T cells at the tumour site is linked to better survival across different cancer types (Nakakubo et al., 2003; Idos et al., 2020; Stumpf et al., 2009).

We now know that cancerous cells can develop a phenotype that permit the immune system to distinguish them from healthy cells (Cooper & Hausman, 2000). One such example is tumour associated antigens, which are antigens that are overexpressed on tumour cells but are also present on a subset of healthy cells. Tumour cells may also express neoantigens that arise from the genetic mutations within cancer cells (Zarour et al., 2003). Some stress ligands and damage-associated molecular patterns also serve as key markers for immune recognition.

Schreiber built on Burnet's immunosurveillance theory when he proposed the cancer immunoediting hypothesis, which describes the mechanism by which cancer evades immune surveillance (Dunn et al., 2004; Hanahan & Weinberg, 2011). Immunoediting is composed of three distinct phases: elimination, equilibrium, and escape. The elimination phase describes the recognition and elimination of transformed cells by the immune system before tumours are clinically detectable. When the immune system fails to eradicate all transformed cells, the equilibrium phase initiates, where cancer cells endure selective pressures. A small subset of cells that have selective advantage can elude immune surveillance. In a phase that can last for years, latent tumor cells coexist with the immune system without being eliminated, and it is this process that selects for tumour cells that can escape immune clearance (Dunn et al., 2004). The escape phase marks clinical tumor appearance, characterized by genetic instability, invasion, and metastasis of adaptive tumour cells. Such transformed cells evade immune recognition through a myriad of tactics, including upregulating of anti-apoptotic proteins, inhibition of immune checkpoints, and tumour microenvironment modelling (Dunn et al., 2004). These adaptive strategies prevent immune-mediated tumour control, allowing cancer growth to proceed uninhibited and clinically manifest (Tang et al., 2020).

The tumour microenvironment promotes immunosuppression by recruiting and retaining myeloid-derived suppressor cells, regulatory T cells, and type 2 macrophages that secrete inhibitory mediators including transforming growth factor (TGF)-β and IL-10 (Hinshaw & Shevde, 2019). Chronic inflammation mediated by TGF-β promotes angiogenesis and regulatory T cell recruitment (Kim et al., 2022). Nutrient deprivation and accumulation of tumour metabolites also impede T cell function and differentiation (Lasek, W, 2022).

Despite immune evasion tactics and the immunosuppressive microenvironment, the presence and activity of T cells within the tumour can influence the therapeutic response and patient prognosis. For example, a high infiltration of effector T cells at the tumour site correlates with favorable clinical outcomes in certain cancers (Shi et al., 2022). The anti-cancer potential of the immune system, particularly T cells, holds significant promise for therapeutic interventions. A review of T cell biology is required to understand the anti-cancer properties possessed by T cells.

1.3 An Overview of T cell biology

An Introduction to T cells

T cells have a remarkable capacity to survey, target, eliminate, and generate a memory response against cancer cells (Sun et al., 2023). T cells are part of the adaptive immune system for their ability to mount an acquired immune response. Almost every T cell expresses an antigen receptor with a unique target specificity, known as the T cell receptor (TCR) (Tripodo & Pileri 2021). During T cell development, the gene segments of the TCR are somatically rearranged in a process known as V(D)J recombination to generate a TCR with a unique binding capacity (Alt et al., 1992).

The lifetime of a T cell can be broadly categorized into four stages: *(i) T cell development*, where progenitor T cells develop antigen specificity, *(ii) T cell activation*, whereby progenitor T cells with functional TCRs, “naïve T cells”, are primed with their antigen and stimulatory signals; *(iii) Effector phase*: activated naïve T cells, “effector T cells,” circulate and perform their effector function upon antigen ligation; *(iv) Memory phase:* a small subset of effector T cells become long-lived T cells that perform effector function upon target re-exposure.

T cell development initiates from hematopoietic stem cells in the bone marrow that give rise to common lymphoid progenitors and migrate to the thymus (Kumar et al., 2018). Within the thymic cortex, early thymic progenitors undergo TCR gene rearrangement. Conventional αβ T cells express a heterodimeric TCR that is composed of a TCRα and TCRβ chain. The TCR lacks signalling capacity on its own and associates with an immunoreceptor tyrosine-based activation motif (ITAM) containing CD3 protein complex to transmit intracellular signals and activate a T cell. The TCR-CD3 complex, associating with a CD8 or CD4 co-receptor, can bind to peptide antigens from processed proteins presented on a major histocompatibility complex (MHC). Immature T cells undergo positive selection in the thymus cortex, where only cells bearing a functional TCR that binds to peptide-MHC (pMHC) with an intermediate affinity are provided survival signals. Binding to either MHC class I or II determines differentiation to the CD8+ or CD4+ subsets, respectively. Immature T cells traverse to the thymus medulla, where they are exposed to the medullary thymic epithelial cells and antigen presenting cells with many tissue-type antigens. T cells with TCRs that bind too strongly to self-pMHC are eliminated by negative selection. This process is important in limiting self-reactive T cells with potential autoimmune characteristics. However, negative selection in the thymus also eliminates most T cells capable of responding to cancer cells which are derived from self-tissues (Chao et al., 2005).

TCR: MHC – Signal 1

Upon thymic egress, naïve T cells populate lymphoid tissues and interact with antigen presenting cells. In the rare event the naïve T cell ligates to an antigen presenting cell bearing its processed antigen on an MHC molecule, this initiates the first stage of T cell 'priming' (Smith-Garvin et al., 2009; Lanzavecchia et al., 1999). The TCR: pMHC ligation is considered Signal 1 of T cell activation. Upon TCR: pMHC binding, Lck is recruited to the TCR/CD3 complex and phosphorylates ITAMs on CD3 moieties. Subsequent recruitment and phosphorylation of Zap70 results in the phosphorylation of the linker for activation of T cells, which ensues downstream signaling cascades mediated by phosphorylation events. These events culminate to activate transcriptional regulators that result in cytoskeletal re-arrangements, metabolic changes and protein synthesis in preparation for T cell activation and expansion (Courtney et al., 2018).

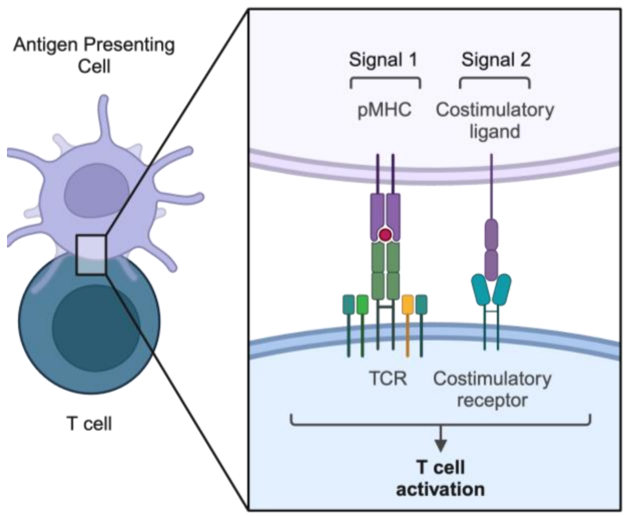

Figure 1. Activation of a naïve T cell. Signal 1 - The TCR binds to its cognate antigen presented by MHC on an antigen presenting cell. Signal 2 – a costimulatory ligand on the antigen presenting cell binds to its corresponding costimulatory receptor on the T cell surface. Created with BioRender.

Costimulation – Signal 2

Ligation of TCR alone is insufficient to induce complete activation of a naïve T cell (Song et al., 2008). A second ligand-receptor interaction (Signal 2) on antigen presenting cells and T cells is required (**Figure 1**). Costimulation, resulting from a costimulatory ligand (antigen presenting cell) binding to its receptor on the T cell, provides signals to naïve T cells to reach their activation threshold. Without signal 2, naïve T cells will enter an anergic state or undergo apoptosis (Song et al., 2008). Moreover, antigen recognition (Signal 1) leads to the formation of the immunological synapse which comprises of a central supramolecular activation complex (c-SMAC) and peripheral SMAC (p-SMAC) (Monks et al., 1998; Dustin, 2014). The c-SMAC region comprises of the TCR, co-receptors, costimulatory receptors, whereas the p-SMAC region comprises of integrins and adhesion molecules. The synapse synergizes TCR-derived and costimulatory signals to augment phosphorylation events required for T cell activation, survival and expansion (Dustin & Shaw, 1999).

Many costimulatory molecules have been identified, most of which belong to the immunoglobulin superfamilies (IgSF), tumour necrosis factor receptor superfamily (TNFRSF) or integrin family (Song et al., 2008). The IgSF (or B7 family) is composed of six ligands expressed on T cells with characterized costimulatory capacity, including CD86/CD80, CD2, PDL1, PDL2, B7-H3 and B7-RP-1 (Song et al., 2008). The receptors for IgSF ligands include CD20, cytotoxic T-lymphocyte antigen 4 (CTLA-4), inducible costimulatory (ICOS), lymphocyte function-associated antigen-3 (LFA-3) and programmed death 1 (PD-1). TNF family members, 4-1BB and OX40 bind to specific TNF receptor family members on T cells. Integrin molecules include LFA-1 and very late activated antigen-4 (VLA-4) (Song et al., 2008). See **Table 1** for a summary of costimulatory molecules and a short description of their activity.

Costimulatory signals augment IL-2 production, growth factor secretion, cell cycle progression, effector cytokine synthesis, suppression of cell death and memory T cell development (Sharpe, 2009; Croft, 2003). For instance, CD28-mediated costimulation promotes T cell proliferation and survival by activating downstream transcriptional targets such as NF-kB, NFAT, and AP1/2 (Ebrahimi et al., 2024). NF-κB regulates DNA transcription, cytokine production, and cell survival (Oeckinghaus, A., & Ghosh, 2009). Transcriptional regulators, NFAT and AP1/2, also support the synthesis of pro-inflammatory signals, and regulate cell survival (Crabtree & Clipstone, 1994).

Members of the TNFRSF synergize with TCR-CD3 signaling to promote cytokine secretion, cell cycle progression, cytokine production, and T cell persistence (Croft, 2009). CD2-LFA-3 ligation augments TCR aggregation and signaling by elongating the immunological synapse (Demetriou, 2019). In addition, CD2 engagement enhances TCR signaling via phosphorylation of CD3ζ (Umehara et al., 1998).

VLA-4 mediates aggregation of T cells and T cell ligation to target cells. Moreover, VLA-4 signalling can enhance the proliferation and cytokine production of T cells (López-Hoyos et al., 1999). LFA-1 is a well-established intercellular adhesion molecule that plays a key role in several stages of T cell activation and effector function. Furthermore, LFA-1 increases the accumulation of TCR/class II complexes within the cSMAC and increases TCR engagement during synapse formation. Functionally, LFA-1 has been shown to enhance IL-2 expression leading to the induction of T cell proliferation (Graf et al., 2007; Tiefenthaler & Hünig, 1989).

Table 1. Costimulatory ligands and their major cellular effects. Adapted from Inman et al., 2007.

Family	Ligand (T cell)	Receptor (APC)	Major Cellular Effects
B7/CD28	CD28	CD80/CD86	IL-2-R upregulation IL-2, IL-3 and IFN-γ secretion Reduction of Bcl-xL Decrease TCR signalling threshold

	CTLA-4	CD80	Compete with CD28, blocks T cell activation and proliferation by reducing IL-2, Cell cycle arrest
	ICOS	B7-H	Inducible; only found on activated T cells, B cell development (increase in IL-4, IL-10, and CD40L)
	PD1	PD-L1	Inhibition of T cell proliferation, IFN-γ, TNF-α, IL-2, cell cycle arrest
		B7-H3	Block T cell activation and proliferation
		B7-H4	Block T cell activation and proliferation, cell cycle arrest
	BTLA	HVEM	Block T cell activation and proliferation
Integrin	LFA-1	ICAM-1	T cell stimulation
TNFRF	CD2	LFA-3	Formation stable immune synapses between T cells and APCs or target cells
	OX40	OX40L	IL-2-R upregulation, IL-2, IL-3 and IFN-γ secretion
	4-1BB	4-1BBL	Increased IL-8, TNF-α, ICAM1
	CD40	CD40L	T cell activation and proliferation
	CD27	CD70	Low IL2, High TNF-α
	Light-R	Light	Amplifies NF-kB, induces IFN-γ

T cell function

Upon receiving Signal 1 and signal 2, the naïve T cell becomes a full-fledged effector T cell. Effector T cells circulate the body and mount a cytotoxic response upon interaction with their target antigen. To mediate killing, effector T cells require antigen presentation (Signal 1) but not costimulation (Signal 2). Two categories of effector T cells mediate anti-tumour immunity: CD8+ cytotoxic T cells and CD4+ helper T cells. CD8+ T cells release apoptotic soluble agents or receptor-mediated mechanisms to induce direct cytotoxic killing (Goldstein & Griffiths, 2018). Cytotoxic perforin and granzyme molecules are released by the T cell into the synaptic cleft to initiate apoptosis in the target cell. Perforin functions as a pore-forming protein, enabling granzymes to enter the cytosol of target cells. Once inside, granzymes cleave intracellular substrates that regulate cell death and survival. Additionally, death receptors such as FasL/Fas trigger apoptotic cascades in the target cells (Waring, & Müllbacher, 1999).

CD4+ T cells function as the regulators of other immune cells. CD4+ T cells amplify the CD8+ cytotoxic T cell anti-tumour response through secretion of supportive cytokines (e.g., IL-2 and IFN-γ) and recruiting immune cells (e.g., B cells and macrophages) (Luckheeram et al., 2012). Both CD4+ and CD8+ T cells mediate serial killing by inducing cell death (Weigelin & Friedl, 2022; Wiedemann et al., 2006). Additionally, CD4+ and CD8+ T cells can migrate to tumors, where they can persist for years to maintain tumour control (Han et al., 2021). High local densities of cytotoxic T cells enhance their effector function by increasing the frequency of contact and the likelihood of encountering targets, emphasizing the importance of maximizing T cell presence at the tumour site (Jansen et al., 2019; Budhu et al., 2010; Halle et al., 2017).

1.4 Engineered T cells for cancer

T cell engineering and synthetic receptors

One treatment that (i) considers the importance of maximizing effector T cell numbers, and (ii) exploits the endogenous anti-tumour activity possessed by T cells is adoptive cellular therapy (ACT) (Rosenberg & Restifo, 2015). ACT is composed of three key stages: the collection of T cells, their *ex vivo* expansion using supportive medium and cytokines to generation millions of activated T cells with known selectivity and potency, and the infusion of expanded T cells into the patient to overwhelm and eliminate the tumour (Rosenberg & Restifo, 2015; Marcus & Eshhar, 2011) (**Figure 2**). One ACT strategy is to infuse genetically modified T cells that express a tumour targeting receptor to redirect antigen specificity and augment anti-tumour activity. The antigen specificity of T cells can be redirected using either transgenic TCRs or synthetic antigen receptors.

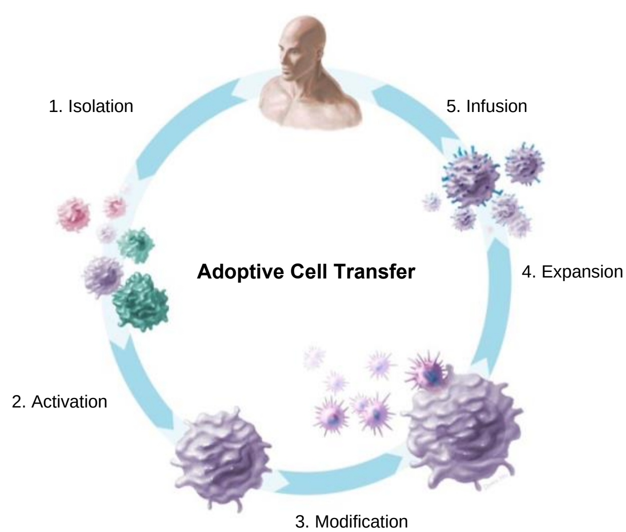

Figure 2. Adoptive cell transfer. T cells are sourced from the patient, activated, (sometimes) modified to enhance efficacy, expanded, and infused into a patient as cancer treatment.

Transgenic TCR

The antigen specificity of T cells depends on the TCRα and TCRβ chain (Janeway et al., 2001). A transgenic TCR with modified TCRα and TCRβ chains can recognize selected tumour antigens through pMHC presentation (Chandran & Klebanoff, 2019). Adoptive transfer of TCR modified T cells are advantageous because it allows for the infusion of large numbers of antigen-specific T cells (Leung & Heslop, 2019). Additional benefits to using transgenic TCRs include: (i) canonical signalling pathways to active the T cell; (ii) target antigens that are not limited to membrane proteins, both of which are barriers for some synthetic receptors (Baulu et al., 2023). However, transgenic TCRs are MHC-restricted and can be ineffective due to a loss of MHC expressing tumour cells due to immune evasion (Cornel et al., 2020).

Chimeric antigen receptor (CAR)

The antigen specificity of T cells can also be redirected with genetically engineered receptors ("synthetic antigen receptors"), that can ligate to a chosen antigen and activate a T cell to perform its effector function. The most notable example is the chimeric antigen receptor (CAR), which circumvents key challenges associated with TCR-based binding, including MHC-restriction (June & Sadelain, 2018). CAR-engineered T cells express a tumour targeting synthetic receptor with specificity towards a desired antigen. The first-generation CAR has three key components: an extracellular antigen binding domain, a transmembrane domain and a single intracellular signalling domain (June & Sadelain, 2018) (**Figure 3**). The antigen binding domain is typically a single-chain fragment variable (scFV) composed of a variable light and heavy chain from an antigen-specific immunoglobulin. The scFV is fused to the transmembrane domain through a flexible linker. The transmembrane domain is required for surface expression and stability of the receptor complex (Bridgeman, 2010). The intracellular domain CD3ζ contains three immunoreceptor tyrosine-based activation motifs (ITAMs) and is required for signal transduction (Eshhar et al., 1993; Rafiq et al., 2010). Following antigen binding, the CD3ζ domain undergoes conformational changes that promotes the recruitment and phosphorylation of intracellular signalling proteins to activate the T cell (Cantrell et al., 2002; Su & Vale, 2018).

CARs can recognize surface expressed proteins in the absence of MHC presentation, circumventing challenges that arise with MHC-downregulation in the context of TCR-based binding (Lim & June, 2017). CARs are also not restricted to peptide antigens and can ligate antigens from glycans, carbohydrates and proteins, should a suitable antigen-binding domain exist. For this reason, antigens which were previously undetectable via TCR-based recognition (which are restricted to processed peptides) can be recognized by T cells through the CAR.

Initial studies with the first-generation CAR T cells demonstrated poor proliferation and tumour killing due to poor cytokine secretion and costimulatory signalling (Brocker, & Karjalainen, 1995; Hege et al., 2017; Till et al., 2008). A major predictor of CAR T cell efficacy is the level of T cell expansion and persistence post-ACT (Porter et al., 2015; Maude et al., 2014; Hsieh et al., 2020). Thus, strategies to promote *in vivo* anti-tumour efficacy of CAR T cells focused on expanding the number of effector cells at the tumour site. One such strategy to enhance CAR T cell function is the incorporation of intracellular costimulatory signalling moieties such as CD28 or 41BB to the CAR itself to promote T cell expansion and survival (Maher et al., 2002; Imai et al, 2004). Indeed, second-generation CAR T cells that incorporated costimulatory domains into the intracellular signalling domain demonstrated superior T cell expansion, cytotoxicity, survival and response durability (**Figure 3**). CD28 and 4-1BB are the two most common costimulatory domains and have demonstrated high response rates in the clinic (Smirnov et al., 2024).

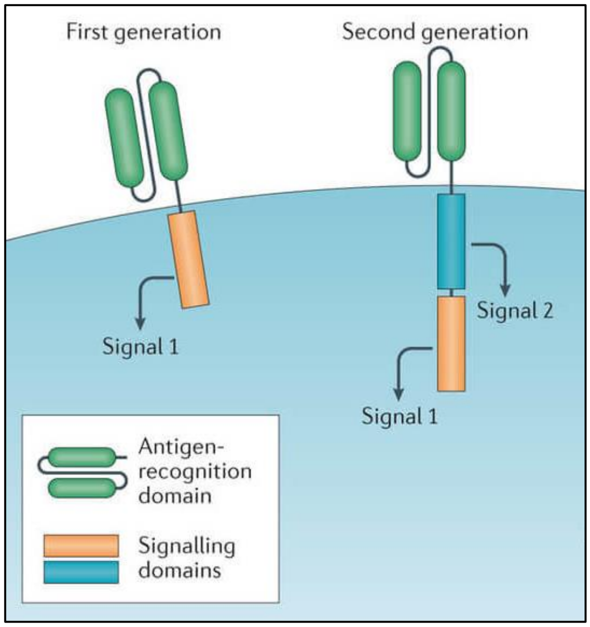

Figure 3. The first-generation CAR is composed of an antigen-binding domain, transmembrane scaffold and intracellular signalling domain. The second-generation CAR T cell includes an additional costimulatory domain. Adapted from (Brentjens et al., 2016).

These advancements led to clinically effective therapeutic responses in hematological malignancies, with FDA approved therapies targeting CD19+ and BCMA+ B cell malignancies, such as B-cell acute lymphoblastic leukemia, B-cell non-Hodgkin lymphoma, follicular lymphoma, mantel cell lymphoma, and multiple myeloma (Sterner & Sterner, 2021). The efficacy of second-generation CAR T cells are currently being investigated in solid tumors, including sarcoma, ovarian cancer, glioblastoma, advanced sarcoma and pancreatic cancer (Van Der Stegen et al., 2015).

Challenges with CAR T cells

Although CAR T cell therapy has revolutionized the treatment of some cancers, high rates of CAR T cell-mediated toxicity, which can be lethal if unchecked, remain a concern (Sterner & Sterner, 2021). In acute lymphoblastic leukemia patients treated with CAR T cells, nearly all experience mild toxicity, while a smaller subset of patients experience adverse effects such as excessive cytokine production and massive T cell proliferation *in vivo* (Frey & Porter, 2016; Morris et al., 2022).

The three most notable toxicities are cytokine release syndrome, immune effector cell-associated neurotoxicity syndrome and macrophage activation syndrome. Cytokine-release syndrome is defined by excessive cytokine production, wherein, IL-6 and IFN-γ are elevated. Symptomatically, raised IFN-γ levels can result in fever, headache, dizziness, and fatigue; and mechanistically, elevated IFN-γ levels induce the activation of other immune cells, such as macrophages (June et al., 2018; Matthys et al., 1993). IL-6 also contributes to characteristic symptoms, such as vascular leakage and inflammatory and coagulation cascades (Tanaka & Kishimoto, 2016; Shimabukuro-Vornhagen et al., 2018).

Immune effector cell-associated neurotoxicity syndrome is characterized by the disturbance of the blood-brain barrier and elevated cerebrospinal fluid cytokine levels (Santomasso et al., 2018). The symptoms resembled that of toxic encephalopathy, aphasia, dysregulation of fine motor function and reduced level of attention (Herr et al., 2020). The presence of central nervous system inflammation was demonstrated by CAR T cells infiltration and raised cerebrospinal fluids levels of IL-6, IL-1, TNF-α and IFN-γ (Hett et al., 2020; Hu et al., 2016). Macrophage activation syndrome, which is characterized by uncontrolled T cell and macrophage proliferation, is a severe hyperinflammatory condition defined by cytokine-release syndrome, pulmonary edema, elevated liver enzymes and kidney failure (Sadelain et al., 2013).

Severe toxicities observed with CAR T cell therapy have been generally attributed to the inclusion of costimulatory domains due to enhanced cytokine production and expansion *in vivo* in second-generation CARs compared to first-generation CARs (Jensen et al., 2010; Kershaw et al., 2006; Till et al., 2008).

The KIR CAR

Although the CAR is very well-described and the only synthetic receptor clinically approved for genetic re-targeting of T cells, researchers are exploring other synthetic antigen receptor designs. Wang et al. (2015) described a DAP12-based synthetic antigen receptor (*referred to as DAP12 SAR hereon*) with three components – an extracellular binding domain fused to a transmembrane scaffold that non-covalently associates to an adaptor signalling protein, known as DAP12 (**Figure 4**).

An scFv based antigen binding domain was fused to the extracellular hinge, transmembrane and cytoplasmic domain of KIR2DS2, a stimulatory killer immunoglobulin-like receptor (KIR). The KIR's short cytoplasmic tail lacks a classical ITAM and cannot signal on its own (Yawata & Yawata, 2010). It thus relies on ITAM containing adapter molecule DAP12 (short-form of DNAX-activating protein of 12 kDa) for its transmission of intracellular signals (Yawata & Yawata, 2010). DAP12 and KIR2DS2 form a non-covalent bond, for which their crosslinking activates the cell through recruitment of Zap70 and Syk tyrosine kinases (Lanier et al., 1998). KIR2DS2 is found primarily on Natural killer (NK) cells, but also on some differentiated T cells (Mora-Bitria, & Asquith, 2023). Thus, the DAP12-based SAR design seeks to naturally regulate T cell activation by exploiting the endogenous association of KIR2DS2 and DAP12 (Wang et al., 2015).

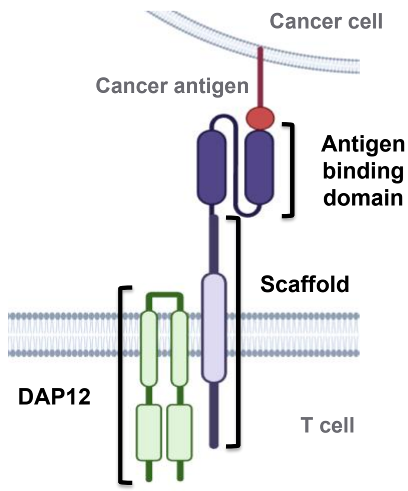

Figure 4. The DAP12 SAR is a tumour redirecting synthetic receptor comprised of an antigen-binding domain, a transmembrane scaffold, and DAP12 adaptor signalling protein.

DAP12 SAR engineered T cells targeting HER2, CD133 and BCMA effectively detect and suppress tumour growth on cells expressing their corresponding antigens (data not published). Despite lacking a synthetic costimulatory domain, they displayed superior anti-tumour activity compared to both first and second generation CD3ζ-based CARs in a xenograft model of immunotherapy-resistant mesothelioma (Wang et al., 2015). **This suggests DAP12 SAR T cells do not require costimulation for function.** A variation of the DAP12 SAR substituted the KIR2DS2 with the transmembrane and cytoplasmic domain of triggering receptor expressed on myeloid cells 1 (TREM1) (Chen et al., 2019). TREM1-based DAP12 SAR also demonstrated anti-tumour efficacy *in vitro* and *in vivo* (Chen et al., 2019).

A few potential mechanisms could explain the DAP12 SAR T cell's superior anti-tumour activity. Unlike CD3ζ-based CARs, DAP12 SAR expression is retained by T cells in the tumour microenvironment, likely an attribute of KIR/DAP12 complex stability within the plasma membrane (Wang et al., 2015). Moreover, traditional CARs incorporate all three CD3ζ ITAMs in contrast to DAP12 proteins that contain only 1 ITAM. It is hypothesized that the redundancy of ITAM signalling in traditional CARs may result in T cell exhaustion, and lack thereof in DAP12 SAR T cells (Feucht et al., 2019).

The T cell antigen coupler

The T cell antigen coupler (TAC) is a synthetic antigen receptor was developed by the Bramson Lab. It consists of two binding components: an extracellular tumour antigen binding linked to a CD3ε-targeting scFv, which are fused to the T cell by the CD4 co-receptor (Helsen et al., 2018) (**Figure 5**). Incorporating the TAC into the TCR/CD3 complex redirects T cell specificity and leverages canonical signaling pathways to employ an endogenous TCR signal (Helsen et al., 2018).

TAC T cells have shown effective anti-tumour activity within *in vitro, in vivo* studies (Helsen et al., 2018; Bezverbnaya et al., 2021) and have also demonstrated safety in a phase I/II dose-escalation trial for HER2-positive cancers (unpublished). TAC T cells generate fewer inflammatory cytokines than CAR T cells and circumvent the severe toxicities seen with 28ζ CAR T cells in mouse models (Helsen et al., 2018). **TAC T cells do not require a costimulatory domain for *in vivo* efficacy.** Despite this, they exhibit strong anti-tumour activity without evidence of tonic signaling *in vivo* (Helsen et al., 2018).

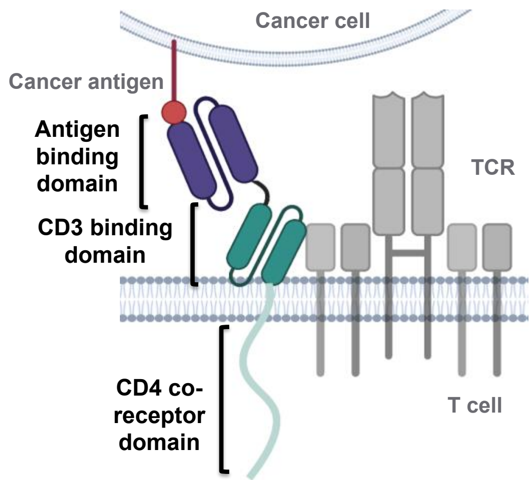

Figure 5. The TAC receptor is a tumour-redirecting synthetic receptor that is composed of an antigen-binding domain, a CD3-epsilon binding domain, and a CD4 transmembrane and intracellular domain. Created with Biorender.

While KIR CAR and TAC T cells function effectively without costimulation, there is potential for enhancement through bolstering persistence and proliferative capacity. Genetic incorporation of costimulation in CAR T cells is known to be crucial for clinical efficacy but underpins toxicity. However, chemical biology offers a promising approach to incorporate the benefits of costimulation to a variety of synthetic antigen receptor engineered T cell products (including KIR CAR and TAC) without the challenges of genetically introducing costimulation. A "druggable" method to provide costimulatory signals could be a strategy to tune *in vivo* T cell expansion (**Figure 6**). For this reason, we are investigating the use of small molecule drugs in KIR CAR and TAC T cells as agents that can provide costimulation.

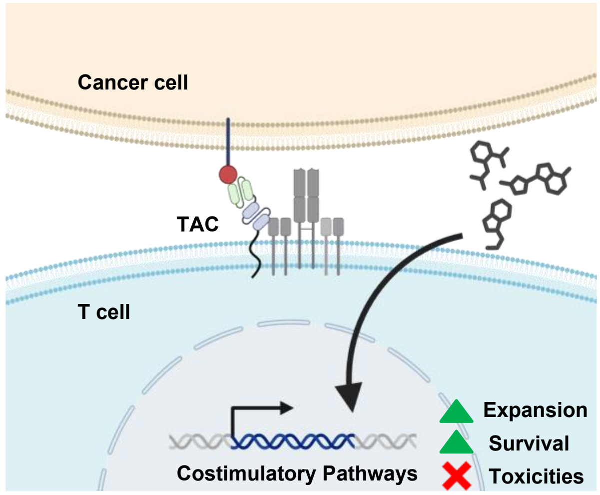

Figure 6. Hypothesis. Small molecules can deliver costimulation to TAC T cells, enhancing their proliferative and survival capacity, without toxicities.

1.5 Research Context

Previous research in the lab found that TAC T cells did not proliferate in response to antigen loaded beads but demonstrated enhanced survival and proliferation via CD28-mediated and CD2-mediated costimulation, respectively. In particular, when stimulated with synthetic beads loaded with recombinant costimulatory ligands CD86-Fc and LFA3-Fc, TAC T cell proliferation and survival increased. Together, these findings formed the rational to conduct a high throughput screen (HTS) of the Bioactive A Library (N=4000 molecules) from CMCB to identify compounds that enhanced TAC T cell proliferation (Bacchiocchi, 2021). The HTS, which employed a bioluminescence reporter and robust assay controls (luciferase^{+} TAC T cells and DMSO, stimulated with HER2-Fc loaded beads (negative control) or HER2-Fc, CD86-Fc & LFA3-Fc loaded beads (positive control)), found 30 hits that enhanced TAC T cell number. Validation assessments that rigorously confirmed the biological activity of the hits narrowed down the actives to a lead candidate, Ferutinin.

Ferutinin is a non-steroidal phytoestrogen derived from the Ferula *tenuisecta* species. Ferutinin is poorly described in the literature. Some reports describe it is a naturally occurring phytoestrogen with selective estrogen receptor activity and anti-cancer activity *in vitro* and *in vivo* experiments (Naji Reyhani Garmroudi et al., 2021). Ferutinin has not yet been characterized for its immunomodulatory activity. Subsequent to Ferutinin's discovery, the Magolan

Lab at McMaster generated a small library (N=25) of Ferutinin analogues based on structure-activity relationship studies, which serve to (i) identify the biologically active structural components of the parental compound and (ii) optimize its potency and drug-likeness. Here, we explore the use of Ferutinin analogues as costimulatory agents.

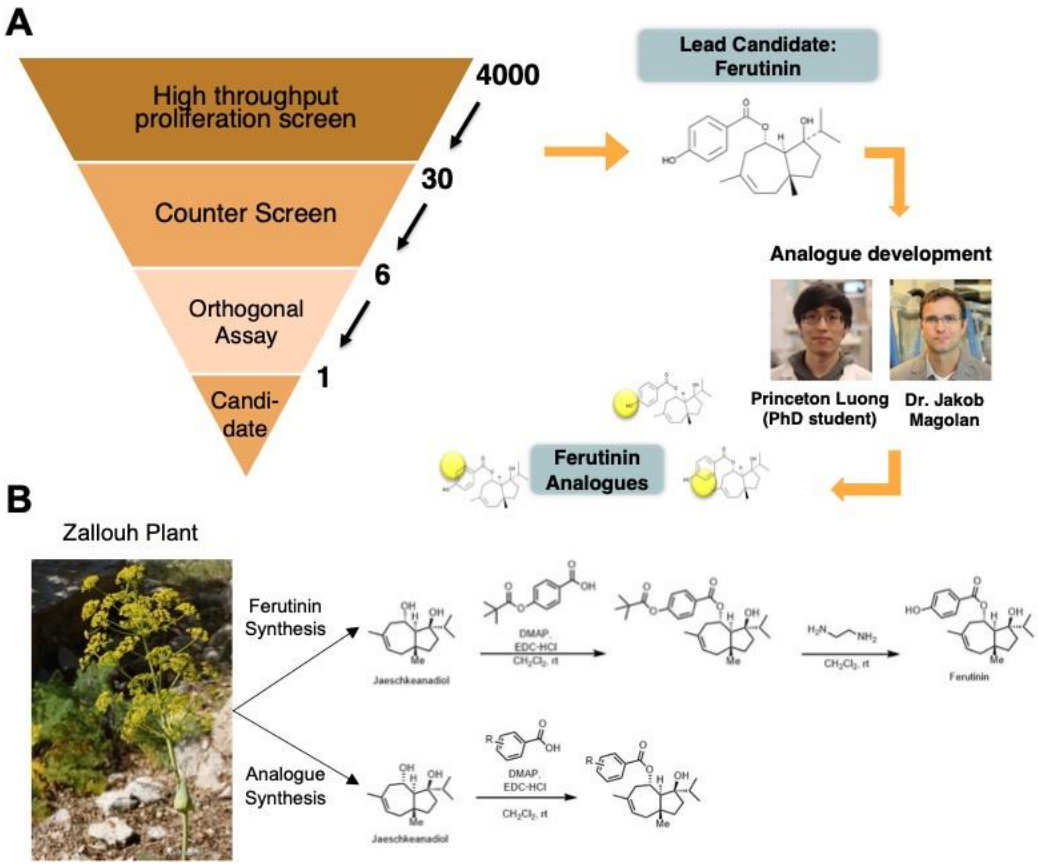

Figure 7. A. A summary of the research context. **B.** Starting with Jaeschkeanadiol extracted and isolated from the Zallouh root tea, it is esterified to give a protected Ferutinin precursor, and subsequently deprotected under basic conditions to give Ferutinin. general synthesis of an ester analogue, where a different benzoic acid is coupled in similar fashion with the Jaeschkeanadiol starting material. The modified ester compounds made up the bulk of the analogue library.

Additionally, a new library of 11K+ biologically active compounds has been obtained at the Centre for Microbial and Chemical Biology, which has limited overlap with the original compound library. Therefore, to extend our investigations to additional possible chemical matter, we developed a reporter-based proliferation and screened the new library. We then validated the biological activity of the 'hit' compounds that emerged from the HTS.

2.0 OBJECTIVES

2.1 Assess the functional changes to DAP12 SAR and TAC T cells when treated with Ferutinin and Ferutinin analogue(s).

Our first objective was to identify candidate(s) within the Ferutinin analogue library that augmented engineered T cell function. The results of the initial screen informed the design and synthesis of novel analogues with structures optimized to better maximize their functional activity. Subsequent analogues were evaluated for their functional benefit to engineered T cells.

2.2 Develop an automated reporter-based proliferation assay

Our second objective was to develop an automated reporter-based proliferation assay based on the previous HTS that identified Ferutinin. We evaluated a range of engineered T cell candidates and conducted a series of optimization experiments to ensure a reliable and robust assay.

2.3 High throughput screening of biologically active compounds

Our final objective was to conduct a HTS assessing over 15,000 biologically active molecules for their effect on engineered T cell proliferation. Hits from the screen were advanced to secondary assays that served to validate their biological activity in various biological contexts. Candidates that demonstrate reproducible enhancement to engineered T cell function were advanced to detailed assessment and characterization studies.

3.0 RESULTS

3.1 Validation of Ferutinin and analogues on enhancing engineered T cell performance

Commercial Ferutinin provides greater functional benefit than Ferutinin synthesized at McMaster

We first assessed Ferutinin mediated enhancement to DAP12 SAR and TAC T cell cytotoxicity (see Appendix for chemical structures and descriptions). T cells engineered with a DAP12 SAR or a TAC (both synthetic antigen receptors were directed against HER2) were co-cultured with various sources of Ferutinin at 10 μM and fluorescent HER2 expressing HCT-116 human colorectal cancer cells. When comparing the functional response to Ferutinin synthesized in-house (2102A, 2102B, 2102C) versus commercially available (P2101 and P2205), the commercial products, in particular P2205, elicited greater suppression of tumour growth by the DAP12 SAR- and TAC-engineered T cells compared to the in-house synthesized Ferutinin (**Figure 8A, 8B**). A similar conclusion was reached by interrogating the functional differences between in-house and commercially generated Ferutinin in a dye-dilution proliferation assay. CellTrace™ Violet (CTV) stained DAP12 SAR T cells were co-cultured with HCT-116 cells and Ferutinin for 72 hours. At assay endpoint, more DAP12 SAR T cells were enumerated in the presence of commercial Ferutinin (again, P2205 was most potent) in comparison to in-house Ferutinin (**Figure 8C**). In addition, DAP12 SAR T cells treated with commercial Ferutinin underwent additional cycles of cellular division (**Figure 8D**). ^{1}H NMR and mass spectrometry analysis of both commercial Ferutinin products P2101 and P2205 suggested the presence of a contaminant or degradation product (see Appendix to view **Figure 27**).

We speculated that this unknown component could be mediating enhancement of engineered T cell function. When considering the mechanism by which Ferutinin could degrade, we considered the possibility that long term exposure to DMSO in storage increased the likelihood degradation. To test this hypothesis, our collaborators in the Magolan Lab exposed in-house synthesized Ferutinin to DMSO at either 60°C or room temperature and open air or argon for seven days. The solvents containing Ferutinin, and possible degradation products (2214-2218) were evaluated for their impact on TAC T cell cytotoxicity. TAC T cells were co-cultured with compounds at 10 μM and green, fluorescent HCT-116 cells for 3 days. None of the degradation products enhanced the tumor growth control by the TAC T cell cytotoxicity (**Figure 9A**).

To further interrogate Ferutinin's active chemical structure, the Magolan Lab isolated natural products from Ferutinin's starting material, zallouh root tea, via a Soxhlet extraction. The crude extracts were preliminarily purified using phase flash chromatography, separated and concentrated. The extraction products (2118-2221) were co-cultured with DAP12 SAR T cells with compounds at 10 μM and HCT-116 cells for 3 days. They failed to enhance DAP12 SAR T cell survival and expansion, as measured in a dye-dilution proliferation assay (**Figure 9B, 9C**). At this stage, we centred our efforts on investigating the Ferutinin analogue library.

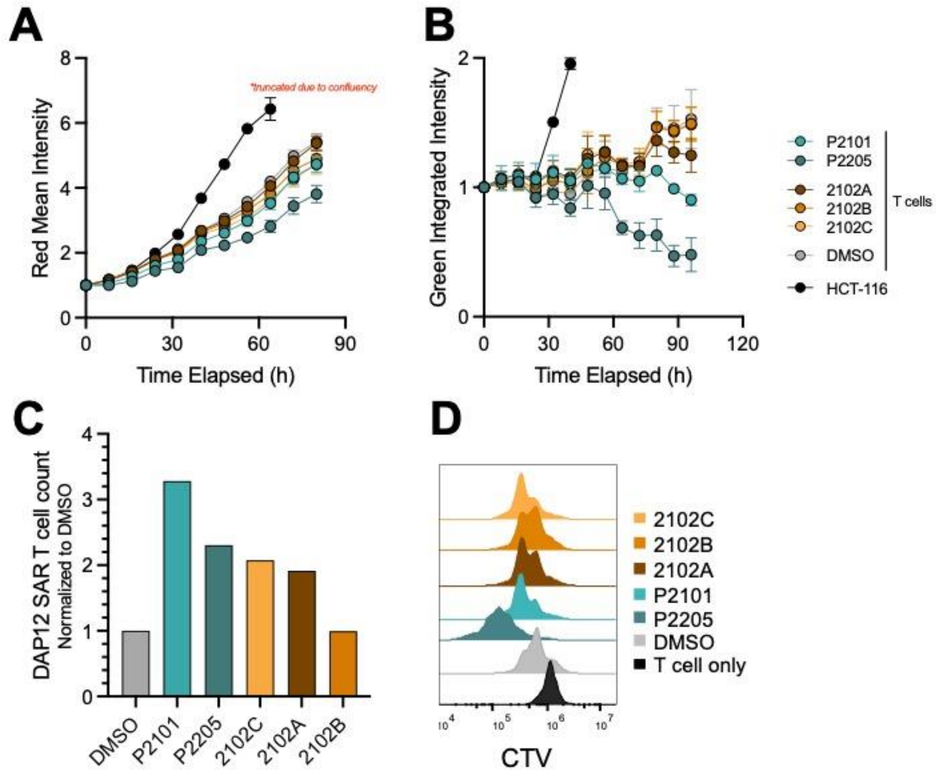

Figure 8. A. Ferutinin mediated DAP 12 SAR T cell cytotoxicity was assessed in an IncuCyte killing assay using HCT-116 tumour cells engineered to express red fluorescent protein. Analysis normalized to T=0. **B.** Ferutinin mediated TAC T cell cytotoxicity was assessed in an IncuCyte killing assay using HCT-116 tumour cells engineered to express green fluorescent protein. **C.** DAP12 SAR T cell count following 72-hour co-culture with HCT-116 tumour cells and Ferutinin. DAP12 SAR T cells were enumerated with counting beads, as measured Live SAR+ cells by Flow Cytometry. **D.** DAP12 SAR T cell count was measured by CellTrace Violet dye-dilution following 72-hour co-culture with HCT-116 tumour cells and Ferutinin.

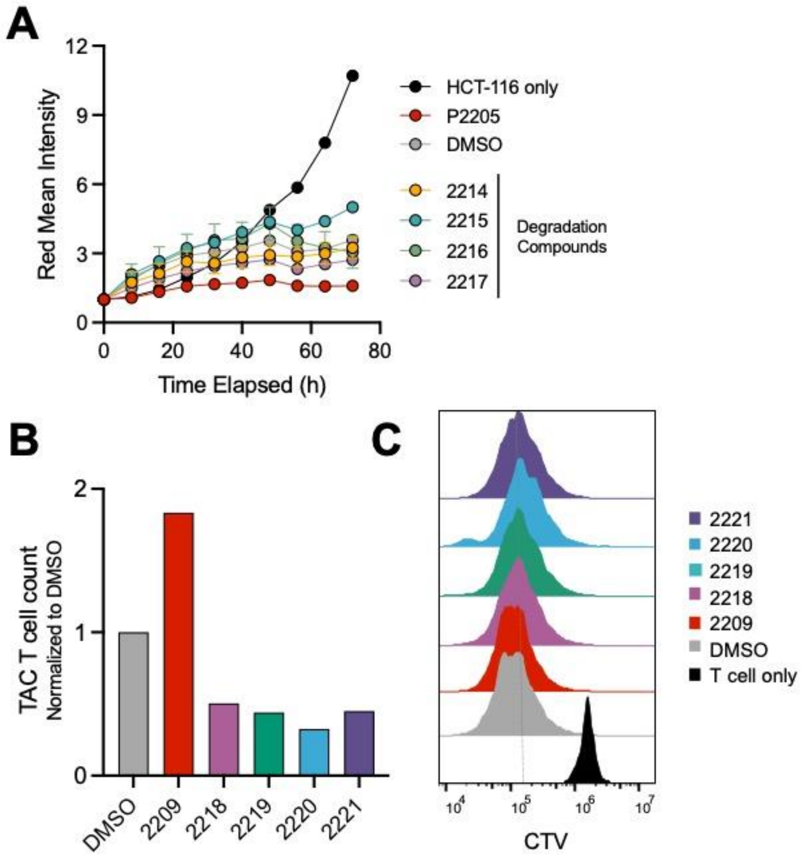

Figure 9. A. Degradation compound mediated DAP 12 SAR T cell cytotoxicity was assessed in an IncuCyte killing assay using HCT-116 tumour cells engineered to express red fluorescent protein. **B.** TAC T cell count following a 72-hour co-culture with HCT-116 tumour cells and extraction compounds. TAC T cells were enumerated with counting beads, as measured Live SAR+ cells by Flow Cytometry. **C.** TAC T cell count was measured by CTV dye-dilution following 72-hour co-culture with HCT-116 tumour cells and Ferutinin**.**

Ferutinin analogues intermittently augment DAP12 SAR and TAC T cell function

We first sought to exclude analogues toxic to human cells. Of 25 Ferutinin analogues, only 2204 (one of two single-blinded compounds) inhibited tumour growth in the absence of T cells (**Figure 10A**). At unblinding, it was revealed that 2204 is a steroid rather than an analogue of Ferutinin. Thus, neither Ferutinin nor any of the synthetic analogues displayed direct cytotoxicity to the tumour cells. Most analogues mildly enhanced tumour growth suppression by DAP12 SAR and TAC T cells but none achieved the tumour growth suppression noted with the commercial Ferutinin (P2101 and P2205) (data not shown). Additionally, we observed considerable variability in the enhancing properties of the analogues' activity across the following parameters: order of potency, class of synthetic receptor and effector to target ratio (data not shown). Analogues 2209, 2210 and 2211 demonstrated consistent enhancement of T cell cytotoxicity using T cells from multiple donors and engineering with both TAC receptors and DAP12 SARs (**Figure 10B, 10C**). We also found that 2209, 2210 and 2211 reproducibly increased DAP12 SAR and TAC T cell count in a 72-hour dye dilution proliferation assay (**Figure 10D**). The reproducible functional enhancement mediated by 2209, 2210 and 2211 led to the generation of 12 derivatives (2300 series).

The 2209-2211 derivatives elicited a moderate enhancement to DAP12 SAR and TAC T cell cytotoxicity compared to DMSO control (**Figure 10E, 10F**). Repeat assessments of the 2300 series and 2209-2211 demonstrated variation with respect to the compound order of potency and across synthetic receptors, and thus, did not clearly identify structural features of the compounds that influence engineered T cell cytotoxicity (data not shown). Our subsequent objective sought to identify optimal analogue doses and validate their performance across multiple T cell donors, antigen binders, receptors and stimuli. For these reasons, we elected to employ a high throughput assay. We elected to employ a variation of the automated reporter-based screen that was originally used to identify Ferutinin.

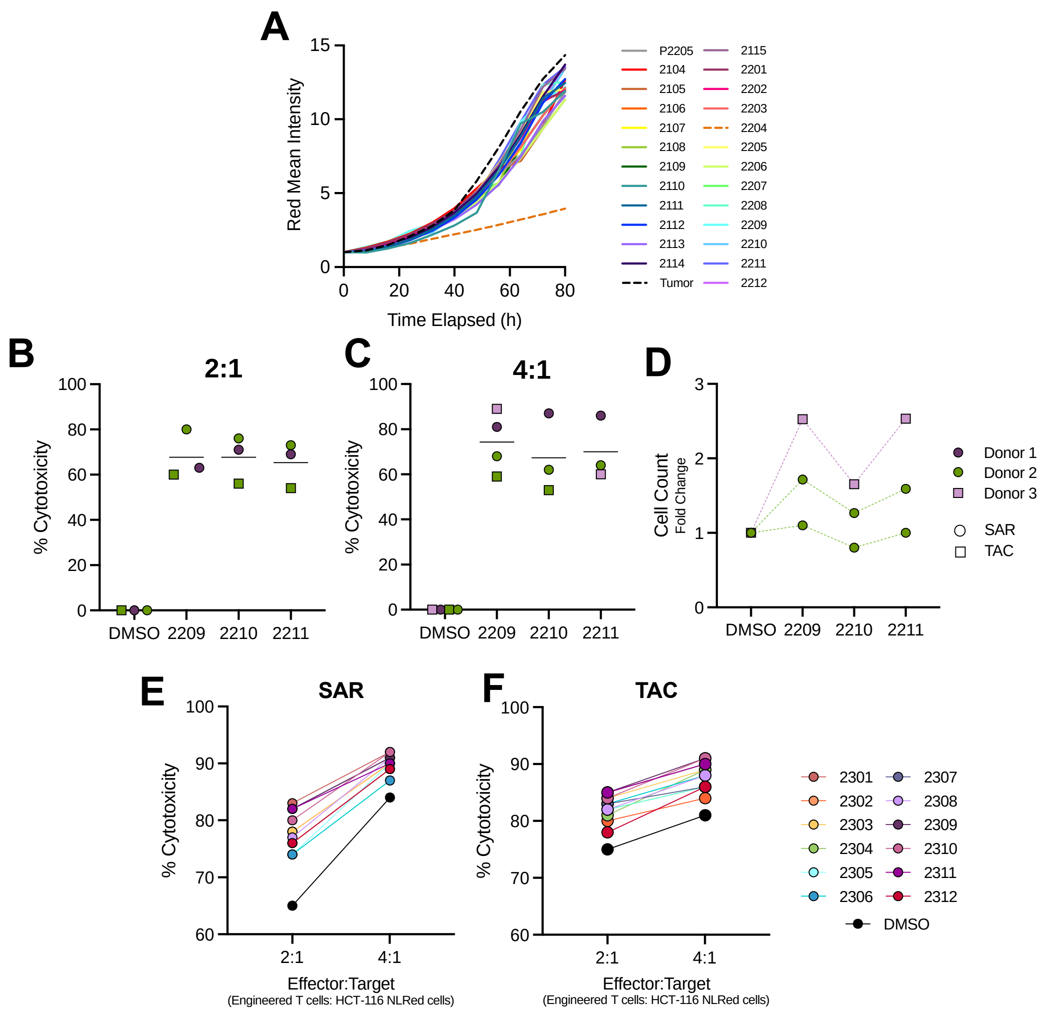

Figure 10. A. Tumour and analogue alone monitored in an Incucyte killing assay using HCT-116 tumour cells engineered to express red fluorescent protein. **B.** Analogue mediated T cell cytotoxicity was assessed in an IncuCyte killing assay using HCT-116 tumour cells at a 2:1 ratio of engineered T cells to tumour cells. Tumour cell killing was measured using the IncuCyte Live Cell Analysis Software and is presented using inverse Area Under the Curve analysis normalized to DMSO only. **C.** Analogue mediated T cytotoxicity was assessed in an IncuCyte killing assay using HCT-116 tumour cells at a 4:1 ratio of engineered T cells to tumour cells. **D.** Engineered T cell count following 72-hour co-culture with HCT-116 tumour cells and analogue. Engineered T cells were enumerated with counting beads, as measured Live receptor+ cells by Flow Cytometry. Lines represent samples from the same experiment. **E.** Analogue mediated engineered T cell cytotoxicity was assessed in an IncuCyte killing assay using HCT-116 tumour cells at multiple ratios of engineered T cells to tumour cells. Tumour cell killing was measured using the IncuCyte Live Cell Analysis Software and is presented using inverse Area Under the Curve analysis normalized to DMSO only.

3.2 Developing an automated reporter-based proliferation assay

Luciferase possesses distinct advantages from fluorescence

An automated assay using a rapid and simple approach to experimental design and data analysis leverages optical readouts such as colorimetry, luminescence and/or fluorescence. We first explored the utility of a fluorescence reporter system for the automated proliferation screen. TAC T cells were manufactured from healthy donor peripheral blood mononuclear cells and transduced with a bicistronic lentivirus vector encoding a HER2 directed TAC receptor and fluorescent reporter, mStrawberry (**Figure 11A**). To validate the accuracy of the mStrawberry reporter system, we plated $2x10^5$ to 300 TAC T cells per well was quantified on a plate reader. The correlation between TAC T cells and mStrawberry signal intensity (R^2=0.9129) was moderately linear and demonstrated substantial variation at lower cell densities **(Figure 11C, 11D**). In addition, the fluorescent readout did not achieve a similar magnitude of reporter signal that can be obtained with a Luciferase reporter system (data not shown). The mStrawberry reporter system presents an additional drawback as it cannot discriminate between live and dead cells, whereas the luminescence from firefly luciferase is dependent upon ATP which is only produced in live cells. Therefore, we elected to proceed with a firefly luciferase-based reporter system.

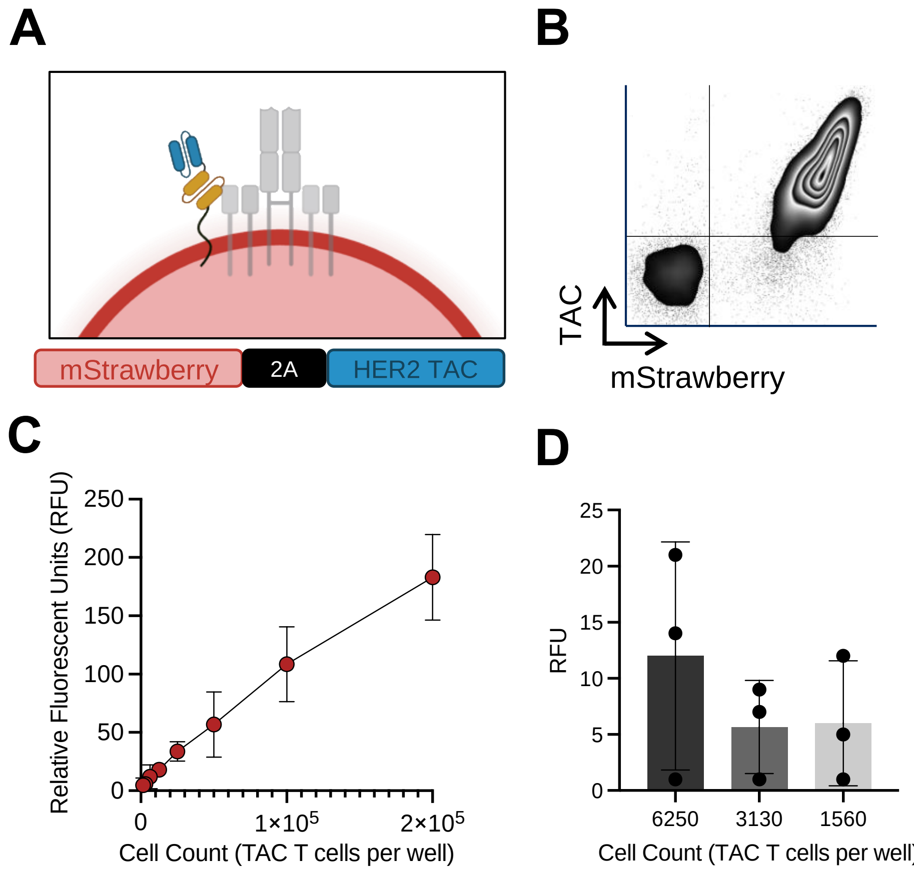

Figure 11. A. Schematic representation of HER2 directed TAC T cell expressing mStrawberry. **B.** TAC and mStrawberry expression on the final day of culture measured by flow cytometry. TAC T cells were stained for and gated on TAC. TAC expression was detection by cell surface staining with HER2-Fc; upstream gating on live singlets **C.** Fluorescence signal intensity correlation with mStrawberry TAC T cell number. mStrawberry TAC T cells were plated at $2x10^5$ per well in triplicate and diluted two-fold eight times over (n=3). Fluorescence signal intensity was measured by a Neotek plate reader. **D.** Fluorescence signal intensity at the low TAC T cell seeding densities.

DAP12 SAR T cells are amenable to a Luciferase reporter system

DAP12 SAR T cells were engineered to express red-shifted Luciferase (rsLuc) using two approaches (for the remainder of the text, T cells that co-express a DAP12 SAR and rsLuc will be called rsLuc SAR T cells). We generated a tricistronic lentivirus vector encoding rsLuc, DAP12 and a HER2 directed SAR (**Figure 12A**). We also generated a bicistronic lentivirus vector encoding rsLuc and transduction marker, tNGFR, to be co-transduced with a lentivirus encoding DAP12 and a HER2 directed SAR (**Figure 12B**). We sought to optimize the lentiviral multiplicity of infection to obtain Luciferase/receptor expression in ~70% of the cellular population. We titrated lentivirus on HEK293T cells and measured expression via flow cytometry. We found that the tricistronic vector transduced 83 % of the population at an MOI of 1 (**Figure 12B**). However, the expression of luciferase in the co-transduced T cells never exceeded 50% even at the highest multiplicity of infection (**Figure 12B**). The co-transduction engineering approach also resulted in a small population of rsLuc+ SAR- T cells, which could skew luminescence activity in the context of the screen. To confirm the functionality of the T cell products co-expressing the HER2-specific DAP12 SAR and luciferase, the T cells were co-cultured with HER2-positive HCT116 tumour cells, and we assessed cytotoxicity, proliferation and survival (**Figure 12C**). No differences were observed between the T cells that co-expressed the DAP12 SAR and luciferase compared to the T cells that expressed the DAP12 SAR alone.

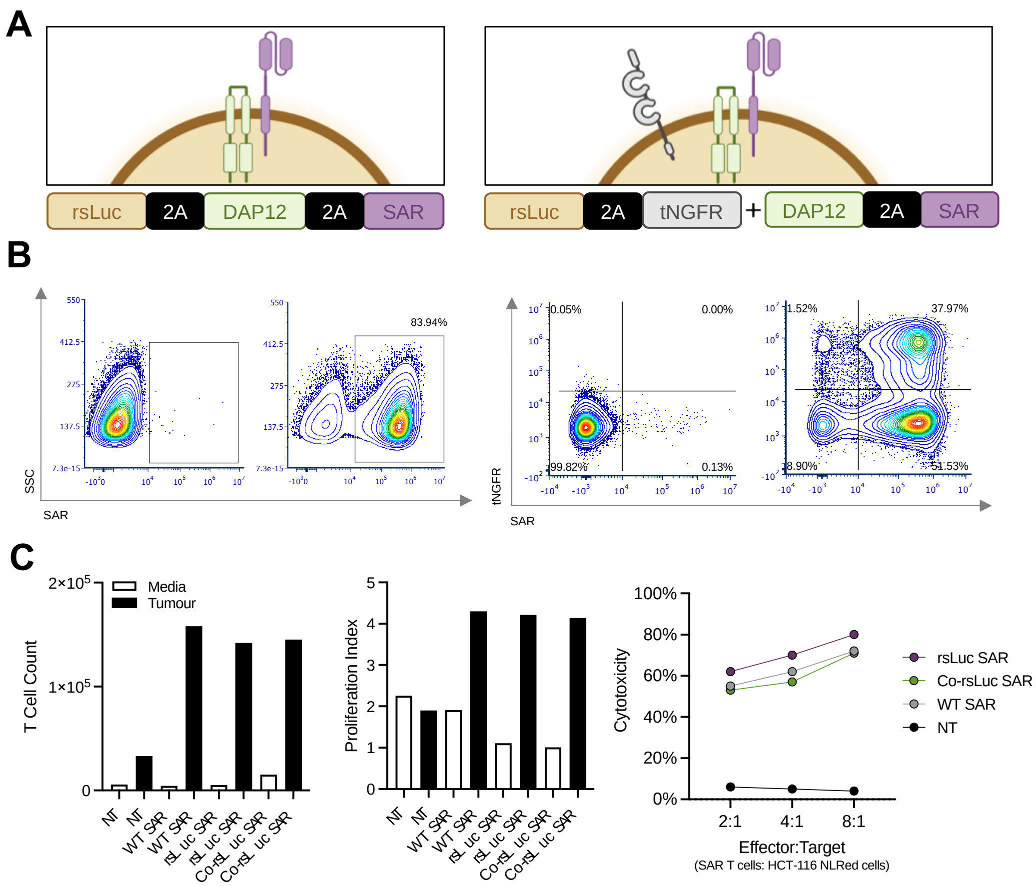

Figure 12. A. Approaches to manufacturing Luciferase expressing DAP12 SAR T cells. LEFT: Tricistronic DNA vector encoding Red Shift Luciferase and DAP12 SAR, separated by 2A sequences. RIGHT: Bicistronic vector encoding Red Shift Luciferase and a tNGFR, separated by 2A sequences. Co-transduction combines rsLuc and tNGFR with a separate vector encoding DAP12 SAR to generate a Luciferase DAP12 SAR T cell. **B.** SAR expression in DAP12 SAR T cells (day 14 of culture) was measured by flow cytometry. DAP12 SAR T cells were stained for and gated on SAR. tNGFR and SAR surface co-expression on T cells (day 14 of culture) was measured by flow cytometry. **C.** SAR T cell proliferation was measured by CellTrace Violet dye-dilution following 72-hour co-culture with HCT-116 tumour cells. DAP12 SAR T cells were enumerated with counting beads, as measured Live SAR+ cells by Flow Cytometry. A proliferation fit model using FCS Express was applied, with a proliferation index representing the average fold expansion. SAR T cell mediated cytotoxicity was assessed in an IncuCyte killing assay using HCT-116 tumour cells engineered to express red fluorescent protein. Tumour cell killing was measured using the IncuCyte Live Cell Analysis Software and is presented using Area Under the Curve analysis normalized to tumour only.

We next assessed the luciferase reporter system as an effective surrogate for T cell count. The luminescent signal resulting from plate $2x10^5$ to 300 SAR T cells per well was quantified on a luminometer. This confirmed that both engineered cell populations exhibited a linear association between luciferase signal intensity and T cell number (**Figure 13A, 13B**). We elected to proceed with the T cells engineered with tricistronic vector as the luminescence values were greater at the same seeding densities.

We then assessed the ability of the T cell engineered with the tricistronic vector to respond to the bead-based stimuli that will be used in the original HTS. We assessed both beads loaded with antigen alone (HER2-Fc), which will ultimately serve as the basal stimulus in the high throughput assay and beads loaded with antigen and costimulatory ligands (HER2-Fc, CD86-Fc and LFA3-Fc), which serve as a positive control for the assay. Controls for a HTS should possess a large signal difference between the negative and positive controls. RsLuc+ SAR T cells were stimulated with loaded beads at a 1:1 ratio and luciferase was measured on day 3, 4 and 5 post-stimulus. At day 3, we observed significant increase in luciferase in the HER2-stimulated cultures compared to those stimulated with negative control beads that were loaded with an irrelevant antigen (BCMA) and this signal gradually declined over the next two days, demonstrating that antigen-on-bead is insufficient to support robust proliferation from the rsLuc+ SAR T cells. Unlike our previous work with TAC T cells, the inclusion of costimulatory ligands, CD86 and LFA-3, did not augment rsLuc+ SAR T cell proliferation (**Figure 13C**). Give that the antigen and costimulatory ligand loading of the beads was optimized for TAC T cells, we reasoned that the conditions may need to be altered for DAP12 SAR T cells.

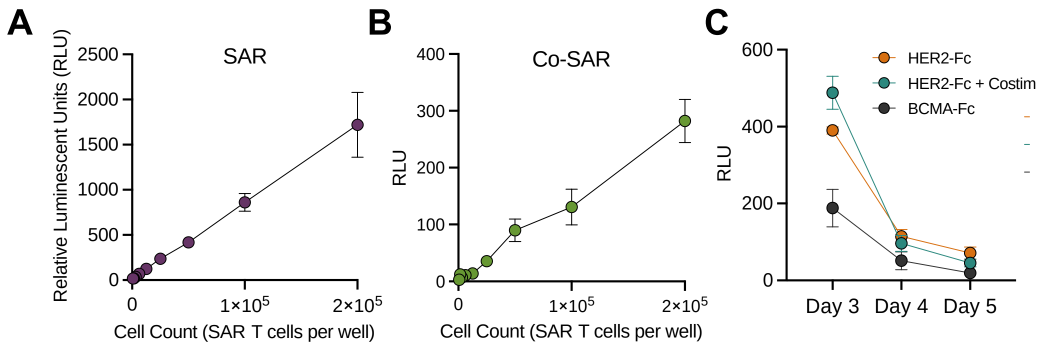

Figure 13. A. Luminescent signal intensity correlation with rsLuc+ SAR T cell number. rsLuc+ SAR T cells were plated at 2x10⁵ per well in triplicate and diluted two-fold eight times over (n=3). Signal intensity was measured by a Neotek plate reader. **B.** Luminescent signal intensity correlation with co-transduced rsLuc+ SAR T cell number. rsLuc+ SAR T cells were plated at 2x10⁵ per well in triplicate and diluted two-fold eight times over (n=3). Signal intensity was measured by a Neotek plate reader. **C.** rsLuc+ SAR T cells stimulated with Her2-Fc coated beads, Her2-Fc + CD86-Fc + LFA-3-Fc coated beads and BCMA-Fc coated beads (n=3). Signal intensity was measured by a Neotek plate reader at 120-hours.

We first sought to optimize HER2-Fc bead loading concentrations for rsLuc+ SAR T cells by titrating HER2-Fc. Protein G polystyrene beads were coated with increasing quantities of Fc-conjugated recombinant HER2 and co-cultured with rsLuc+ SAR T cells at a 1:1 ratio for 3 days. Luminescence peaked at 50 ng/1E6 beads (**Figure 14A**). At all antigen concentrations, the luminescence following stimulation with beads was markedly lower than the luminescence following tumour stimulation, suggesting antigen-on-bead does not provide a complete activation signal. We selected HER2-Fc at peak luminescence signal (100 ng/1E6 beads). We then sought to optimize the costimulatory ligand loading concentrations. Protein G polystyrene beads were coated with HER2-Fc at 100 ng/1E6 beads, increasing quantities of Fc-conjugated recombinant LFA-3 and CD86 and co-cultured with rsLuc+ SAR T cells at a 1:1 ratio for 3 days. Response to all concentrations of costimulatory ligands and HER2-Fc were roughly equivalent (**Figure 14B**), suggesting a difference in the DAP12 SAR T cell and TAC T cell response to bead stimuli.

To explore this hypothesis, we conducted a head-to-head proliferation assay comparing the rsLuc+ SAR T cells to T cell engineered with a bicistronic vector expressing rsLuc+ and HER2-TAC (rsLuc+ TAC T cells) following bead-based stimulation. As seen before, there was little luciferase production in the cultures of rsLuc+ TAC T cells stimulated with antigen-on-bead alone (**Figure 14C**; brown squares) and robust luciferase expression in cultures of rsLuc+ TAC T cells stimulated with beads carrying antigen and costimulatory ligands (**Figure 14C**; turquoise squares). In contrast, the rsLuc+ SAR T cells displayed markedly higher levels of luciferase in response to antigen-on-bead alone and this signal was not affected by the presence of costimulatory ligands. (**Figure 14D**). These results demonstrate that the rsLuc+ SAR T cells are fundamentally different from rsLuc+ TAC T cells. Thus, even though the Bramson lab is actively investigating DAP12-based SAR-T cells as potential therapeutics for a variety of cancers, we elected to proceed with rsLuc+ TAC T cells for the assessment of the Ferutinin analogues because TAC T cells were used in the original screen that identified Ferutinin. Should any strong hits emerge from the screen, they will be assessed in the context of DAP12-SAR-engineered T cells to understand that general utility of the analogue(s) beyond TAC T cells.

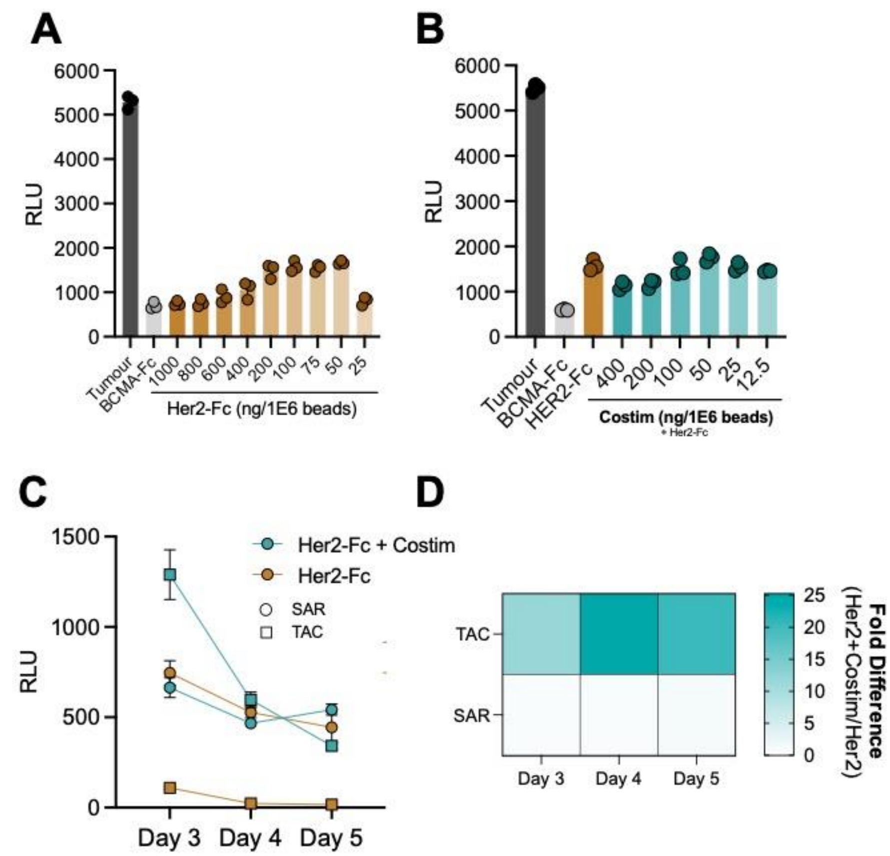

Figure 14. A. DAP12 SAR T cells were plated at 1x10[5] per well in triplicate and stimulated with HER2-Fc coated beads or HCT-116 (HER2+) tumour cells at a 1:1 ratio for three days (n=3). D-Luciferin was added, and luminescence was measured with a plate reader. **B.** DAP 12 SAR T cells were plated at 1x105 per well in triplicate and stimulated with protein-coated beads or HCT-116 tumour cells at a 1:1 ratio for three days (n=3). HER2 was loaded at 100 ng/1E6 beads for all beads loaded with HER2. Luminescent signal intensity peaks when costimulatory ligands are at a concentration of 50 ng/1E6 beads. **C.** DAP 12 SAR T cells were plated at 1x10[5] per well in triplicate and stimulated with protein-coated beads or HCT-116 tumour cells at a 1:1 ratio for three days (n=3). Luminescence of DAP12 SAR T cells was measured by the addition of D-Luciferin and captured on a plate reader on Day 3, 4, and Day 5. TAC T cells were plated at 1x105 per well in triplicate and stimulated with protein-coated beads or HCT-116 tumour cells at a 1:1 ratio for five days (n=3). Luminescence of TAC T cells was measured by the addition of D-Luciferin and captured on a plate reader on Day 3, 4, and Day 5. TAC T cells exhibit a large differential between the positive control (HER2-Fc + Costim.) and negative control (HER2-Fc).

Engineering TAC T cells with Luciferase

RsLuc+ TAC T cells were manufactured from healthy donor peripheral blood mononuclear cells, and co-transduced with two bicistronic lentiviral vectors encoding HER2 TAC & mStrawberry, as well as rsLuc+ & tNGFR. 62% of all cells co-expressed HER2 TAC and rsLuc+, as measured by Flow Cytometry, based on mStrawberry and tNGFR expression respectively (**Figure 15A**). Functional evaluation established that rsLuc+ TAC T cells functioned comparably to their parental TAC T cells (**Figure 15B, 15C, 15D**).

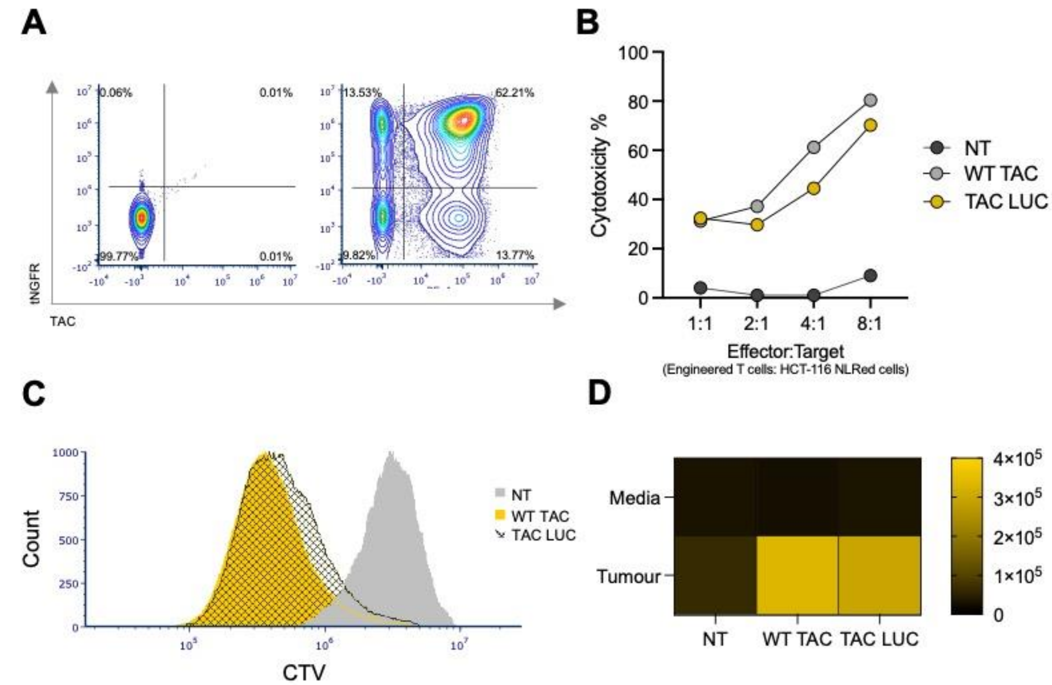

Figure 15. A. tNGFR and SAR surface co-expression on rsLuc+ TAC T cells (day 14 of culture) was measured by flow cytometry and compared to NT. **B.** rsLuc+ TAC T cell mediated cytotoxicity was compared to WT TAC T cell and assessed in an IncuCyte killing assay using HCT-116 tumour cells engineered to express red fluorescent protein. Tumour cell killing was measured using the IncuCyte Live Cell Analysis Software and is presented using Area Under the Curve analysis normalized to tumour only. **C.** T cell proliferation was measured by CellTrace™ Violet dye-dilution following 72-hour co-culture with HCT-116 tumour cells. **D.** T cells were enumerated with counting beads, as measured Live TAC+ cells by Flow Cytometry.

To ensure luminescence was an accurate measure of live TAC T cells a known number of TAC T cells were seeded into microwells followed by a luminescence readout. This confirmed the relationship between the luminescence signal intensity and TAC T cell density was linear (R^2=0.9898) (**Figure 16A**). A dilution series, plating a known number of TAC T cells per well (1x10^6 to 60 cells per well), established the biphasic trend in a 384-well flat bottom plate (R^2=0.9539) (**Figure 16B**). Higher seeding densities observed greater variability in signal (**Figure 16B**). All densities at 1x10^5 cells per well and below represented a stronger relationship (R^2=0.9976) (**Figure 16C**). When selecting an optimal TAC T cell seeding density, were sought to: (i) retain luminescence resolution at high cell densities and (ii) ensure experimental feasibility. Considering both factors, we selected a density of 3.13x10^4 cells per well, which was the same seeding density used in the original screen.

A range of T cell to bead (effector to target; E:T) ratios were evaluated to optimize separation between the basal stimulus (antigen-on-bead alone) and the positive control (antigen-on-bead with costimulatory ligands). RsLuc+ TAC T cells were co-cultured with beads at varying ratios and luciferase was measured after 3 days and 4 days of co-culture. The signal fold-difference was determined by dividing the signal produced by positive stimulus by the signal produced by the basal stimulus. The peak signal fold-difference was 8.13, which was measured in cultures consisting of T cells:beads at a 2:1 ratio and a culture time of 96 hours (**Figure 16D**).

The Z-factor is a statistical indicator of data quality for HTS bioassays. In most HTS programs in drug discovery, each compound in a chemical library is evaluated in a single test during primary screening. Therefore, the assay must be highly accurate and sensitive to identify active compounds, or "hits." However, unavoidable sources of error introduce variability and reducing variability improves the reliability of the data. Thus, when designing and validating HTS assays, assessing screening data variability with metrics such as the standard deviation of replicate data is crucial for determining whether an assay can reliably identify hits.

With the optimal seeding density, co-culture period and E:T established, we conducted a Z-factor assay to determine the quality of the proposed proliferation screen. A Z-factor score, determined by the standard deviation and average of the assay controls, categorizes an assay as either ideal (Z-factor = 1), excellent (Z-factor = 0.5-1), marginal (Z-factor > 0 but <0.5) or not useful (Z-factor = 0). The screen's negative controls (rsLuc+ TAC T cells, HER2-Fc beads, and

DMSO) and positive controls (rsLuc+ TAC T cells, HER2-Fc and Costim, and DMSO) were plated at a high number of replicates (N=192) and co-cultured for 96 hours. The Tempest and Multidrop Combi from the CMCB at McMaster were used to dispense T cells, coated beads, and DMSO – as would be the case in the actual HTS. We assessed a number of conditions, including the co-culture period (72- vs 96-hours), incubation period post D-Luciferin addition (10 min vs 40 min) and plate reader (Neotek or Integrated). The Z-Factor peaked at 0.85, following a 96-hour co-culture and measuring luciferase 40-minutes post-addition of D-Luciferin (**Figure 16E, 16F**).

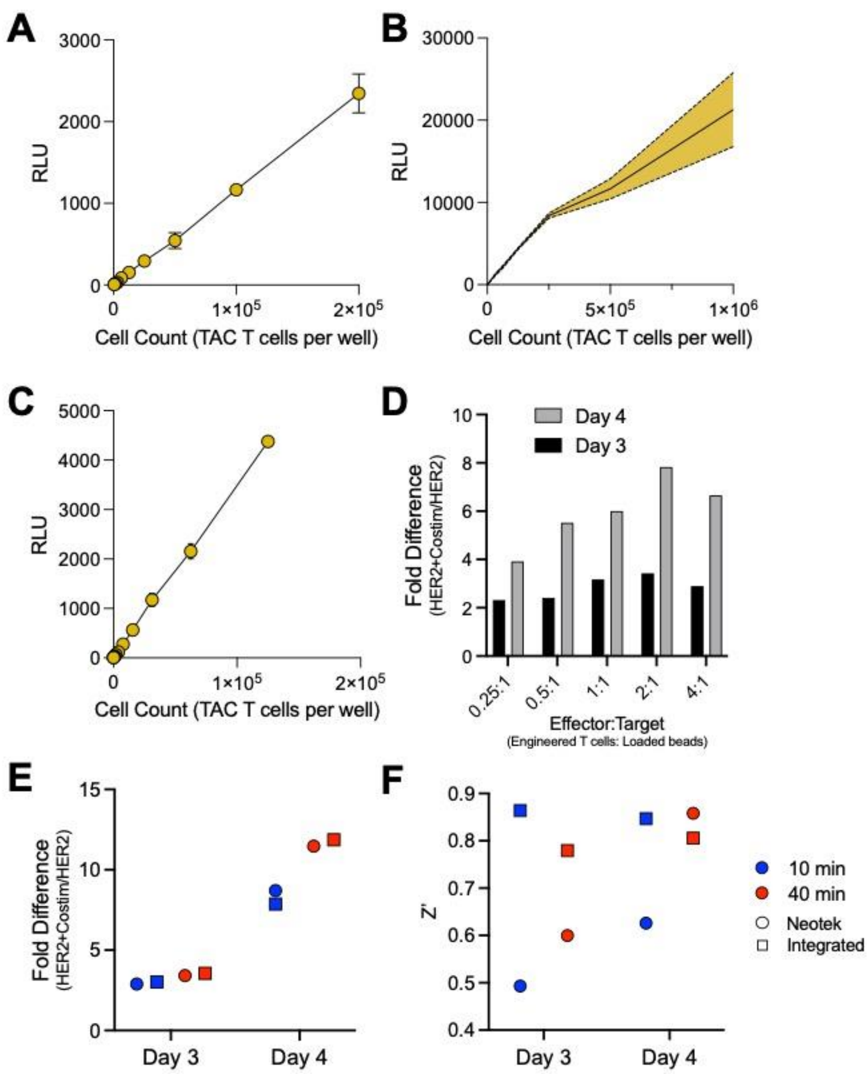

Figure 16. A. Luminescence correlation with rsLuc+ TAC T cell number in a 96-well plate. rsLuc+ TAC T cells were plated at 2x10⁵ per well in triplicate and diluted two-fold eight times over (n=3). **B.** All TAC T cell densities from $1x10^6$ to 50 cells per well fall within a linear range. TAC T cells were plated at 2x106 per well in triplicate and diluted two-fold 12 times over (n=3). **C.** Replotted from $1.5x10^5$ cells per well and below. **D.** TAC T cells were plated at 3.14x104 per well in triplicate and stimulated with protein coated beads at 5 different effector to target ratios for 4 days (n=3). Luminescence of TAC T cells was measured by the addition of D-Luciferin and captured on a plate reader on Day 3, 4, and Day 5. **E.** TAC T cells were plated at $3.14x10^4$ per well in triplicate and stimulated with protein coated beads for 4 days (n=3). Luminescence of TAC T cells was measured by the addition of D-Luciferin and captured on a plate reader on Day 3, and Day 4, at different read times and plate readers. **F.** TAC T cells were plated at $3.14x10^4$ per well in triplicate and stimulated with protein coated beads for 4 days (n=3). Luminescence of TAC T cells was measured by the

addition of D-Luciferin and captured on a plate reader on Day 3, and Day 4, at different read times and plate readers.

To assess the potential utility of the Ferutinin analogues synthesized by the Magolan lab, rsLuc+ TAC T cells were co-cultured with Ferutinin analogues at 10 μM and Her2-Fc coated beads according to the optimized assay conditions. We conducted one screen with one replicate and a subsequent screen with two replicates (**Figure 17A**). The analogues did not demonstrate enhancement to TAC T cell proliferation across all replicates (**Figure 17A**). The results of the screen were challenged with low luminescent signal in replicate one and marginal Z-Factor scores across replicates two and three (**Figure 17B**). In addition, the separation between assay controls were lower than demonstrated during assay optimization (**Figure 17C**). We suspected the rsLuc+ TAC- population may have elicited additional background signal. Moving forward, we elected to employ a bicistronic vector that expresses rsLuc and a HER2-specific TAC to ensure that all TAC+ cells also express rsLuc. This was the same vector used to prepare T cells for the original screen.

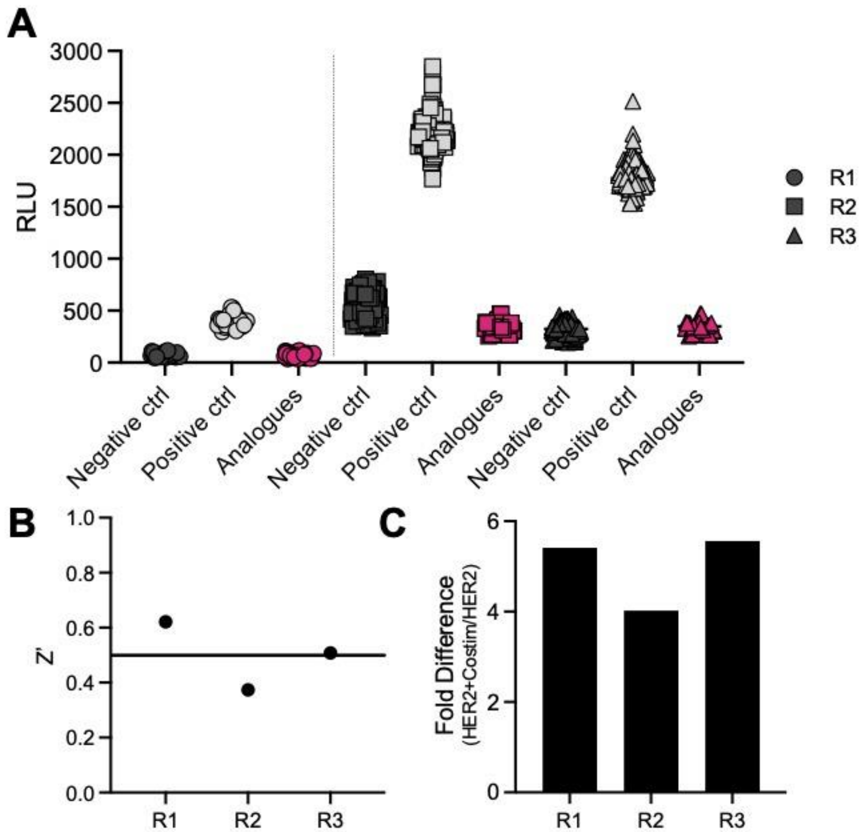

Figure 17. A. TAC T cells stimulated with antigen coated beads and Ferutinin analogues at 10 μM (N=38) in triplicate. **B.** Values represent the fold-difference in luminescence signal between controls (antigen + costim bead/antigen) for each replicate. **C.** Values represent Z' score for each replicate.

We generated a large batch of gRV-based rsLuc+ TAC T cells and validated the linearity of the luciferase reporter system in a 384-well plate (R^2=0.9916) (**Figure 18A, 18B**). To determine the optimal number of T cells per well, we co-cultured varying densities of gRV-based rsLuc+ TAC T cells with loaded beads at 1:1 ratio in a 96-hour proliferation assay. As found with LV-based rsLuc+ TAC T cells, a seeding of 3.13×10^4 TAC T cells per well provided the greatest separation between the positive and negative assay controls (**Figure 18D**). We also validated that a 2:1 ratio (1.57×10^4 beads per well) of T cells to beads provided optimal separation (**Figure 18E**). A Z-Factor score of 0.61 and a 20.4-fold difference between the positive and negative controls gave confidence to the reliability and quality of the assay (**Figure 18F**).

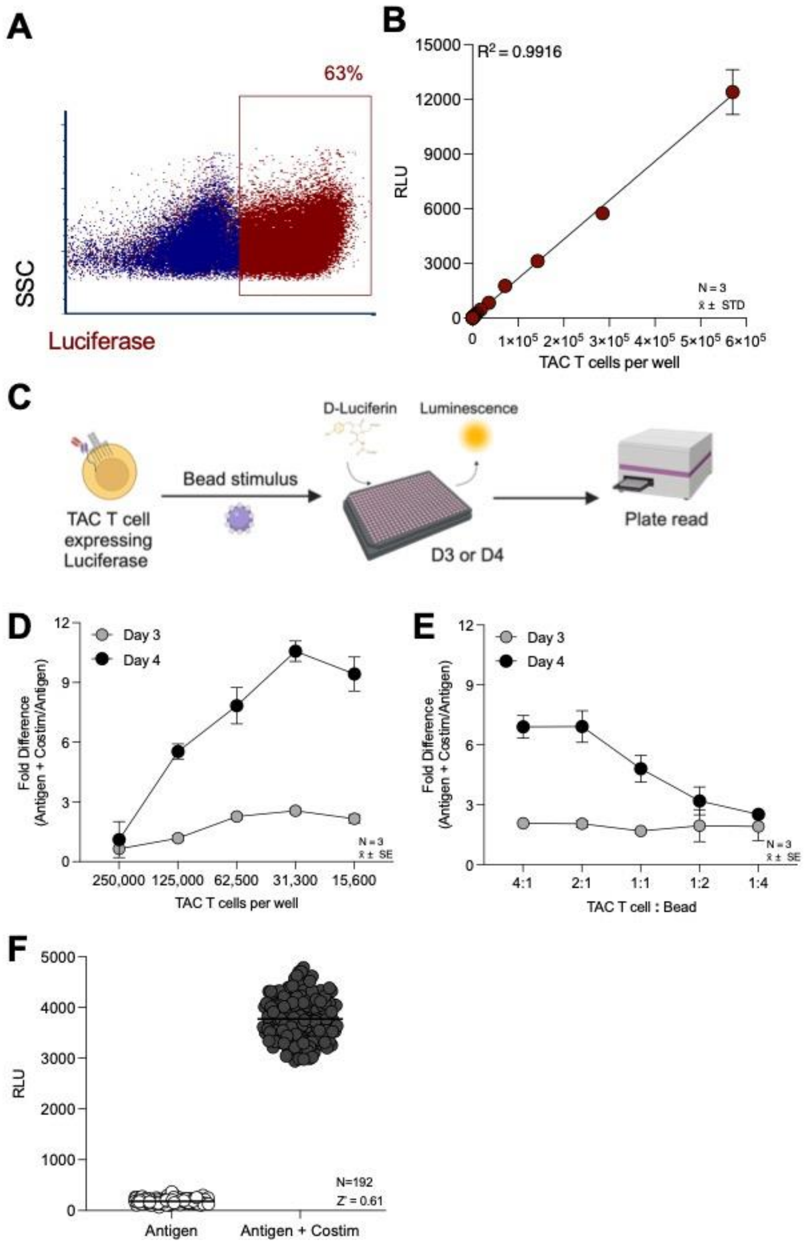

Figure 18. A. Live rsLuc expressing cells, as measured by flow cytometry on day 14 of culture. **B.** Luminescence of rsLuc+ T cells plated at varying cell densities. (N=3). Error bars represent SD. **C.** Schematic of the bioluminescence bead-based proliferation assay. RsLuc+ TAC T cells are stimulated with antigen-on-beads for multiple days, and luminescence is measured by a plate reader on the final day. **D.** rsLuc+ TAC T cells co-cultured with antigen or antigen and costim. on beads. Values represent the fold-difference in luminescence signal between rsLuc+ TAC T cells stimulated with antigen or with antigen/costim. (N=3). **E.** rsLuc+ TAC T cells co-cultured with antigen or antigen + costim. on beads at different ratios. Values represent the fold-difference in

luminescence signal between rsLuc+ TAC T cells stimulated with antigen or with antigen/costim. (N=3). **F.** rsLuc+ TAC T cells co-cultured with antigen or antigen or costim. (N=192).

3.3 Screening the Ferutinin analogue library

We re-screened the Ferutinin analogue library (N=38) and hits from the original HTS screen to serve as positive compound controls (N=12). Across three replicates, the analogues reproducibly failed to enhance luciferase signal (**Figure 19B**). In addition, commercial Ferutinin (see 'prior hits' in **Figure 19B**) increased TAC T cell luciferase activity more than synthesized Ferutinin (see analogues) (**Figure 19C**). This is consistent with observations from early functional experiments where commercial Ferutinin repeatedly outperformed Ferutinin synthesized at McMaster, which reaffirms the likelihood that the activity observed in the screen is due to a contaminant and not Ferutinin (**Figure 19C**). Measures of assay quality, including the Z-Factor and fold-difference between positive and negative controls, were consistent and acceptable across all replicates (**Figure 19D, 19E**). This experiment concluded our investigation into Ferutinin and the Ferutinin analogues.

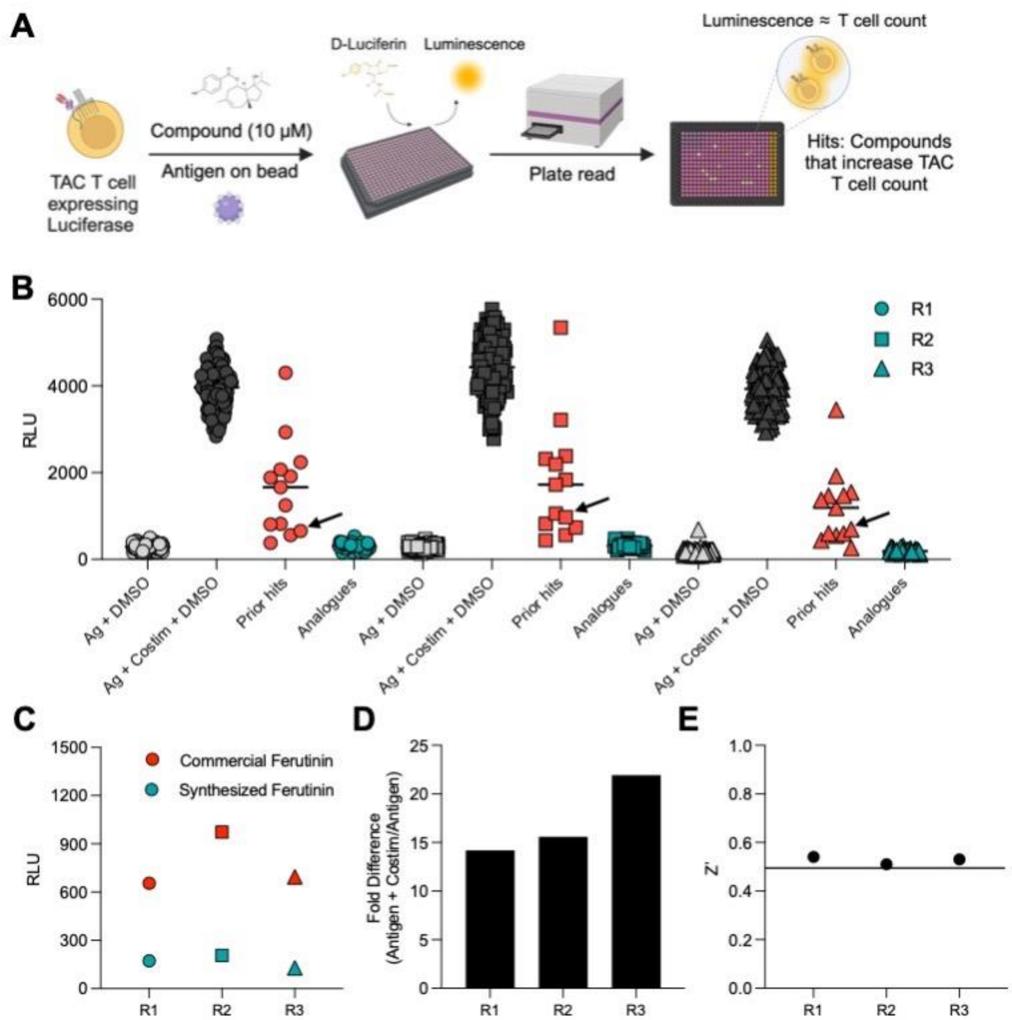

Figure 19. A. Schematic of the automated reporter-based proliferation compound screen. rsLuc+ TAC T cells are co-cultured with antigen coated beads compounds at 10 µM for 4 days. Luminescence is measured by a plate reader as an indirect measure of TAC T cell number. **B.** Relative luminescence of rsLuc+ TAC T cells after 4-days of stimulation from antigen-coated beads and compound or antigen + costim coated beads (N=3). Commercial Ferutinin annotated with arrows. **C.** Relative luminescence of rsLuc+ TAC after 4-days of stimulation with antigen on bead and Ferutinin from different sources (N=3). **D.** Values represent the fold-difference in luminescence signal between rsLuc+ TAC T cells stimulated with antigen or with antigen/costim. (N=32). **E.** Z-Factor score of each assay plate.

3.4 High throughput screening bioactive compound libraries

Screening 11,428 molecules from the Bioactive 2 Library

We remained interested in the utility of small molecules as costimulatory agents for engineered T cells. Since the bioluminescence proliferation assay was developed based on the original HTS, we sought to re-purpose our assay and a screen a large volume of chemical compounds. Using the optimized assay parameters, we screened a large compound library (11,428 molecules) ("Bioactive 2 Library") with known biological activity from the CMCB. Compounds were screened at a standard concentration (10 μM) with the integrated HTS instruments, including the Echo 650 Series Acoustic Liquid Handler, Tempest® Liquid Dispenser and Multidrop Combi nL to dispense compounds, cell culture reagents, and D-Luciferin, respectively. Compound library plates (N=37) containing master stocks were dispensed in duplicate, resulting in a total of 74 assay plates. We required a large volume of rsLuc+ TAC T cells for each assay plate, and thus, screened 10 assay plates per run to minimize the risk of error. The assay plates included a high number of negative and positive control replicates (N=32) to monitor plate to plate variability. A large batch of gRV-based rsLuc+ TAC T cells were generated from two manufacturing runs from the same donor.

We normalized the relative luminescence value of each experimental well to the interquartile mean (IQM) of the assay plate. The IQM is the average of the middle 50% of rank ordered values. We selected this normalization approach as it considers plate-to-plate variation and positional effects due to bias in columns, rows or wells, such signal spillover in wells adjacent to positive controls (Mangat et al., 2014). When we defined hits as equivalent to or greater than three standard deviations above the IQM of the assay plate, we identified 869 hits from Bioactive 2 library plates 1-36 (**Figure 20A, 20B**). While HTS for drug-like compounds typically yield hit rates in the range of 0.01 to 1% (Dreiman et al., 2021; Woodward et al., 2006), the high hit rate from the Bioactive 2 library screen (7.6%) was not unexpected as the library is enriched for cell permeable and biologically active compounds. Low variability across replicates and high Z-Factor score values demonstrate the reliability of the screen results (**Figure 20C, 20D**). Moreover, many of the hits which demonstrated the greatest enhancement to rsLuc+ TAC T cell expansion have been previously characterized for their immunomodulatory activity. Many of the top hits also share the same target and/or fall in the same class of chemicals based on their biological function. For instance, within the top 30 hits, 13 compounds are immunomodulatory (IMiDs) drugs, 2 are Protein Kinase C (PKC) effectors, and 3 are inhibitors of apoptosis (IAP) antagonists – all classes of compounds which have demonstrated costimulatory activity (Li et al., 2023; Marro et al., 2019; Afsahi et el., 2023) (**Figure 20E**).

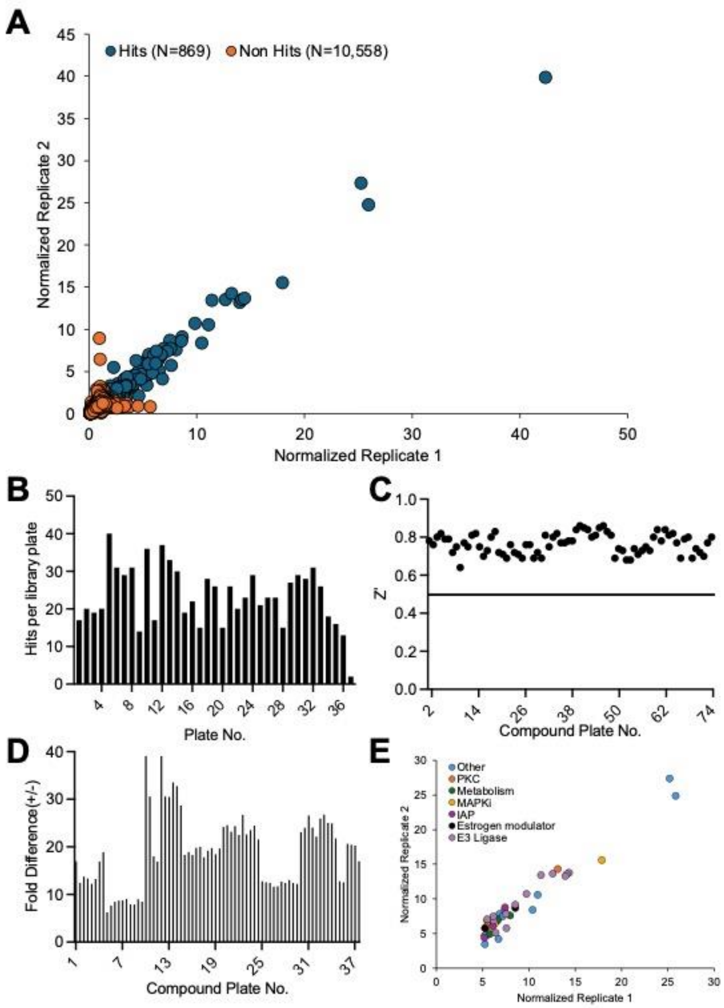

Figure 20. A. Replicate plot of the relative luminescence of each sample normalized to the interquartile mean of the respective assay plate. **B.** The number of hits per Bioactive 2 Library plate. **C.** The Z-Factor score for each assay plate. **D.** The luminesce signal fold difference (rsLuc+ TAC T cells stimulated with DMSO and either antigen + costim or antigen). **E.** The chemical class, based on biological activity, of the top 40 hits.

Table 2. Top 30 compounds from the Bioactive 2 Library HTS and their corresponding chemical family.

Compound	Family	Known immunomodulatory activity
DMT-dC(bz) Phosphoramidite	Other	
20-Deoxyingenol	Other	Enhances NK cell degranulation and cytokine (INF-γ) secretion (Szymański, 2011)
Soyasaponin Ab	Other	Activates NF-κB signalling in murine macrophages (Shen et al., 2023).
MAPK13-IN-1	Kinase Inhibitor	
Pomalidomide	Ligand for E3 Ligase	
Avadomide	Ligand for E3 Ligase	
Iberdomide	Ligand for E3 Ligase	
Ingenol-5,20-acetonide-3-O-angelate	PKC activator**Error! Reference source not found.**	
PF-4618433	Kinase Inhibitor	
Thalidomide-NH-CH2-COOH	Ligand for E3 Ligase	
8-Geranyloxypsoralen	Other	
Endoxifen (E-isomer hydrochloride)	Kinase inhibitor (PKC); Estrogen receptor modulator	Estrogen receptor signaling has been linked with T cell expansion and persistence (Arghiani, 2014).
Thalidomide-O-C8-Boc	Ligand for E3 Ligase	
BAY 60-6583	Other	Increases cytokine production in CAR T cells (Tang et al., 2021).
Sirtuin modulator 1	Other	
QS 11	Other	
Cbl-b-IN-1	Ligand for E3 Ligase	
3-(4-Hydroxy-1-oxoisoindolin-2-yl)piperidine-2,6-dione	Ligand for E3 Ligase	
p38-α MAPK-IN-1	Kinase Inhibitor	
Lenalidomide-Br	Ligand for E3 Ligase	
LCL161	SMAC Mimetic	
Deltorphin I(TFA)	Other	
FKBP12 PROTAC RC32	Ligand for E3 Ligase	
TD-106	Ligand for E3 Ligase	
TMX-4100	Other	
CUDC-427	SMAC Mimetic	
TRPV4 agonist-1 free base	Other	Agonist to TRPV4, which regulates Ca^{2+} signalling in T cells (Acharya, 2023).
Endoxifen (Z-isomer hydrochloride)	Kinase inhibitor (PKC); Estrogen receptor modulator	Estrogen receptor signaling has been linked with T cell expansion and persistence (Arghiani et al., 2014).
Allosteric WNK Kinase Inhibitor	Kinase Inhibitor	

Screening 3840 molecules from the Bioactive A Library

We also re-screened the original HTS (3840 molecules) library ("Bioactive A") to assess for additional and/or different hits when using the modified screening parameters and an alternative normalization approach. Similar to the Bioactive 2 library screen, compounds from 12 library plates were screened at 10 μM in duplicate. The screen, which was completed in two runs, identified 149 hits from all library plates but primarily from library plate one (**Figure 21A**). The original HTS found 25 hits that also primarily originated from library plate one and generally repeated in the re-screen (**Figure 21B**). In particular, 22 compounds that were hits in the original screen re-emerged as hits our re-screen. We did not pursue further investigation with Bioactive A library as most hits did not pass subsequent validation assessments (see Appendix for **Table A2**).

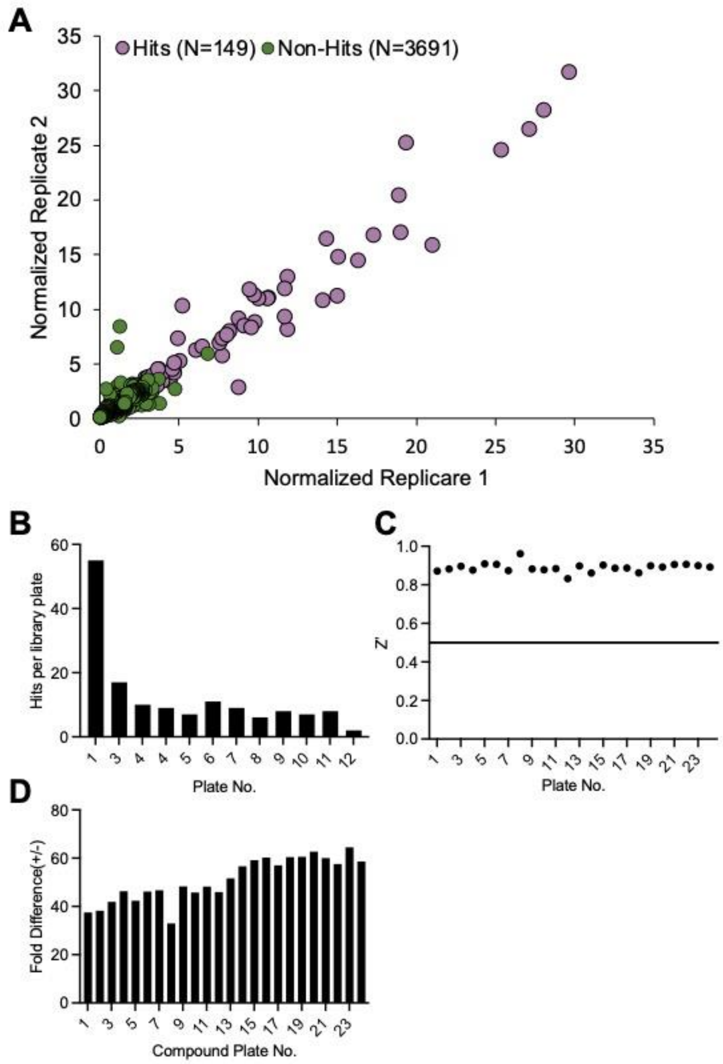

Figure 21. Rescreen of Bioactive A Library. **A.** Replicate plot of the relative luminescence of each sample normalized to the interquartile mean of the respective assay plate. **B.** The number of hits per Bioactive 2 Library plate. **C.** The Z-Factor score for each assay plate. **D.** The luminesce signal fold difference (rsLuc+ TAC T cells stimulated with DMSO and either antigen + costim or antigen).

3.5 Secondary screening to validate HTS hit activity

Secondary Assay - Stage I: Validating Compound Specificity

Following the primary screen (HTS), a series of secondary assays are used to validate the activity of hits and determine compound properties, such as the dose-response (Hughes et al., 2011; Thorne et al., 2010). Demonstrating activity in secondary experiments will lead to compound assessment in robust, medium throughput *in vitro* and *in vivo* assessments of the lead candidate(s) (Hughes et al., 2011; Thorne et al., 2010).

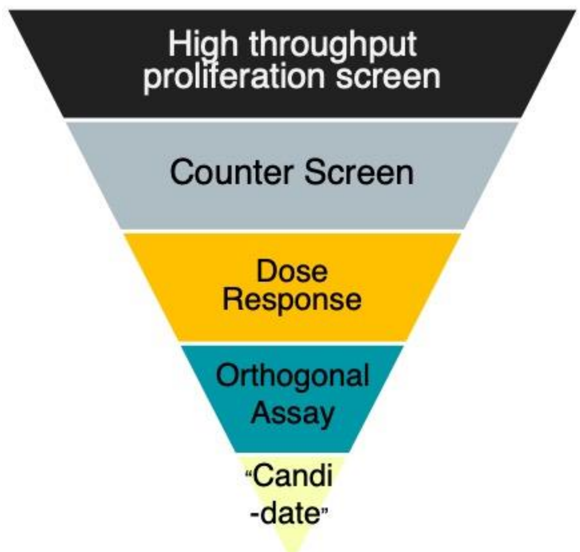

Figure 22. The HTS hits were assessed in a series of secondary assessments. Only the hits that demonstrate activity in all secondary assessments are categorized as 'candidates.'

Thus, we evaluated the HTS actives in a secondary assessment pipeline that included a counter screen, dose response assay and orthogonal assay to identify robust and reproducible small molecule candidate(s) with costimulatory activity (**Figure 22**). The counter screen serves to distinguish false positives from compounds that are genuinely active against the target but not for determining the presence of biological activity (Thorne et al., 2010). Since luminescence can be elicited through mechanisms independent of T cell proliferation, we first sought to exclude hits that increased luciferase activity independent of TAC-based activation. From the Bioactive 2 HTS to stage one of the secondary assessments, we advanced 297 hits that increased luminescence activity greater than or equivalent to two-fold of the interquartile mean.

To exclude false positives, we compared the luciferase activity of gRV-based rsLuc+ TAC T cells in the presence of hits and its target antigen (HER2) or irrelevant antigen (BCMA) after 4 days. The relative luminescence of each well was normalized to the negative control mean of the respective assay plate. When we defined hits as greater than or equivalent to three standard deviations above the negative control mean, we found that 129 of the 297 compounds re-emerged as hits (**Figure 23A**). In addition, very few compounds elicited luciferase activity independent of TAC-based activation (**Figure 23B**). We repeated this assessment with T cells generated from a different donor, which saw similar results – few false positives and 161 of the 297 compounds re-emerged as hits, most of which (N=116) were also hits in the first counter-screen (**Figure 23C**).

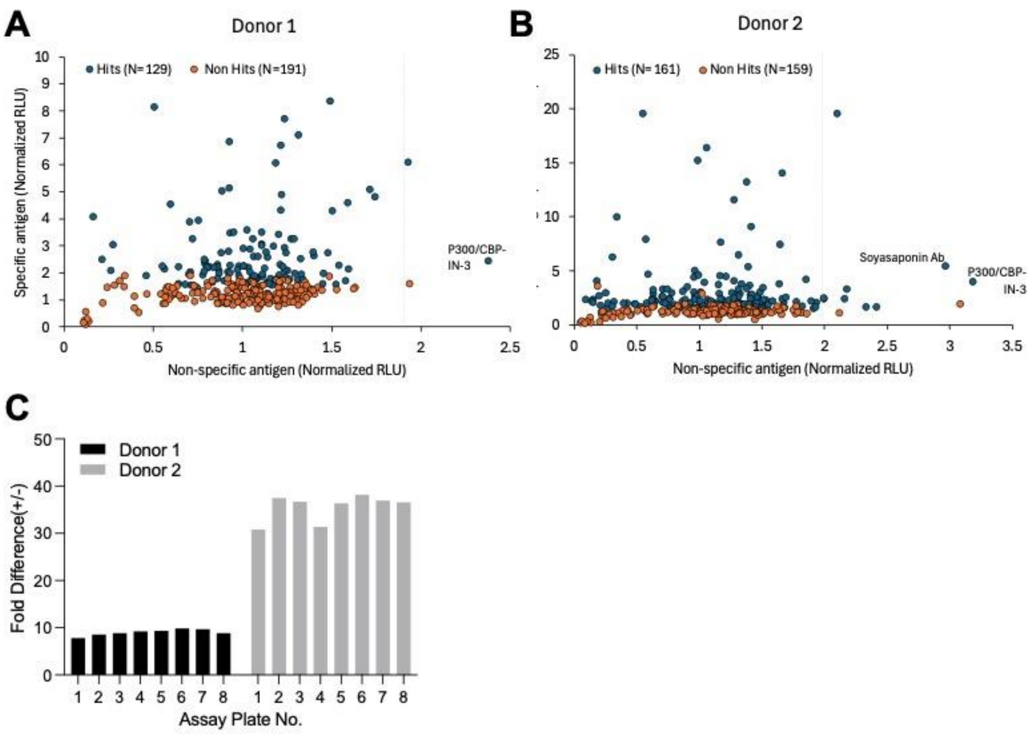

Figure 23. A. Normalized RLU of gRV-based rsLuc+ TAC T cells when stimulated with HER2 (y-axis) or BCMA (x-axis) after 4 days. Data normalized to the negative control mean. Technical replicate not shown. Hits that elicit high (≥ 3-fold x̄neg ctrl) non-specific activity are annotated. **B.** Donor repeat. Normalized RLU of gRV-based rsLuc+ TAC T cells when stimulated with HER2 (y-axis) or BCMA (x-axis) after 4 days. Data normalized to the negative control mean. Technical replicate not shown. Hits that elicit high (≥ 3-fold x̄neg ctrl) non-specific activity are annotated. **C.** The luminesce signal fold difference (rsLuc+ TAC T cells stimulated with DMSO and either antigen + costim or antigen) across assay plates.

Secondary Assay - Stage II: Determining the Dose Response

We next sought to determine the optimal dose of Bioactive 2 Library hits as the dose used for the screen (10 μM) may be on the higher end of activity. For this reason, we elected not to exclude compounds that were either categorized as 'non-hits' or 'false positives' and advanced all 297 Bioactive 2 Library hits from stage one to stage two of the secondary assessments. gRV-based rsLuc+ TAC T cells from a unique donor were co-cultured with antigen-coated beads and 297 hit compounds at 11 concentrations, ranging from 10 μM down to 10 nM in two-fold serial dilutions, for 4 days. The conformation of the assay plate permitted fewer technical replicates of the negative (N=16) and positive (N=16) controls than the HTS and stage one of the secondary assessments. Moreover, we seeded technical replicates on the same assay plate.

The relative luminescence of each well was normalized to the negative control mean of its respective assay plate. 61 compounds demonstrated activity greater than or equivalent to two-fold of the negative control mean at one, or more, of the tested concentrations. 27 of these compounds increased rsLuc+ TAC T cell luciferase activity at 4 or more of the 11 tested concentrations, with some being effective at picomolar doses (**Figure 24A**). Many of the 27 compounds fall into chemical categories with characterized T cell enhancing activity, including PKC effectors (Ingenol 3,20-dibenzoate, Ingenol Mebutate); IMiDs/E3 ubiquitin ligase PROTACs/CelMods (Iberdomide, TD-106, BTX161, Thalidomide, ALV2, Lenalidomide, Pomalidomide, Cbl-b-IN-1); and IAPs (CUDC-427, GDC0152, LCL161). These also included various kinase inhibitors (c-Fms-IN-10, TGFβRI-IN-3, PF-4618433, Regorafénib N-oxyde (M2)) and other chemical classes (BAY 60-6583, Kansuinine A, TMX-4100, Emricasan, P300/CBP-IN-3). The chemical classes with well-characterized for their T cell enhancing activity (i.e., PKC activators and IMiDs) delivered the greatest boost to rsLuc+ TAC T cell luciferase activity and were active across almost all doses (data not shown). Although we observed variability across technical replicates (see difference in range between the x- and y-axis in **Figure 24A**) and atypically high signal from the positive controls in the dose-response assay, we were confident with the reliability of the results because of high Z-scores and reproducible hits (**Figure 24B, 24C**). Some of the more potent hits from the HTS and stage one, including DMT-dC(bz) Phosphoramidite, did not reveal activity in stage two.

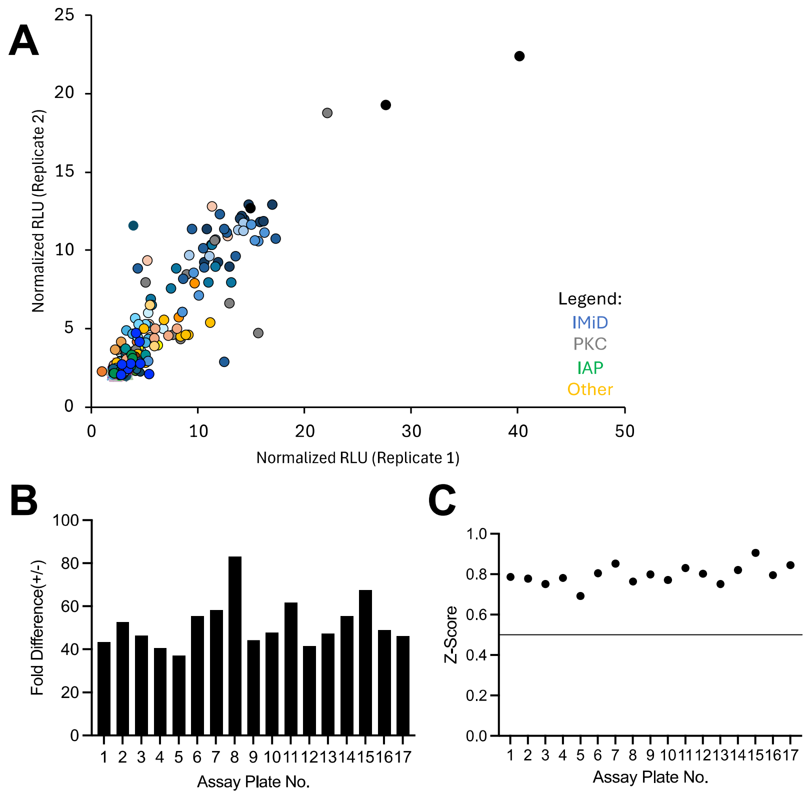

Figure 24. A. Normalized RLU of gRV-based rsLuc+ TAC T cells co-cultured with hits (N=61 compounds; N=236 conditions) at varying concentrations and antigen coated beads for 4 days. Colours represent each compound (multiple doses per compound). Select chemical classes are annotated by colour scale: IMIDs/blue; PKC/grey scale; IAP/green; Other/orange. **B.** The luminesce signal fold difference (rsLuc+ TAC T cells stimulated with DMSO and either antigen + costim or antigen). **C.** Z-Factor scores.

Secondary Assay - Stage III: Multi-donor CellTraceTM Violet Proliferation and Survival

We then sought to complete the validation series with an orthogonal assay, which analyzes the same biological outcome as tested in the primary assay, but uses independent assay readouts (Auld & Inglese, 2018). We validated the activity of select compounds using a dye dilution-based proliferation and survival experiment that provides a direct readout of TAC T cell number. From stage two to stage three, we advanced 7 of the 61 hits based on the following criteria that they are among the top 20 compounds and have demonstrated little to no immunomodulatory activity in the literature (**Table 3**).

Table 3. Compounds advanced to Stage Three of the Secondary Assessments.

Compound Name	Optimal Dose (μM)	Bioactivity
TGFBR1-IN-3	10	TGFβRI-IN-3 inhibits TGFβR1 with selectivity against MAP4K4.
BAY 60 6538	10	BAY 60-6583 is a potent and high-affinity agonist of adenosine A2B receptor.
ML327	10	ML327 is a blocker of MYC.
Emricasan	5	Effective and irreversible pan-caspase inhibitor.
CK1-IN-1	2.5	Casein kinase 1 inhibitor, with an IC50s of 73 nM for p38σ MAPK.
Desacetylcinobufagin	5	Natural product, shows potent activities against Hela and A375 cells *in vitro*.
8-Geranyloxypsoralen	10	Inhibits α^2-secretase (BACE1) activity.

Two distinct PBMC donors were used to generate gRV rsLuc+ TAC T cells. Multi-donor gRV rsLuc+ TAC T cells stained with CellTrace™ Violet were co-cultured with the select compounds at their optimal dose (as determined the by the dose-response experiment) and antigen-loaded beads or media at a 1:1 ratio for 4 days. We included biological replicates to capture potential donor dependent effects. Unlike luminescence-based proliferation assays, we seeded $5x10^5$ TAC T cells per well in a 12-well clear bottom plate. On day 4, we stained the co-cultures with fluorophore conjugated antibodies to tag markers, CD4 and CD8, and measured their surface expression and CellTrace™ Violet using flow cytometry. We monitored cell division by tracking CellTrace™ Violet dilution, which found that BAY 60 6583 and 8-Geranyloxypsoralen resulted in robust TAC T cell proliferation, where some cells underwent four division cycles (**Figure 25A**). With the exception of Desacetylcinobufagin which elicited negligible TAC T cell proliferation, in order from greatest to least, Emricasan, TGFBR1-IN-3, ML327 and CK1-IN-1 resulted in some TAC T cell proliferation (albeit the ranking may slightly differ donor-to-donor) (**Figure 25A**).

We also quantified the number of live cells at the end of culture by measuring the ratio of cells to counting beads. Results were normalized to their respective negative control to permit comparison between donors. In line with CellTrace™ Violet proliferation curves, BAY 60 6583 and 8-Geranyloxypsoralen enhanced live cell count compared to the negative control in the presence of their target (**Figure 25B**). We saw see these effects independent of donor, albeit the enhancement to donor 1 was greater than to donor 2 generated TAC T cells. All other compounds but ML327 enhanced the number of live cells generated from donor 1 and not donor 2 in the order from greatest to least: Emricasan, TGFBR1-IN-3, CK1-IN-1 and Desacetylcinobufagin (**Figure 25B**). ML327 resulted in fewer live cells than DMSO control, independent of T cell donor and with or without stimulus (**Figure 25B, 25C**).

We then sought to assess the toxicity of compounds by measuring their effect to TAC T cell survival in the absence of a stimulus. The compounds that provided the most benefit to TAC T cell survival, BAY 60 6583 and 8-Geranyloxypsoralen, were toxic to T cells in the absence of stimulus in a donor independent manner (**Figure 25B**). Among the less potent compounds, TGFBR1-IN-3 but not Emricasan, CK1-IN-1 or Desacetylcinobufagin resulted in fewer TAC T cells than DMSO control (**Figure 25B**).

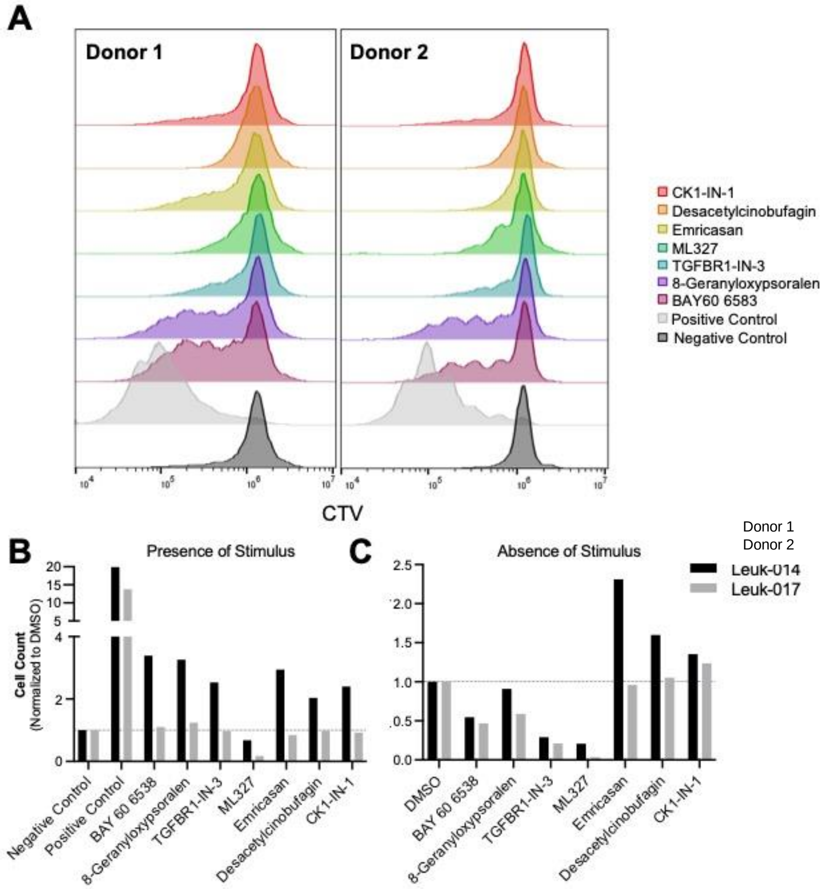

Figure 25. A. Live T cell proliferation was measured by CellTrace™ Violet dye-dilution following 96-hour co-culture with Antigen-loaded beads and compounds at optimal doses. **B.** Live cell count following 96-hour co-culture with Antigen loaded beads and compound at optimal doses. Live T cells were enumerated with counting beads, as measured Live cells by Flow Cytometry. **C.** Live cell count following 96-hour co-culture in the absence of antigen loaded beads and compound at optimal doses. Live T cells were enumerated with counting beads, as measured Live cells by Flow Cytometry. Data generated by Ariya Shiwram.

4.0 DISCUSSION

Commercial Ferutinin provides greater functional benefit than Ferutinin synthesized at McMaster

We investigated the utility of small molecules as agents to costimulate TAC- and DAP12 SAR-engineered T cells. Our first approach sought to assess the impact of Ferutinin and Ferutinin analogues on engineered T cell function. Our comparison of Ferutinin from different sources revealed that Ferutinin obtained from commercial sources could enhance cytotoxic, proliferative and survival outcomes for TAC and DAP12 SAR T cells whereas pure Ferutinin synthesized at McMaster could not. When we interrogated potential differences in the molecular composition, ^{1}H-NMR and mass spectrometry studies identified an unknown structure in Ferutinin from commercial vendors, suggesting that the active component was not Ferutinin itself but rather an undefined contaminant.

Although most compounds are stable in DMSO at sub-zero degree centigrade, some are susceptible to degradation over long storage periods and multiple freeze-thaw cycles (Engeloch et al., 2009; Kozikowski et al., 2003). For this reason, we suspected the presence of a contaminant and/or degradation of Ferutinin given that P2101 and P2205 were stored in DMSO for 2 years and 6 months at time of analysis, respectively. Our collaborators conducted Soxhlet extractions to obtain potential contaminants and co-cultured Ferutinin with DMSO at different conditions to generate degradation products, none of which provided enhancement to DAP12 SAR or TAC T cell function. It is possible a 7-day incubation period was insufficient to appreciably degrade Ferutinin where previous studies used a 7-week or longer period to assess DMSO caused degradation (Kozikowski et al., 2003). Likewise, it is possible that additional rounds of extraction were required to obtain a product that elicited sufficient change to T cell activity.

Ferutinin analogues intermittently augment DAP12 SAR and TAC T cell function

Assessments of the Ferutinin analogues found that 2209, 2210 and 2211 enhanced DAP12 and TAC T cell tumour growth suppression, T cell expansion and T cell survival in a number of experiments. Our studies established that the presence of *p*-hydroxybenzoate moiety was required for activity when we compared Ferutinin with the parent compound Jaeshkeanadiol/2101 (without *p*-hydroxybenzoate) (data not shown). For compound 2209, we suspect that inserting the two methylene units between the benzene ring and the carbonyl group subsequently allowed for free rotation of the p-hydroxy moiety in space. We speculate that this could minimize unfavourable steric interactions by allowing the benzene ring to more freely move around compared to its parent molecule and/or permit the molecule to adopt a more optimized orientation to bind to its target and elicit greater activity. For analogues 2210 and 2211, changing the OH to F or Cl could lead to changes in shape, size, hydrogen bonding ability, electron distribution or through another mechanism that conferred favourable biological activity. The subsequently generated analogues provided some but unappreciable enhancement to DAP12 SAR and TAC T cell tumour growth suppression. This outcome was not unanticipated as analogue development requires multiple rounds of lead-to-drug iteration before lead candidates are advanced to *in vivo* and clinical testing (Jorgensen, 2004; Ripphausen et al., 2010).

The results with 2209, 2210 and 2211 notwithstanding, repeat experiments assessing the Ferutinin analogue library could not convincingly establish their functional effect on tumour growth suppression due to inter-experimental variation. Moreover, examination of all Ferutinin analogues on engineered T cell proliferation using flow cytometry-based lab protocols is an arduous approach given the extensive conditions we aimed to include: synthetic receptors, antigen-binders, tumour targets, stimuli and T cell donors. We recognized that a higher throughput biological assessment would enable evaluation of the Ferutinin analogue library in a variety of conditions and offer several advantages: (i) rapidly evaluate numerous conditions in parallel; (ii) automation with minimal manual handling to reduce interexperimental variability; (iii) proven method for identifying compounds that enhance TAC T cell number. Therefore, we sought to develop an automated reporter-based proliferation assay based on the HTS screen that originally identified Ferutinin.

Luciferase possesses distinct advantages from fluorescence

As a first step towards the development of the HTS screen, we compared reporters to serve as indirect measures of T cell numbers. A comparison between the fluorescent mStrawberry protein and red-shifted firefly luciferase (rsLuc) reporter systems revealed distinct advantages to luciferase. It has superior resolution because luminescence is brighter and is exclusively produced by live cells (Fan & Wood, 2007). In addition, we observed that luminescence was a better correlate of engineered T cells than fluorescence. Although the original HTS used luciferase engineered TAC T cells, we chose to explore the impact of Ferutinin analogues on DAP12 SAR T cells in alignment with the lab's research direction.

DAP12 SAR T cells are amenable to a Luciferase reporter system

We found that transducing T cells with a single vector encoding both the DAP12 SAR and rsLuc was superior to co-transducing with two vectors encoding DAP12 SAR and tNGFR rsLuc. Two key technical issues emerged from co-transduction: (1) DAP12 SAR expression was reduced and (2) the presence of T cells that expressed rsLuc+ without the DAP12 SAR meant that some luciferase activity was emerging from cells that could not engage antigen and, thus, yields unwanted background signal. Although functional evaluation confirmed both rsLuc+ DAP12 SAR T cells performed comparably to WT DAP12 SAR T cells, we chose to screen T cells manufactured using the single vector that co-expressed the DAP12 SAR and luciferase given higher SAR expression and superior rsLuc reporter efficacy.

To confirm that the DAP12 SAR-engineered T cells could be used in the HTS set up, we assessed the proliferative response of rsLuc+ DAP12 SAR T cell to polystyrene beads loaded with either antigen alone or antigen and costimulatory ligands. Unlike TAC T cells, the rsLuc+ DAP12 SAR T cells failed to respond robustly to beads loaded with antigen and costimulatory ligands. Numerous optimization steps were employed to assess whether the densities of the antigen and/or costimulatory ligands could influence the outcome, but none could promote significant expansion, which indicated that the DAP12 SAR T cells may not be suitable for this HTS set up. Indeed, a direct comparison between DAP12 SAR T cells and TAC T cells confirmed robust proliferation of TAC T cells when stimulated with antigen and costimulatory ligands on bead and lack of proliferation by the DAP12 SAR T cells.

While we do not have an explanation for the differences in proliferation, it may be due to differential expression of the receptors for the costimulatory ligands (CD2, CD28) or it may be a consequence of differential requirements for costimulation. For example, DAP12 SAR T cells may be preferentially activated by other costimulatory receptors, such CD40, ICOS, OX40, or 4-1BB. Further investigation is required to elucidate the mechanisms underpinning this difference.

Engineering TAC T cells with Luciferase

Given that the DAP12 SAR T cells did not appear suitable for the HTS, we elected to reboot the assay with the TAC T cells that were previously established for use in a reporter-based screen. The rsLuc+ TAC T cells employed in the original HTS were engineered using gamma retrovirus (gRV), whereas the rsLuc+ DAP12 SAR T cells were engineered using lentivirus (LV). Due to technical challenges obtaining optimal receptor expression and engineered T cell yields with the gRV protocol, we generated LV-based rsLuc+ TAC T cells. To bypass cloning procedures, we co-transduced with existing vectors. Although co-transduction hampered TAC expression, LV-based rsLuc+ TAC T cells were functionally comparable to WT TAC T cells and demonstrated an effective rsLuc reporter system. When we assessed the LV-based rsLuc+ TAC T cell response to bead-based assay controls, in line with historic observations, TAC T cells robustly active when stimulated with antigen and costimulatory and non-responsive to antigen alone.

When seeded in a 384-well plate, the rsLuc reporter system demonstrated less variability in luminescent signal at lower cell densities. We selected an 'optimal' seeding concentration of 3.14×10^4 TAC T cells per well because it is (i) well within the linear range; (ii) experimentally practical; (iii) comparable to the seeding density used in the original HTS. Our 384-well plate assays which assessed for optimal bead: TAC T cell ratio and incubation period, found that a 2:1 relationship and 4 days of co-culture maximized the signal difference between negative and positive controls. This contrasts with the original HTS parameters that employed a 1:1 ratio and 3-day incubation period. The original HTS did not assess ratios greater than 1:1 or optimize the incubation period. Thus, the updated screen employed slightly modified parameters, which seemed to yield an improved signal: noise.

Statistical validation of the assay quality confirmed the efficacy of the optimized controls, as measured by the Z-Factor score test. Having established the assay parameters, the first run of the Ferutinin analogue screen was executed using HTS equipment. In contrast to optimization assays, low levels of signal were detected across both controls and experimental conditions. We suspected user error in the dispensing of reagents. A subsequent run with two replicate plates detected higher signal but no activity by TAC T cells treated with the Ferutinin analogues. This run failed to conclusively report Ferutinin analogue activity due to suboptimal Z-Factor scores across both replicates. We considered the possibility of a bystander effect from a large subpopulation of non-transduced cells (>40%) and a smaller but relevant population of receptor- rsLuc+ cells that could skew the reporter information intended to detect receptor+ cells. The discrepancy between the optimization assays and HTS could be attributed to different TAC and rsLuc expression levels and differences in the frequencies of TAC-positive/rsLuc-positive and TAC-negative/rsLuc-positive cells in the various assays. These are the same caveats that emerged earlier when we considered co-transduction of viruses expressing the DAP12 SAR and rsLuc. Thus, we chose to use a single vector approach where both the TAC and rsLuc are expressed from the same vector.

Therefore, the next stage of the HTS development employed gRV-engineered rsLuc+ TAC T cells.

Screening the Ferutinin analogue library

The assay parameters were confirmed with gRV-based rsLuc+ TAC T cells and the Z-Factor scores confirmed the utility of the assay, so we proceeded to evaluate the Ferutinin analogues. As observed in the low throughput assays, commercial Ferutinin reproducibly augmented TAC T cell number more than Ferutinin synthesized at McMaster; however, none of the Ferutinin analogues offered any evidence of enhanced T cell proliferation. Altogether, our findings suggest that Ferutinin was a false hit, with an uncharacterized entity likely responsible for affecting change in engineered T cell function. While the reason(s) for variable outcomes across experiments assessing Ferutinin analogues remains unclear, false hits in HTS are not atypical. Previous reports show multiple freeze/thaw cycles can profoundly affect the integrity of a compound, particularly for those insoluble in DMSO, due to sample degradation or precipitation (Kozikowski et al., 2003). The hygroscopic nature of DMSO can affect compound concentration, solubility and/or degradation at room temperature (Kozikowski et al., 2003). Indeed, 12 months after storage, one report assessing 7200 compounds stored in DMSO at ambient conditions found that the probability of observing a compound in DMSO was 52% after one year (Kozikowski et al., 2003).

High throughput screening bioactive compound libraries

Given that we had rebooted the HTS screen with a robust Z-Factor score, we elected to revisit our original HTS of the Bioactive A Library and evaluate a new chemical repository ("Bioactive 2") containing 11,427 biologically active compounds. This Bioactive 2 library was selected for three reasons: (i) it was recently acquired in February 2023, and therefore, less likely to contain degradation products or contaminants that may be present in older libraries with an extended history of freeze-thaw cycles and compound transfers; (ii) the library is enriched for natural products, FDA-approved drugs and clinical compounds that are cell-permeable, and therefore, more likely to demonstrate biological activity than non-curated chemical libraries; (iii) it has only a 5% overlap with the chemical library assessed in the original screen.

We identified nearly 3 times the hits in the Bioactive A library re-screen (N=149) compared to the original screen (N=30). It is likely we picked up on additional less potent actives due to an additional day in culture and a different data analysis approach, as the previous screen normalized the RLU values to their respective negative and positive controls. Among the more potent hits, we recapitulated the same screen outcomes, where 22 compounds were the exact same even though the hits did not pan out in the original secondary assessments. We identified 869 hits from the Bioactive 2 library screen. Among the more potent hits, we found that many compounds were from the same chemical classes, some of which have been characterized for their costimulatory activity, such as IMiDs, PKC modulators, and IAP effectors.

IMiDs, also known as Cereblon E3 ligase modulators, are a class of drugs that possess anti-multiple myeloma and costimulatory properties. These drugs mediate Cereblon-dependent engagement and degradation of transcription factors, Ikaros and Aiolos, resulting in the de-repression of the IL-2 gene locus (Costacurta et al., 2021). Following CD3 ligation, IMiDs stimulate T cell proliferation and IFN-γ production and have been found to activate CD28 downstream signalling via NF-kB (Corral et al., 1999; LeBlanc et al., 2004). Reports support the costimulatory activity of various IMiDs, most notably thalidomide (Corral et al., 1999), lenalidomide (Davies et al., 2001), Iberdomide (Amatangelo et al., 2018), and pomalidomide (Schafer et al., 2003). The combination of anti-multiple myeloma and costimulatory properties have formed the rational of an Exploratory Phase 1/2 trial investigating the safety, tolerability and efficacy of anti-BCMA CAR T cell therapy in combination with Iberdomide in Replased/Refractory Multiple Myeloma patients (NCT04855136).

Phorbol esters ("PKC modulators") were also among the top hits of the HTS. Phorbol esters are natural products that mimic diacylglycerol (DAG) and bind to Protein Kinase C (PKC), which is downstream of TCR signaling. PKC is from a family of enzymes involved in signalling pathways that specifically phosphorylates substrates at serine/threonine residues, influencing a variety of cellular events such as cell proliferation and the regulation of gene expression (Wang et al., 2012). TCR activation and costimulation by the native CD28 receptor triggers PKC-θ catalytic activation and translocation to the immunological synapse. These events initiate downstream signals to increase proliferation, including the activation of NF-κB, AP-1 and NFAT pathways (Wang et al., 2012). Phorbol ester compounds function to activate PKC-θ directly and bypass the need for CD28 receptor stimulation, synergizing with TCR engagement in T cells to increase intracellular Ca2+ and induce activation, proliferation, and cytokine production (Kim et al., 2018). This activity recapitulates CD28 costimulatory signaling, providing T cells with signal 2 via chemical costimulation. They are, however, characterized for their cariogenic activity and are unlikely to be suitable for combinatorial therapies with engineered T cells.

Second mitochondrial-derived activator of caspases (SMAC) mimetics were among the top hits of the HTS. SMAC mimetics are a class of compounds that antagonize inhibitors of apoptosis (IAP), which are a family of negative regulators of caspases and cell death. Since IAP's are linked to cancer development, SMAC mimetics have been investigated for their utility as anti-cancer drugs (Probst et al., 2010). SMAC mimetics have also shown to augment T cell proliferation and survival by non-canonical NF-kB activation (Dougan et al., 2010). LCL 161 is one such SMAC mimetic that emerged as a hit from our screen and has been shown by our lab to enhance BCMA-TAC T cell function when exposed to antigen on bead (Afsahi et al., 2023). Others have also demonstrated that SMAC mimetics can be used in combination with CAR T cells to augment anti-tumour activity through enhancement of TNF-α-dependent bystander effects (Song et al., 2022). To this point, SMAC mimetics are still finding a place in the armamentarium of oncologists and have not yet been combined with T cell therapy in human trials.

Mitogen-activated protein kinases (MAPK) inhibitors reproducibly emerged as hits, too. MAPK are protein kinases that convert extracellular stimuli into cellular responses, regulating fundamental processes including proliferation, metabolism, and survival (Cargnello & Roux, 2011). Some reports have demonstrated the costimulatory activity of MAPK inhibitors, such as the pharmacological p38 MAPK inhibitor BIRB796 that enhanced T cell cytokine production and tumour killing (Chan et al., 2020). The transfer of BIRB796 preconditioned TCR T cells or gene-engineered anti-CD19 CAR T cells results in more effective anti-tumour responses and long-term survival in mouse models. This was attributed to a more favourable memory-like phenotype, as measured by CD62L and CD27 expression (Chan et al., 2020).

We conducted a counter screen using two donors to exclude false positives that generated signal in the context of irrelevant antigen. Almost all hits, except for P300/CBP-IN-3 and Soyasaponin B, demonstrated on-target activity. Histone acetyltransferase CREB-binding protein (CBP) and its closely related p300 protein (CBP/p300) are required for histone acetylation. CBP/p300 inhibitors are being investigated as anti-cancer agents as CBP/p300 has been identified as a tumorigenic driver (Chen et al., 2022). Soyasaponin Ab is from a class of compounds 'group A soyasponins,' that demonstrated enhancement to TNF-α and IL-1β in a mouse macrophage RAW264.7 line *in vitro* (Sun et al., 2014). The reason for the non-specific activity by P300/CBP-IN-3 and Soyasaponin B is unclear.

Although luminescence is also susceptible to inhibition by small molecules in the library, we did not re-evaluate the compounds to detect for false negatives (Yonchev, & Bajorath, 2020). Only some hits from the HTS were also hits in the first donor counter screen (N=129) and second donor counter screen (N=161).

When making our selection of compounds to advance for more detailed assessment in the orthogonal assay, we excluded compounds IMiDs, phorbol esters and SMAC mimetics (IAP) because they are well described for their costimulatory activity in the literature. We chose to evaluate 7 compounds that demonstrated potent activity in stage two: TGFBR1-IN-3, BAY 60 6538, ML327, Emricasan, CK1-IN-1, Desacetylcinobufagin and 8-Geranyloxypsoralen.

8-Geranyloxypsoralen and BAY 60 6538 demonstrated the most potent enhancement to TAC T cell proliferation and survival in the orthogonal assay. Although 8-Geranyloxypsoralen has not yet been characterized for its effect on immune cell function, we do know that it inhibits Cytochrome P450 (CYp) 3A4 and β-secretase 1 (BACE1). CyP3A4 contributes to bile acid detoxification, elimination of food phytochemicals, and the metabolism of most drugs (Chen, 2014; Basheer & Kerem, 2015). Contrast to our findings, cytochrome P450 inhibitors, such as miconazole, clotrimazole, and econazole, have been shown to hamper CD3-induced T cell proliferation by impairing Ca^{2+} influx and IL-2 production (Aussel et al., 1994). Thalidomide, which belongs to IMiDs and is expected to have costimulatory activity, was found to increase hepatic CYP3A4 (Murayama et al., 2014). The inactivation of CYP3A4, and thus the inhibition of drug metabolism, can have significant consequences due to an increased risk of toxic levels of drug exposure (Walsh & Miwa, 2011).

The inhibition of another CYP variant CYP1, increased stem cell factor receptor (c-Kit) and IL-22 expression and promoted CD4+ T cells that co-express c-Kit and IL-22 simultaneously (Effner et al., 2017). C-Kit is a receptor tyrosine kinase expressed in stem cell populations and plays a crucial role in cell proliferation and differentiation (Kagoya et al., 2018). Intracellular expression of c-Kit in first-generation CAR T cells demonstrated IFN-γ mediated costimulation, which resulted in improved survival and cytotoxicity in low-antigen-expressing solid tumor models (Xiong et al., 2023).

It is also possible 8-Geranyloxypsoralen is acting through BACE1, which is a beta-site amyloid precursor protein cleaving enzyme that is found in neural cells but also T cells. Contrast to our observations that support 8-Geranyloxypsoralen as a T cell boosting agent, one study found that knocking out BACE1 from murine

CD4+ T cells enhanced Akt activation, which is downstream of costimulatory pathways (Hernandez-Mir, 2019).

Activation of BACE1 promotes PGE2 production (Dai et al., 2021). PGE2 has demonstrated both agonist/antagonist effects on TCR signalling in a concentration-dependent manner. Suppressive function to T cell activation, proliferation, migration and differentiation is thought to occur at micromolar concentrations of PGE2 (Sreeramkumar et al., 2012). Multiple reports show that PGE2 impairs the anti-tumour efficacy of CD8+ tumour infiltrating lymphocytes, restricting sensitivity to IL-2 and expansion of tumour-infiltrating stem-like CD8+ T cells (Morotti et al., 2024; Lacher et al., 2024). Nanomolar concentrations of PGE2 have been shown to potentiate CD4+ T cell responses and augment T cell proliferation (Sreeramkumar et al., 2012). Thus, it is possible that 8-Geranyloxypsoralen promotes T cell proliferation by inhibiting or reducing PGE2 levels.

BAY 60 6583 also demonstrated potent enhancement to T cell proliferation in the orthogonal assay. BAY 60 6583 is a selective agonist to the G-protein coupled adenosine A2B receptor agonist (Hinz et al., 2014). BAY 60 6583 has previously demonstrated costimulatory effects as it was found to significantly increase cytokine secretion, cytotoxicity and proliferation of CD133- and HER2-specific CAR T cells when co-cultured with their respective target expressing tumour cells (Tang et al., 2021). These effects were recapitulated *in vivo*, as BAY 60 6533 augmented anti-HER2 CAR T cell mediated tumour suppression in a xenograft mouse model (Tang et al., 2021). Knocking out adenosine A2b receptor in CAR T cells, however, did not hamper its functional benefits (Tang et al., 2021). Several predicted targets of BAY 60 6583, such as pyruvate kinase M, Talin-1, Plastin-2, and lamina-associated polypeptide 2, were generated with computational methods (Tang et al., 2021).

ML327 treatment was toxic to TAC T cells. ML327 inhibits c-Myc, which regulates global gene expression, cell proliferation, differentiation, metabolism and apoptosis (Llombart, & Mansour, 2022). Myc is typically overexpressed in most cancer cells, where it seizes regenerative programs that drive normal cell expansion (Llombart, & Mansour, 2022). Myc inhibition induces the regression of tumours, but can have profound effects on normal regenerating tissues. However, these effects are tolerated over long periods and are reversible (Soucek et al., 2008). This may explain the observed toxic effects to TAC T cells.

TGFβRI-IN-3 inhibits TGFβR1 and has selectivity against MAP4K4. It is possible that enhancement to TAC T cell survival was a result of MAP4K4 inhibition, as it has been found to negatively regulate CD8 T cell-mediated anti-tumour immunity (Esen et al., 2020). For example, the deletion of MAP4K4 augmented LFA-1 activation and thus, binding to its ligand in CD8+ T cells (Esen et al., 2020). It also enhanced CD8+ T cell priming and resulted in improved antigen-dependent activation, proliferation, cytokine production, and tumour growth suppression (Esen et al., 2020).

It is also possible that TGFβRI-IN-3 enhances T cell survival via inhibition of TGFβR1, which is the receptor for TGF-β1. TGF-β1 is a cytokine that activates regulatory proteins, inducing the transcription of target genes that are responsible for differentiation, chemotaxis, proliferation, and the activation of many immune cells (Massagué, 2012). TGF-β1 restricts T cell growth, which may be an attribute of its inhibition of IL-2 expression and secretion (Thomas & Massagué, 2005). In addition to reducing T cell proliferation, TGF-β1 signals directly target CD8+ T cells, restricting the expression of genes for IFN-γ, granzyme and perforin (Thomas & Massagué, 2005). TGF-β1 has also increased co-inhibitory PD-1 expression on human CD8+ and CD4+ T cells *in vitro* (Park et al., 2016).

Emricasan, CK1-IN-1 and Desacetylcinobufagin moderately improved TAC T cell survival and proliferation. Emricasan is a pan-caspase inhibitor with antiapoptotic effects. Multiple caspase inhibitors have been created for use as a treatment of cell death-related pathologies, but a limited number have been evaluated for clinical use due to poor efficacy, target specificity and side effects (Dhani et al., 2021). CK1-IN-1 is an inhibitor of casein kinase 1, where are enzymes that regulate signal transduction pathways. For example, CK1 play a role in DNA repair and DNA transcription (Eide et al., 2001). It is unclear how CK1 inhibition would improve T cell functional outcomes. It is also possible that CK1-IN-1 is acting through the suppression of p38 MAPK, which is improved anti-tumour efficacy of CD19-CAR T cells *in vitro* and *in vivo* (Chan et al., 2020).

Desacetylcinobufagin is produced from the microbial biotransformation (i.e., the transformation of a lipophilic to a hydrophilic compound) of cinobufagin (He et al., 2012). Cinobufagin is derived from dried white secretion of Chinese toads, which is from traditional Chinese medicine (Aprayni et al., 2020). Although there is little known about the immunomodulatory effects of Desacetylcinobufagin, Cinobufagin treatment increased cytokine production, including IFN-γ and TNF-α in CD4+ T cells. Cinobufagin also improved the proliferative and phagocytic capacity of macrophages (Wang et al., 2011).

Future Directions

Following the completion of the high throughput screen, secondary assessments and brief characterization of the lead actives, key research questions have emerged as future directions.

1. How can we validate the functional effects of the lead compounds? What are the mechanisms underpinning biological activity?

Thus far, all HTS compounds have been evaluated for their impact on the proliferative capacity of TAC T cells stimulated by antigen-on-bead. It is possible some compounds do not recapitulate these effects in the context of a tumour-based stimulus. This was observed with LCL-161 which enhanced the proliferation of BCMA-TAC T cells stimulated by BCMA-loaded beads but not BCMA expressing tumour cells (Afsahi et al., 2023). It is also possible some compounds have undesirable effects on tumour cells, such PKC modulators, which potently enhance T cell proliferation but are carcinogenic (Garg et al., 2014). For these reasons, the lead compounds should be evaluated in the presence of a tumour-based stimulus.

To validate that the biological activity of the lead compounds is not restricted to one setting, it would be pertinent to assess their impact in different conditions, e.g., different synthetic receptors, antigen-binders, tumour targets, and T cell donors. Other readouts, such as activation (e.g., CD69 expression), cytotoxicity, effector cytokine production, and division (e.g., Ki-67 staining), will provide a broader understanding of the functional effects to T cells. Furthermore, the most potent compounds, 8-Geranyloxypsoralen and BAY 60 6538, appeared toxic to T cells in the absence of a stimulus. It is possible micromolar concentrations are too high. This forms the rationale for additional dose response assessments to determine a safe concentration that would not hamper TAC T cell survival.

To elucidate the mechanisms underpinning the biological activity, RNA sequencing is one approach that could shed light on changes to gene expression within the TAC T cell transcriptome. More specific approaches can be used to determine mechanisms. For example, the ablation of predicted 8-Geranyloxypsoralen targets, CYP3A4, BACE1 or PGE2, may reveal their importance. Similarly, the overexpression by genetic modification or quantifying the changes to CYP3A4, BACE1 or PGE2 may aid in our understanding of 8-Geranyloxypsoralen. For example, there are luminescent assays for measuring changes to CYP3A4 activity (Kabir et al., 2022). Given the role of CYP3A4 in drug metabolism, it could be worthwhile to explore the effect of concurrent delivery of 8-Geranyloxypsoralen delivery and marketed drug metabolized by CYP3A4 to validate concerns about toxicity. Similarly, measuring the quantity, deletion or overexpression of the predicted targets of other relevant compounds may aid in our investigation.

2. How can we use the findings of this screen to develop more potent small molecules?

The findings of this screen can be used to develop a library of compounds with a greater likelihood of desirable biological activity. This is possible through both conventional methods (e.g., analogue development using synthetic chemistry) and innovative computational tools (e.g., artificial intelligence). The lead compounds will require validation in multiple contexts to confirm that their effects are 'real'.

Conventionally, upon validation of compound biological activity, one or multiple lead compounds will be selected for analogue generation. The selection criteria can vary but may consider the novelty, potency and drug-likeness of the lead compounds. Structure activity relationship studies, which combine basic computational methods and synthetic chemistry expertise, serve to identify the specific structural characteristics of compound that are associated with its biological activity (Guha, 2013). Analogues of the parental compound are evaluated to determine those that provide desirable biological activity. Subsequent rounds of structural activity relationship studies aim to optimize analogue structure to improve potency and drug-likeness to eventually be studied *in vivo* and clinically testing.

Artificial intelligence has emerged as an alternative approach to the analogue generation. It been used to develop a novel library of compounds with that to predict preclinical candidates with antibiotic activity (Catacutan et al., 2024). We can feed a machine learning-based algorithm the HTS actives and their respective compound structures. The model will assess the library of actives to predict functionally active chemical characteristics and sift through a massive chemical space for candidates. Based on a defined set of chemical reactions and building-blocks, the model will generate a library of novel compounds that are scored based on their predicted level of activity (Swanson et al., 2024). For that reason, the model would not propose a chemical structure that requires a synthesis approach beyond the defined chemical reactions. The use of generative artificial intelligence has been demonstrated the development of original, synthesizable and effective preclinical antibiotic candidates from a large chemical library (Swanson et al., 2024).

5.0 MATERIALS & METHODS

Lentivirus production

Lentivirus encoding receptor or reporter transgene were generated using a 3rd generation packaging system. 12x10^6 HEK293T cells were cultured on a 15-cm dish (NUNC; Thermo Fisher Scientific) and transfection with packaging plasmids pRSV-Rev (6.25 µg), pMD2.G (9 µg), pMDLg-pRRE (12.5 µg) and transfer plasmid pCCL or pCDH (32 µg), using Opti-MEM (Gibco) and Lipofectamine 2000 (Thermo Fisher Scientific). At 12-16 hours post-transfection, HEK293T media (10% fetal bovine serum (FBS) (Gibco), 50 mg/mL Normocin, 10 mM HEPES (Roche), 2 mM L-glutamine (BioShop)) was replaced with fresh HEK293TM media (100 U/mL penicillin (Gibco), 100 µg/mL streptomycin (Gibco) supplemented with sodium butyrate (Sigma-Aldrich). 24-37 hours later, supernatants were harvested. Lentiviral particles were filtered with a 0.45 µM Polyethersulfone filter, concentrated with the Amicon® Ultra Centrifugal Filter (EMD Millipore) and stored at -80°C. Viral titer (TU/mL) was determined by serial dilution, transduction of HEK293T cells, and enumeration of percent transduction marker positive cells by flow cytometry.

Gamma retrovirus production

3x10^6 PG13 cells stably expressing gamma retrovirus particles generated by Bonnie Bojovic were seeded in a T-75 flask (Falcon). At 72 hours, PG13/gRV cells are lifted with Tryspin+EDTA, split and transferred depending on their confluency. 144 hours later, 2x10^6 PG13/gRV cells are seeded in T-75 flasks. Viral supernatants are harvested 48 hours later, filtered with a 0.45 µM Polyethersulfone filter and stored at -80°C.

Generation of engineered human T cell products with lentivirus

Peripheral blood mononuclear cells (PBMC) were obtained from healthy donors from commercial leukapheresis products (HemaCare, Northridge, CA, and STEMCELL Technologies, Vancouver, BC, Canada). Leukapheresis products were obtained by Ficoll-Paque Plus gradient centrifugation, shipped at 24°C and cryopreserved in inactivated human AB serum containing either CryoStor10 (STEMCELL Technologies) or 10% DMSO (Sigma-Aldrich) within 24 hours of collection. PBMCs were stored in an isopropanol freeze (Thermo Fisher Scientific) at-80°C for 24 hours before storage in liquid nitrogen. PBMCs were transported on dry ice, thawed in a 37°C water bath and washed in 10x volume of standard T cell media (RPMI 1640 (Gibco), 10% FBS (Gibco), 2mM L-glutamine (BioShop), 10 mM HEPES (Roche), 0.5 mM sodium pyruvate (Sigma Aldrich), 1 mM non-essential amino acids (Gibco), 55 µM B-mercaptoethanol (Gibco), 100 U/mL penicillin (Gibco), 100 µg/mL streptomycin (Gibco)). PBMCs were activated ImmunoCult soluble CD3/28/2 tetrameric complexes (STEMCELL Technologies) and cultured in T cell media supplemented with 1.5 ng/mL rhIL-2 and 10 ng/mL rhIL-7 (Peprotech) at $1x10^5$ cells per well in a 96-well round bottom plate. 16-24 hours later, activated T cells were transduced with a lentivirus at an experimentally determined MOI. T cells were washed with 1x PBS on day 4 to remove the soluble activator. Cells were enumerated every 2 days and cultured with cytokine-supplemented T cell media to a concentration of $1x10^6$ cells/mL. On day 14 of culture, TAC T cells were cryopreserved in CryoStor10 at $20x10^6$ or $30x10^6$ cells/mL in cryovials and stored at -80°C. 24 hours later, cryovials were transferred to liquid nitrogen for long term storage.

Phenotyping

Surface expression of engineered products was determined by staining either mStrawberry+, NGFR+ or with recombinant HER2-Fc protein (R&D Systems), followed by anti-human IgG and surface markers CD4 and CD8. Staining was measured by flow cytometry. Luciferase expression was determined by permeating cells with Cytofix/CytoPerm followed by staining of Red Shift Luciferase, followed by anti-rabbit IgG.

Generation of engineered human T cell products with gammaretrovirus

PBMCs were transported on dry ice, thawed in a 37°C water bath and washed in 10x volume of T cell media. PBMCs were activated ImmunoCult soluble CD3/28/2 tetrameric complexes (STEMCELL Technologies) and cultured in T cell media supplemented with 1.5 ng/mL rhIL-2 and 10 ng/mL rhIL-7 (Peprotech) at $1x10^5$ cells per well in a 96-well round bottom plate (Falcon). The following day, non-tissue culture treated 24-well plates (Falcon) are coated with 1µg/µL recombinant RetroNectin at 4°C overnight. 24 hours later, activated T cells were transduced with a gamma retrovirus supernatant at an experimentally determined volume. T cells were washed with 1x PBS on day 5 to remove the soluble activator. The procedure for day 6 to 14 is the same as human engineered T cells products generated with lentivirus.

Flow cytometry

Flow cytometry data were collected with Beckman Coulter CytoFLEX LX (NUV/V/YG/B/R laser configuration) or CytoFLEX S (V/YG/B/R). Flow cytometry data were analyzed using FCS Express Software (DeNovo Software) or Flow Jo.

Microbead antigen loading

Protein G-conjugated ~6-7 μM polystyrene beads (Spherotech, Lake Forest, IL, USA) were loaded with 200 ng HER2-Fc chimera protein (R&D Systems), 200 ng BCMA-Fc chimera protein (R&D Systems), X ng LFA3-Fc chimera protein (Abcam), CD86-Fc chimera protein (Biolegend) per 10^6 beads in PBS + 0.1% Bovine Serum Albumin (BSA), at a concentration of $5x10^6$ beads/mL and rotated overnight at 4°C. Prior to use, beads were resuspended in T cell medium without cytokines at the desired concentration.

Cell Maintenance

Adherent HER2+ cell lines HCT-116 tumour cells were cultured in NCI-60 (RPMI 1640, 10% FBS (Gibco), 2mM L-glutamine (BioShop), 10 mM HEPES (Roche), 100 U/mL penicillin (Gibco), 100 μg/mL streptomycin (Gibco)). Suspension BCMA+ cell lines RPMI-8226 were cultured in RPMI 1640 (Gibco supplemented with 10% FBS (Gibco), 2mM L-glutamine (BioShop), 10 mM HEPES (Roche), 0.5 mM sodium pyruvate (Sigma Aldrich), 1 mM non-essential amino acids (Gibco), 55 μM B-mercaptoethanol (Gibco), 100 U/mL penicillin (Gibco), 100 μg/mL streptomycin (Gibco)). All cell lines were cultured at 5% CO_2 and 37°C. Cell lines were regularly examined for the presence of mycoplasma with the PlasmoTest mycoplasma detection kit (Invivogen).

In Vitro Cytotoxicity Assay

$2.0x10^3$ fluorescent HCT-116 cells were seeded in a 96-well round bottom plate (Falcon). 24 hours later, engineered T cells were co-cultured in triplicate with HCT-116 cells in the presence of presence of DMSO or compound at ranging effector: target ratios for 4-5 days at 37°C in an IncuCyte® Live-Cell Imaging System. Tumour viability was quantified using the IncuCyte® Live-Cell Analysis Software.

CellTrace™ Violet Proliferation Assay

Engineered T cells were labelled using a CellTrace® Violet Cell Proliferation kit (ThermoFisher). Following stimulation under different conditions for 72-hours, T cell subsets were stained with LIVE/DEAD NearIR Viability Dye (Invitrogen), followed by surface antibodies against CD4, CD8 and a receptor or transduction marker and mixed with absolute 123E counting beads (Thermo Fisher Scientific). Flow cytometry data was acquired from was conducted on CytoFlex and analyzed by FCS Express.

Luminescence Proliferation Assay

Engineered T cells were co-cultured with tumour or bead-based stimuli for 72, 96 or 120 hours in the presence of DMSO or compound at 37°C. Following co-culture, 0.15 mg/mL D-Luciferin (Perkin Elmer, Waltham, MA) was added, and luminescence was measured with luminescence fibers using a Neo2 Plate Reader (Biotek). Where appropriate, wells were pooled and stained for LIVE/DEAD NearIR Viability Dye (Invitrogen), followed by surface antibodies against CD4, CD8 and a receptor or transduction marker and mixed with absolute 123E counting beads (Thermo Fisher Scientific).

High Throughput Screen

The protocol was operated at the high throughput screening centre at McMaster University's Centre for Chemical Microbial Biology. DMSO or compounds were dispensed in 384-well Low Range White Flat Bottom Polystyrene TC-treated Microplate (Corning) by the Echo Ecoustic Dispenser. The Tempest Liquid Handler dispensed $3.3\text{x}10^4$ TAC T cells per well and $1.57\text{x}10^4$ beads. The plates were stored at 5 CO_2 and 37°C for 4 days in a Steri-Store. Follow co-culture, 0.15 mg/mL of D-Luciferin (Perkin Elmer) are dispensed with the Multidrop Combi Reagent Dispenser. Luminescence was measured with luminescence fibers using a SynergyNeo2 1.2. Hit analysis was completed using the interquartile mean normalization method on Microsoft Excel (Mangat et al., 2014).

Z-Factor

The quality of an assay can be estimated by determining the Z-factor:

$$Z = 1 - (3\sigma_{c+} + 3\sigma_{c-}) / (|\mu_{c+} - \mu_{c-}|)$$

where (σc+) and (σc−) is the data standard deviation for positive control and negative control, respectively, and |μc+−μc−| is the absolute value of the difference of the two control signal means and it defines linear range of the assay.

Reagent	**Source**	**CAT No.**
Goat anti-human igG -PE	Jackson ImmunoResearch	109-115-098
Goat anti-human igG BV421	Jackson ImmunoResearch	109-675-098
Anti-human CD4-Pacific Blue	BD Biosciences	558116
Anti-human CD4-APC-H7	BD Biosciences	560158
Anti-human CD4-AlexaFluor 700	Thermo Fisher Scientific	1939044
Anti-humanCD8-AlexaFluor 700	Thermo Fisher Scientific	557945
Anti-human CD8-PerCP-Cynanine5.5	Thermo Fisher Scientific	45-0088-42
Anti-human NGFR-VioBright FITC	Miltenyi Biotec	130-113-423
Anti-human CD3-Brilliant Violet 605	BioLegend	300460
LIVE/DEAD fixable Near-IR dead cell stain	Thermo Fisher Scientific	A10628
Cytofix buffer	BD Biosciences	554655
123count eBeads	Thermo Fisher Scientific	01-1234-42
Protein G-conjugated ~6 μM polystyrene beads	Spherotech	PGP-60-5
CellTrace Violet	Thermo Fisher Scientific	C34557
D-Luciferin	Perkin Elmer	122799
rhBCMA-Fc chimera	R&D Systems	NBP2-52270-0.05mg
rhHErRB2-Fc chimera	R&D Systems	1129-ER-050
rhIL-2	PeproTech	200-02-250ug
rhIL-7	PeproTech	200-07-250ug
ImmunoCult™ Human CD3/CD28/CD2 T Cell Activator	STEM Cell Technologies	10990
Anti-rabbit igG PE	Cell Signalling Technology	5742S
Anti-red shifted Luciferase	Abcam	ab185923

6.0 BIBLIOGRAPHY

Acharya, T. K., Kumar, S., Rokade, T. P., Chang, Y. T., & Goswami, C. (2023). TRPV4 regulates mitochondrial Ca2+-status and physiology in primary murine T cells based on their immunological state. *Life Sciences*, *318*, 121493.

Adami, J., Gäbel, H., Lindelöf, B., Ekström, K., Rydh, B., Glimelius, B., ... & Granath, F. (2003). Cancer risk following organ transplantation: a nationwide cohort study in Sweden. British journal of cancer, 89(7), 1221-1227.

Afsahi, A., Silvestri, C. M., Moore, A. E., Graham, C. F., Bacchiochi, K., St-Jean, M., ... & Bramson, J. L. (2023). LCL161 enhances expansion and survival of engineered anti-tumor T cells but is restricted by death signaling. Frontiers in Immunology, 14, 1179827.

Ajina, A., & Maher, J. (2018). Strategies to address chimeric antigen receptor tonic signaling. *Molecular cancer therapeutics*, *17*(9), 1795-1815.

Alt, F. W., Oltz, E. M., Young, F., Gorman, J., Taccioli, G., & Chen, J. (1992). VDJ recombination. *Immunology today*, *13*(8), 306-314.

Amatangelo, M., Bjorklund, C. C., Kang, J., Polonskaia, A., Viswanatha, S., & Thakurta, A. (2018). Iberdomide (CC-220) has synergistic anti-tumor and immunostimulatory activity against multiple myeloma in combination

Apryani, E., Ali, U., Wang, Z. Y., Wu, H. Y., Mao, X. F., Ahmad, K. A., ... & Wang, Y. X. (2020). The spinal microglial IL-10/β-endorphin pathway accounts for cinobufagin-induced mechanical antiallodynia in bone cancer pain following activation of α7-nicotinic acetylcholine receptors. Journal of neuroinflammation, 17, 1-18.

Arghiani, N., Matin, M. M., Bahrami, A. R., Iranshahi, M., Sazgarnia, A., & Rassouli, F. B. (2014). Investigating anticancer properties of the sesquiterpene ferutinin on colon carcinoma cells, in vitro and in vivo. *Life sciences*, *109*(2), 87-94.

Auld, D. S., & Inglese, J. (2018). Interferences with luciferase reporter enzymes. Assay Guidance Manual [Internet].

Aussel, C., Breittmayer, J. P., Ticchioni, M., Pelassy, C., & Bernard, A. (1994). Regulation of T cell activation by cytochrome P450 inhibitors. Cellular immunology, 155(2), 436-445.

Basheer, L., & Kerem, Z. (2015). Interactions between CYP3A4 and dietary polyphenols. Oxidative medicine and cellular longevity, 2015(1), 854015.

Baulu, E., Gardet, C., Chuvin, N., & Depil, S. (2023). TCR-engineered T cell therapy in solid tumors: State of the art and perspectives. *Science Advances*, *9*(7), eadf3700.

Bendle, G. M., Linnemann, C., Hooijkaas, A. I., Bies, L., de Witte, M. A., Jorritsma, A., ... & Schumacher, T. N. (2010). Lethal graft-versus-host disease in mouse models of T cell receptor gene therapy. *Nature medicine*, *16*(5), 565-570.

Bezverbnaya, K., Moogk, D., Cummings, D., Baker, C. L., Aarts, C., Denisova, G., ... & Bramson, J. L. (2021). Development of a B-cell maturation antigen-specific T-cell antigen coupler receptor for multiple myeloma. *Cytotherapy*, *23*(9), 820-832.

Bialer, G., Horovitz-Fried, M., Ya'acobi, S., Morgan, R. A., & Cohen, C. J. (2010). Selected murine residues endow human TCR with enhanced tumor recognition. *The Journal of Immunology*, *184*(11), 6232-6241.

Bonora, M., Patergnani, S., Rimessi, A., De Marchi, E., Suski, J. M., Bononi, A., ... & Pinton, P. (2012). ATP synthesis and storage. Purinergic signalling, 8, 343-357.

Bridgeman, J. S., Hawkins, R. E., Bagley, S., Blaylock, M., Holland, M., & Gilham, D. E. (2010). The optimal antigen response of chimeric antigen receptors harboring the

CD3ζ transmembrane domain is dependent upon incorporation of the receptor into the endogenous TCR/CD3 complex. *The Journal of Immunology*, *184*(12), 6938-6949.
Brocker, T., & Karjalainen, K. (1995). Signals through T cell receptor-zeta chain alone are insufficient to prime resting T lymphocytes. *The Journal of experimental medicine*, *181*(5), 1653-1659.
Budhu, S., Loike, J. D., Pandolfi, A., Han, S., Catalano, G., Constantinescu, A., ... & Silverstein, S. C. (2010). CD8+ T cell concentration determines their efficiency in killing cognate antigen–expressing syngeneic mammalian cells in vitro and in mouse tissues. *Journal of Experimental Medicine*, *207*(1), 223-235.
Burnet, M. (1957). Cancer—a biological approach: I. The processes of control. II. The significance of somatic mutation. British medical journal, 1(5022), 779.
Cantrell, D. A. (2002). T-cell antigen receptor signal transduction. *Immunology*, *105*(4), 369.
Cargnello, M., & Roux, P. P. (2011). Activation and function of the MAPKs and their substrates, the MAPK-activated protein kinases. Microbiology and molecular biology reviews, 75(1), 50-83.
Catacutan, D. B., Alexander, J., Arnold, A., & Stokes, J. M. (2024). Machine learning in preclinical drug discovery. Nature Chemical Biology, 1-14.
Chan, J. D., Beavis, P. A., & Darcy, P. K. (2020). p38 Kinase: a key target for driving potent T cells for adoptive immunotherapy. Cancer cell, 37(6), 756-758.
Chan, J. D., Beavis, P. A., & Darcy, P. K. (2020). p38 Kinase: a key target for driving potent T cells for adoptive immunotherapy. *Cancer cell*, *37*(6), 756-758.
Chandran, S. S., & Klebanoff, C. A. (2019). T cell receptor-based cancer immunotherapy: emerging efficacy and pathways of resistance. *Immunological reviews*, *290*(1), 127-147.
Chao, D. L., Davenport, M. P., Forrest, S., & Perelson, A. S. (2005). The effects of thymic selection on the range of T cell cross-reactivity. *European journal of immunology*, *35*(12), 3452-3459.
Chen, B., Zhou, M., Zhang, H., Wang, C., Hu, X., Wang, B., & Wang, E. (2019). TREM1/Dap12-based CAR-T cells show potent antitumor activity. *Immunotherapy*, *11*(12), 1043-1055.
Chen, Q., Yang, B., Liu, X., Zhang, X. D., Zhang, L., & Liu, T. (2022). Histone acetyltransferases CBP/p300 in tumorigenesis and CBP/p300 inhibitors as promising novel anticancer agents. Theranostics, 12(11), 4935.
Chen, J., Zhao, K. N., & Chen, C. (2014). The role of CYP3A4 in the biotransformation of bile acids and therapeutic implication for cholestasis. Annals of translational medicine, 2(1).
Chruściel, E., Urban-Wójciuk, Z., Arcimowicz, Ł., Kurkowiak, M., Kowalski, J., Gliwiński, M., ... & Marek-Trzonkowska, N. (2020). Adoptive cell therapy—harnessing antigen-specific T cells to target solid tumours. *Cancers*, *12*(3), 683.
Cooper, G. M., & Hausman, R. E. (2000). The development and causes of cancer. The cell: A molecular approach, 2, 725-766.
Cornel, A. M., Mimpen, I. L., & Nierkens, S. (2020). MHC class I downregulation in cancer: underlying mechanisms and potential targets for cancer immunotherapy. *Cancers*, *12*(7), 1760.
Corral, L. G., Haslett, P. A., Muller, G. W., Chen, R., Wong, L. M., Ocampo, C. J., ... & Kaplan, G. (1999). Differential cytokine modulation and T cell activation by two distinct classes of thalidomide analogues that are potent inhibitors of TNF-α. The Journal of Immunology, 163(1), 380-386.

Costacurta, M., He, J., Thompson, P. E., & Shortt, J. (2021). Molecular mechanisms of cereblon-interacting small molecules in multiple myeloma therapy. Journal of Personalized Medicine, 11(11), 1185.

Courtney, A. H., Lo, W. L., & Weiss, A. (2018). TCR signaling: mechanisms of initiation and propagation. Trends in biochemical sciences, 43(2), 108-123.

Crabtree, G. R., & Clipstone, N. A. (1994). Signal transmission between the plasma membrane and nucleus of T lymphocytes. Annual review of biochemistry, 63(1), 1045-1083.

Croft, M. (2003). Costimulation of T cells by OX40, 4-1BB, and CD27. *Cytokine & growth factor reviews*, *14*(3-4), 265-273.

Dai, L., Wang, Q., Lv, X., Gao, F., Chen, Z., & Shen, Y. (2021). Elevated β-secretase 1 expression mediates CD4+ T cell dysfunction via PGE2 signalling in Alzheimer's disease. Brain, Behavior, and Immunity, 98, 337-348.

Davenport, A. J., Cross, R. S., Watson, K. A., Liao, Y., Shi, W., Prince, H. M., ... & Jenkins, M. R. (2018). Chimeric antigen receptor T cells form nonclassical and potent immune synapses driving rapid cytotoxicity. *Proceedings of the National Academy of Sciences*, *115*(9), E2068-E2076.

Davies FE, Raje N, Hideshima T, Lentzsch S, Young G, Tai YT et al. Thalidomide and immunomodulatory derivatives augment natural killer cell cytotoxicity in multiple myeloma. Blood 2001; 98: 210–216.myeloma

De Visser, K. E., & Joyce, J. A. (2023). The evolving tumor microenvironment: From cancer initiation to metastatic outgrowth. *Cancer cell*, *41*(3), 374-403.

Dhani, S., Zhao, Y., & Zhivotovsky, B. (2021). A long way to go: caspase inhibitors in clinical use. *Cell death & disease*, *12*(10), 949.

Dougan, M., Dougan, S., Slisz, J., Firestone, B., Vanneman, M., Draganov, D., ... & Dranoff, G. (2010). IAP inhibitors enhance co-stimulation to promote tumor immunity. Journal of Experimental Medicine, 207(10), 2195-2206.

Dreiman, G. H., Bictash, M., Fish, P. V., Griffin, L., & Svensson, F. (2021). Changing the HTS paradigm: AI-driven iterative screening for hit finding. SLAS DISCOVERY: Advancing the Science of Drug Discovery, 26(2), 257-262.

Dunn, G. P., Old, L. J., & Schreiber, R. D. (2004). The immunobiology of cancer immunosurveillance and immunoediting. Immunity, 21(2), 137-148.

Dustin, M. L. (2014). The immunological synapse. *Cancer immunology research*, *2*(11), 1023-1033.

Dustin, M. L., & Shaw, A. S. (1999). Costimulation: building an immunological synapse. *Science*, *283*(5402), 649-650.

Ebrahimi, N., Abdulwahid, A. H. R. R., Mansouri, A., Karimi, N., Bostani, R. J., Beiranvand, S., ... & Aref, A. R. (2024). Targeting the NF-κB pathway as a potential regulator of immune checkpoints in cancer immunotherapy. *Cellular and Molecular Life Sciences*, *81*(1), 106.

Effner, R., Hiller, J., Eyerich, S., Traidl-Hoffmann, C., Brockow, K., Triggiani, M., ... & Buters, J. T. (2017). Cytochrome P450s in human immune cells regulate IL-22 and c-Kit via an AHR feedback loop. Scientific Reports, 7(1), 44005.

Eide, E. J., & Virshup, D. M. (2001). Casein kinase I: another cog in the circadian clockworks. *Chronobiology international*, *18*(3), 389-398.

Engeloch, C., Schopfer, U., Muckenschnabel, I., Le Goff, F., Mees, H., Boesch, K., & Popov, M. (2008). Stability of screening compounds in wet DMSO. Journal of Biomolecular Screening, 13(10), 999-1006.

Esen, E., Sergin, I., Jesudason, R., Himmels, P., Webster, J. D., Zhang, H., ... & Ye, W. (2020). MAP4K4 negatively regulates CD8 T cell–mediated antitumor and antiviral immunity. *Science immunology*, *5*(45), eaay2245.

Eshhar, Z., Waks, T., Gross, G., & Schindler, D. G. (1993). Specific activation and targeting of cytotoxic lymphocytes through chimeric single chains consisting of antibody-binding domains and the gamma or zeta subunits of the immunoglobulin and T-cell receptors. *Proceedings of the National Academy of Sciences*, *90*(2), 720-724.

Fan, F., & Wood, K. V. (2007). Bioluminescent assays for high-throughput screening. *Assay and drug development technologies*, *5*(1), 127-136.

Frauwirth, K. A., & Thompson, C. B. (2002). Activation and inhibition of lymphocytes by costimulation. *The Journal of clinical investigation*, *109*(3), 295-299.

Frey, N. V., & Porter, D. L. (2016). Cytokine release syndrome with novel therapeutics for acute lymphoblastic leukemia. *Hematology 2014, the American Society of Hematology Education Program Book*, *2016*(1), 567-572.

Garg, R., Benedetti, L. G., Abera, M. B., Wang, H., Abba, M., & Kazanietz, M. G. (2014). Protein kinase C and cancer: what we know and what we do not. Oncogene, 33(45), 5225-5237.

Golstein, P., & Griffiths, G. M. (2018). An early history of T cell-mediated cytotoxicity. *Nature Reviews Immunology*, *18*(8), 527-535.

Graf, B., Bushnell, T., & Miller, J. (2007). LFA-1-mediated T cell costimulation through increased localization of TCR/class II complexes to the central supramolecular activation cluster and exclusion of CD45 from the immunological synapse. The Journal of Immunology, 179(3), 1616-1624.

Guha, R. (2013). On exploring structure–activity relationships. In silico models for drug discovery, 81-94.

Halle, S., Halle, O., & Förster, R. (2017). Mechanisms and dynamics of T cell-mediated cytotoxicity in vivo. *Trends in immunology*, *38*(6), 432-443.

Hamaidi, I., & Kim, S. (2022). Sirtuins are crucial regulators of T cell metabolism and functions. *Experimental & Molecular Medicine*, *54*(3), 207-215.

Han, J., Zhao, Y., Shirai, K., Molodtsov, A., Kolling, F. W., Fisher, J. L., ... & Angeles, C. V. (2021). Resident and circulating memory T cells persist for years in melanoma patients with durable responses to immunotherapy. Nature cancer, 2(3), 300-311.

Han, J., Zhao, Y., Shirai, K., Molodtsov, A., Kolling, F. W., Fisher, J. L., ... & Angeles, C. V. (2021). Resident and circulating memory T cells persist for years in melanoma patients with durable responses to immunotherapy. Nature cancer, 2(3), 300-311.

Hanahan, D., & Weinberg, R. A. (2000). The hallmarks of cancer. *cell*, *100*(1), 57-70.

Hanahan, D., & Weinberg, R. A. (2011). Hallmarks of cancer: the next generation. *cell*, *144*(5), 646-674.

He, X., Hu, H., Wu, Y., & Zeng, X. (2012). Urinary metabolites of cinobufagin in rats and their antiproliferative activities. *Natural Product Research*, *26*(6), 489-499.

Hege, K. M., Bergsland, E. K., Fisher, G. A., Nemunaitis, J. J., Warren, R. S., McArthur, J. G., ... & Sherwin, S. A. (2017). Safety, tumor trafficking and immunogenicity of chimeric antigen receptor (CAR)-T cells specific for TAG-72 in colorectal cancer. *Journal for immunotherapy of cancer*, *5*, 1-14.

Helsen, C. W., Hammill, J. A., Lau, V. W., Mwawasi, K. A., Afsahi, A., Bezverbnaya, K., ... & Bramson, J. L. (2018). The chimeric TAC receptor co-opts the T cell receptor yielding robust anti-tumor activity without toxicity. *Nature communications*, *9*(1), 3049.

Hernandez-Mir, G., Raphael, I., Revu, S., Poholek, C. H., Avery, L., Hawse, W. F., ... & McGeachy, M. J. (2019). The Alzheimer's Disease–Associated Protein BACE1 Modulates T Cell Activation and Th17 Function. The Journal of Immunology, 203(3), 665-675.

Herr, M. M., Chen, G. L., Ross, M., Jacobson, H., McKenzie, R., Markel, L., ... & McCarthy, P. L. (2020). Identification of neurotoxicity after chimeric antigen receptor (CAR) T cell infusion without deterioration in the immune effector cell-associated encephalopathy (ICE) score. Biology of Blood and Marrow Transplantation, 26(11), e271-e274.

Hinshaw, D. C., & Shevde, L. A. (2019). The tumor microenvironment innately modulates cancer progression. Cancer research, 79(18), 4557-4566.

Hinz, S., Lacher, S. K., Seibt, B. F., & Müller, C. E. (2014). BAY60-6583 acts as a partial agonist at adenosine A2B receptors. Journal of Pharmacology and Experimental Therapeutics, 349(3), 427-436.

Hsieh, E. M., Scherer, L. D., & Rouce, R. H. (2020). Replacing CAR-T cell resistance with persistence by changing a single residue. *The Journal of Clinical Investigation*, *130*(6), 2806-2808.

Hu, Y., Sun, J., Wu, Z., Yu, J., Cui, Q., Pu, C., ... & Huang, H. (2016). Predominant cerebral cytokine release syndrome in CD19-directed chimeric antigen receptor-modified T cell therapy. Journal of hematology & oncology, 9, 1-5.

Hughes, J. P., Rees, S., Kalindjian, S. B., & Philpott, K. L. (2011). Principles of early drug discovery. British journal of pharmacology, 162(6), 1239-1249.

Idos, G. E., Kwok, J., Bonthala, N., Kysh, L., Gruber, S. B., & Qu, C. (2020). The prognostic implications of tumor infiltrating lymphocytes in colorectal cancer: a systematic review and meta-analysis. Scientific reports, 10(1), 3360.

Imai, C. M. I. H. A. R. A., Mihara, K., Andreansky, M., Nicholson, I. C., Pui, C. H., Geiger, T. L., & Campana, D. (2004). Chimeric receptors with 4-1BB signaling capacity provoke potent cytotoxicity against acute lymphoblastic leukemia. *Leukemia*, *18*(4), 676-684.

Inman, B. A., Frigola, X., Dong, H., & Kwon, E. D. (2007). Costimulation, coinhibition and cancer. *Current cancer drug targets*, *7*(1), 15-30.

Janeway Jr, C. A., Travers, P., Walport, M., & Shlomchik, M. J. (2001). T-cell receptor gene rearrangement. In Immunobiology: The Immune System in Health and Disease. 5th edition. Garland Science.

Jansen, C. S., Prokhnevska, N., & Kissick, H. T. (2019, August). The requirement for immune infiltration and organization in the tumor microenvironment for successful immunotherapy in prostate cancer. In *Urologic Oncology: Seminars and Original Investigations* (Vol. 37, No. 8, pp. 543-555). Elsevier.

Jensen, M. C., Popplewell, L., Cooper, L. J., DiGiusto, D., Kalos, M., Ostberg, J. R., & Forman, S. J. (2010). Antitransgene rejection responses contribute to attenuated persistence of adoptively transferred CD20/CD19-specific chimeric antigen receptor redirected T cells in humans. *Biology of blood and marrow transplantation*, *16*(9), 1245-1256.

Johnston, C., Hardacre, C., & Migaud, M. E. (2021). Investigations into the synthesis of a nucleotide dimer via mechanochemical phosphoramidite chemistry. Royal Society Open Science, 8(3), 201703.

Jorgensen, W. L. (2004). The many roles of computation in drug discovery. *Science*, *303*(5665), 1813-1818.

June, C. H., & Sadelain, M. (2018). Chimeric antigen receptor therapy. *New England Journal of Medicine*, *379*(1), 64-73.

June, C. H., O'Connor, R. S., Kawalekar, O. U., Ghassemi, S., & Milone, M. C. (2018). CAR T cell immunotherapy for human cancer. *Science*, *359*(6382), 1361-1365.
Kabir, M., Padilha, E. C., Shah, P., Huang, R., Sakamuru, S., Gonzalez, E., ... & Xu, X. (2022). Identification of selective CYP3A7 and CYP3A4 substrates and inhibitors using a high-throughput screening platform. Frontiers in Pharmacology, 13, 899536.
Kagoya, Y., Tanaka, S., Guo, T., Anczurowski, M., Wang, C. H., Saso, K., ... & Hirano, N. (2018). A novel chimeric antigen receptor containing a JAK–STAT signaling domain mediates superior antitumor effects. Nature medicine, 24(3), 352-359.
Kershaw, M. H., Westwood, J. A., Parker, L. L., Wang, G., Eshhar, Z., Mavroukakis, S. A., ... & Hwu, P. (2006). A phase I study on adoptive immunotherapy using gene-modified T cells for ovarian cancer. *Clinical cancer research*, *12*(20), 6106-6115.
Kim, H. J., Ji, Y. R., & Lee, Y. M. (2022). Crosstalk between angiogenesis and immune regulation in the tumor microenvironment. Archives of Pharmacal Research, 45(6), 401-416.
Kim, K. H., Kim, S. H., Jung, H. H., Moon, J. H., Jeong, S. U., Yu, K., & Lee, C. K. (2018). Thapsigargin increases IL-2 production in T cells at nanomolar concentrations. Immune network, 18(4).
Kozikowski, B. A., Burt, T. M., Tirey, D. A., Williams, L. E., Kuzmak, B. R., Stanton, D. T., ... & Nelson, S. L. (2003). The effect of room-temperature storage on the stability of compounds in DMSO. SLAS Discovery, 8(2), 205-209.
Kumar, B. V., Connors, T. J., & Farber, D. L. (2018). Human T cell development, localization, and function throughout life. *Immunity*, *48*(2), 202-213.
Lacher, S. B., Dörr, J., de Almeida, G. P., Hönninger, J., Bayerl, F., Hirschberger, A., ... & Böttcher, J. P. (2024). PGE2 limits effector expansion of tumour-infiltrating stem-like CD8+ T cells. Nature, 1-9.
Lanier, L. L., Corliss, B. C., Wu, J., Leong, C., & Phillips, J. H. (1998). Immunoreceptor DAP12 bearing a tyrosine-based activation motif is involved in activating NK cells. *Nature*, *391*(6668), 703-707.
Lanzavecchia, A., Iezzi, G., & Viola, A. (1999). From TCR engagement to T cell activation: a kinetic view of T cell behavior. *Cell*, *96*(1), 1-4.
Lasek, W. (2022). Cancer immunoediting hypothesis: History, clinical implications and controversies. Central European Journal of Immunology, 47(2), 168-174.
LeBlanc, R., Hideshima, T., Catley, L. P., Shringarpure, R., Burger, R., Mitsiades, N., ... & Munshi, N. C. (2004). Immunomodulatory drug costimulates T cells via the B7-CD28 pathway. Blood, 103(5), 1787-1790.
Leung, W., & Heslop, H. E. (2019). Adoptive immunotherapy with antigen-specific T cells expressing a native TCR. *Cancer immunology research*, *7*(4), 528-533.
Li, J., Slaga, D., Johnston, J., & Junttila, T. T. (2023). IMiDs Augment CD3-Bispecific Antibody–Induced CD8+ T-Cell Cytotoxicity and Expansion by Enhancing IL2 Production. Molecular Cancer Therapeutics, 22(5), 659-666.
Lim, W. A., & June, C. H. (2017). The principles of engineering immune cells to treat cancer. *Cell*, *168*(4), 724-740.
Lindelöf, B., Sigurgeirsson, B., Gäbel, H., & Stern, R. S. (2000). Incidence of skin cancer in 5356 patients following organ transplantation. British Journal of Dermatology, 143(3), 513-519.
Llombart, V., & Mansour, M. R. (2022). Therapeutic targeting of "undruggable" MYC. EBioMedicine, 75.
Loeb, K. R., & Loeb, L. A. (2000). Significance of multiple mutations in cancer. *Carcinogenesis*, *21*(3), 379-385.

López-Hoyos, M., Revilla, C., Conde, C., Del Campo, E. G., González, A., & Merino, J. (1999). Different roles for LFA-1 and VLA-4 integrins in T–B-cell interactions in vivo. Immunology, 97(3), 438.

Luckheeram, R. V., Zhou, R., Verma, A. D., & Xia, B. (2012). CD4+ T cells: differentiation and functions. *Journal of Immunology Research*, *2012*(1), 925135.

Maher, J., Brentjens, R. J., Gunset, G., Rivière, I., & Sadelain, M. (2002). Human T-lymphocyte cytotoxicity and proliferation directed by a single chimeric TCRζ/CD28 receptor. *Nature biotechnology*, *20*(1), 70-75.

Mangat, C. S., Bharat, A., Gehrke, S. S., & Brown, E. D. (2014). Rank ordering plate data facilitates data visualization and normalization in high-throughput screening. Journal of biomolecular screening, 19(9), 1314-1320.

Marcus, A., & Eshhar, Z. (2011). Allogeneic adoptive cell transfer therapy as a potent universal treatment for cancer. *Oncotarget*, *2*(7), 525.

Marro, B. S., Zak, J., Zavareh, R. B., Teijaro, J. R., Lairson, L. L., & Oldstone, M. B. (2019). Discovery of small molecules for the reversal of T cell exhaustion. Cell reports, 29(10), 3293-3302.

Massagué, J. (2012). TGFβ signalling in context. *Nature reviews Molecular cell biology*, *13*(10), 616-630.

Matthys, P., Dillen, C., Proost, P., Heremans, H., And, J. V. D., & Billiau, A. (1993). Modification of the anti-CD3-induced cytokine release syndrome by anti-interferon-γ or anti-interleukin-6 antibody treatment: Protective effects and biphasic changes in blood cytokine levels. European journal of immunology, 23(9), 2209-2216.

Maude, S. L., Frey, N., Shaw, P. A., Aplenc, R., Barrett, D. M., Bunin, N. J., ... & Grupp, S. A. (2014). Chimeric antigen receptor T cells for sustained remissions in leukemia. *New England Journal of Medicine*, *371*(16), 1507-1517.

Monks, C. R., Freiberg, B. A., Kupfer, H., Sciaky, N., & Kupfer, A. (1998). Three-dimensional segregation of supramolecular activation clusters in T cells. *Nature*, *395*(6697), 82-86.

Mora-Bitria, L., & Asquith, B. (2023). Innate receptors modulating adaptive T cell responses: KIR-HLA interactions and T cell-mediated control of chronic viral infections. *Immunogenetics*, *75*(3), 269-282.

Morotti, M., Grimm, A. J., Hope, H. C., Arnaud, M., Desbuisson, M., Rayroux, N., ... & Coukos, G. (2024). PGE2 inhibits TIL expansion by disrupting IL-2 signalling and mitochondrial function. Nature, 1-9.

Morris, E. C., Neelapu, S. S., Giavridis, T., & Sadelain, M. (2022). Cytokine release syndrome and associated neurotoxicity in cancer immunotherapy. Nature Reviews Immunology, 22(2), 85-96.

Murayama, N., van Beuningen, R., Suemizu, H., Guguen-Guillouzo, C., Shibata, N., Yajima, K., ... & Yamazaki, H. (2014). Thalidomide increases human hepatic cytochrome P450 3A enzymes by direct activation of the pregnane X receptor. Chemical research in toxicology, 27(2), 304-308.

Naji Reyhani Garmroudi, S., Karimi, E., Oskoueian, E., Homayouni-Tabrizi, M., & Iranshahi, M. (2021). Ferutinin: A phytoestrogen from ferula and its anticancer, antioxidant, and toxicity properties. *Journal of Biochemical and Molecular Toxicology*, *35*(4), e22713.

Nakakubo, Y., Miyamoto, M., Cho, Y., Hida, Y., Oshikiri, T., Suzuoki, M., ... & Katoh, H. (2003). Clinical significance of immune cell infiltration within gallbladder cancer. British journal of cancer, 89(9), 1736-1742.

Oeckinghaus, A., & Ghosh, S. (2009). The NF-κB family of transcription factors and its regulation. Cold Spring Harbor perspectives in biology, 1(4), a000034.

Park, B. V., Freeman, Z. T., Ghasemzadeh, A., Chattergoon, M. A., Rutebemberwa, A., Steigner, J., ... & Cox, A. L. (2016). TGFβ1-mediated SMAD3 enhances PD-1 expression on antigen-specific T cells in cancer. *Cancer discovery*, *6*(12), 1366-1381.

Parkin, J., & Cohen, B. (2001). An overview of the immune system. The Lancet, 357(9270), 1777-1789.

Porter, D. L., Hwang, W. T., Frey, N. V., Lacey, S. F., Shaw, P. A., Loren, A. W., ... & June, C. H. (2015). Chimeric antigen receptor T cells persist and induce sustained remissions in relapsed refractory chronic lymphocytic leukemia. *Science translational medicine*, *7*(303), 303ra139-303ra139.

Probst, B. L., Liu, L., Ramesh, V., Li, L., Sun, H., Minna, J. D., & Wang, L. (2010). Smac mimetics increase cancer cell response to chemotherapeutics in a TNF-α-dependent manner. Cell Death & Differentiation, 17(10), 1645-1654.

Rafiq, S., Hackett, C. S., & Brentjens, R. J. (2020). Engineering strategies to overcome the current roadblocks in CAR T cell therapy. *Nature reviews Clinical oncology*, *17*(3), 147-167.

Ripphausen, P., Nisius, B., Peltason, L., & Bajorath, J. (2010). Quo vadis, virtual screening? A comprehensive survey of prospective applications. *Journal of medicinal chemistry*, *53*(24), 8461-8467.

Rosenberg, S. A., & Restifo, N. P. (2015). Adoptive cell transfer as personalized immunotherapy for human cancer. *Science*, *348*(6230), 62-68.

Sadelain, M., Brentjens, R., & Rivière, I. (2013). The basic principles of chimeric antigen receptor design. *Cancer discovery*, *3*(4), 388-398.

Santomasso, B. D., Park, J. H., Salloum, D., Riviere, I., Flynn, J., Mead, E., ... & Brentjens, R. J. (2018). Clinical and biological correlates of neurotoxicity associated with CAR T-cell therapy in patients with B-cell acute lymphoblastic leukemia. *Cancer discovery*, *8*(8), 958-971.

Schafer PH, Gandhi AK, Loveland MA, Chen RS, Man HW, Schnetkamp PP et al. Enhancement of cytokine production and AP-1 transcriptional activity in T cells by thalidomide-related immunomodulatory drugs. J Pharmacol Exp Therap 2003; 305: 1222–1232.

Sharpe, A. H. (2009). Mechanisms of costimulation. *Immunological reviews*, *229*(1), 5.

Shen, L., Luo, H., Fan, L., Tian, X., Tang, A., Wu, X., ... & Su, Z. (2023). Potential Immunoregulatory Mechanism of Plant Saponins: A Review. *Molecules*, *29*(1), 113.

Shi, N., Zhou, Y., Liu, Y., Zhang, R., Jiang, X., Ren, C., ... & Luo, L. (2022). PD-1/LAG-3 bispecific antibody potentiates T cell activation and increases antitumor efficacy. Frontiers in Immunology, 13, 1047610.

Shimabukuro-Vornhagen, A., Gödel, P., Subklewe, M., Stemmler, H. J., Schlößer, H. A., Schlaak, M., ... & von Bergwelt-Baildon, M. S. (2018). Cytokine release syndrome. Journal for immunotherapy of cancer, 6, 1-14.

Shurin, M. R. (2012). Cancer as an immune-mediated disease. ImmunoTargets and therapy, 1-6.

Smirnov, S., Mateikovich, P., Samochernykh, K., & Shlyakhto, E. (2024). Recent advances on CAR-T signaling pave the way for prolonged persistence and new modalities in clinic. *Frontiers in Immunology*, *15*, 1335424.

Smith-Garvin, J. E., Koretzky, G. A., & Jordan, M. S. (2009). T cell activation. *Annual review of immunology*, *27*(1), 591-619.

Sommermeyer, D., & Uckert, W. (2010). Minimal amino acid exchange in human TCR constant regions fosters improved function of TCR gene-modified T cells. *The Journal of Immunology*, *184*(11), 6223-6231.

Song, E. Z., Wang, X., Philipson, B. I., Zhang, Q., Thokala, R., Zhang, L., ... & Milone, M. C. (2022). The IAP antagonist birinapant enhances chimeric antigen receptor T cell therapy for glioblastoma by overcoming antigen heterogeneity. Molecular Therapy-Oncolytics, 27, 288-304.

Song, J., Lei, F. T., Xiong, X., & Haque, R. (2008). Intracellular signals of T cell costimulation. *Cellular & molecular immunology*, *5*(4), 239-247.

Soucek, L., Whitfield, J., Martins, C. P., Finch, A. J., Murphy, D. J., Sodir, N. M., ... & Evan, G. I. (2008). Modelling Myc inhibition as a cancer therapy. *Nature*, *455*(7213), 679-683.

Sreeramkumar, V., Fresno, M., & Cuesta, N. (2012). Prostaglandin E2 and T cells: friends or foes?. Immunology and cell biology, 90(6), 579-586.

Sterner, R. C., & Sterner, R. M. (2021). CAR-T cell therapy: current limitations and potential strategies. *Blood cancer journal*, *11*(4), 69.

Stumpf, M., Hasenburg, A., Riener, M. O., Jütting, U., Wang, C., Shen, Y., ... & Lassmann, S. (2009). Intraepithelial CD8-positive T lymphocytes predict survival for patients with serous stage III ovarian carcinomas: relevance of clonal selection of T lymphocytes. British journal of cancer, 101(9), 1513-1521.

Su, X., & Vale, R. (2018). Mechanisms of chimeric antigen receptor (CAR) signaling during T cell activation. *Biophysical Journal*, *114*(3), 107a-108a.

Sun, L., Su, Y., Jiao, A., Wang, X., & Zhang, B. (2023). T cells in health and disease. Signal transduction and targeted therapy, 8(1), 235.

Sun, M., Xu, P., Wang, E., Zhou, M., Xu, T., Wang, J., ... & Chen, B. (2021). Novel two-chain structure utilizing KIRS2/DAP12 domain improves the safety and efficacy of CAR-T cells in adults with r/r B-ALL. *Molecular Therapy-Oncolytics*, *23*, 96-106.

Sun, T., Yan, X., Guo, W., & Zhao, D. (2014). Evaluation of cytotoxicity and immune modulatory activities of soyasaponin Ab: an in vitro and in vivo study. Phytomedicine, 21(13), 1759-1766.

Swanson, K., Liu, G., Catacutan, D. B., Arnold, A., Zou, J., & Stokes, J. M. (2024). Generative AI for designing and validating easily synthesizable and structurally novel antibiotics. Nature Machine Intelligence, 6(3), 338-353.

Szymański, P., Markowicz, M., & Mikiciuk-Olasik, E. (2011). Adaptation of high-throughput screening in drug discovery—toxicological screening tests. *International journal of molecular sciences*, *13*(1), 427-452.

Tanaka, T., Narazaki, M., & Kishimoto, T. (2016). Immunotherapeutic implications of IL-6 blockade for cytokine storm. Immunotherapy, 8(8), 959-970.

Tang, J., Zou, Y., Li, L., Lu, F., Xu, H., Ren, P., ... & Zhu, X. (2021). BAY 60-6583 enhances the antitumor function of chimeric antigen receptor-modified T cells independent of the adenosine A2b receptor. *Frontiers in pharmacology*, *12*, 619800.

Tang, J., Zou, Y., Li, L., Lu, F., Xu, H., Ren, P., ... & Zhu, X. (2021). BAY 60-6583 enhances the antitumor function of chimeric antigen receptor-modified T cells independent of the adenosine A2b receptor. Frontiers in pharmacology, 12, 619800.

Tang, S., Ning, Q., Yang, L., Mo, Z., & Tang, S. (2020). Mechanisms of immune escape in the cancer immune cycle. International Immunopharmacology, 86, 106700.

Tannock, I. F. (1998). Conventional cancer therapy: promise broken or promise delayed?. The Lancet, 351, SII9-SII16.
Thomas, D. A., & Massagué, J. (2005). TGF-β directly targets cytotoxic T cell functions during tumor evasion of immune surveillance. *Cancer cell*, *8*(5), 369-380.
Thorne, N., Auld, D. S., & Inglese, J. (2010). Apparent activity in high-throughput screening: origins of compound-dependent assay interference. *Current opinion in chemical biology*, *14*(3), 315-324.
Tiefenthaler, G., & Hünig, T. (1989). The role of CD2/LFA-3 interaction in antigen-and mitogen-induced activation of human T cells. International Immunology, 1(2), 169-175.
Till, B. G., Jensen, M. C., Wang, J., Chen, E. Y., Wood, B. L., Greisman, H. A., ... & Press, O. W. (2008). Adoptive immunotherapy for indolent non-Hodgkin lymphoma and mantle cell lymphoma using genetically modified autologous CD20-specific T cells. *Blood, The Journal of the American Society of Hematology*, *112*(6), 2261-2271.
Tripodo, C., & Pileri, S. A. (2021). The Fundamentals of T-cell Lymphocyte Biology. *The Peripheral T-Cell Lymphomas*, 1-8.
Umehara, H., Huang, J. Y., Kono, T., Tabassam, F. H., Okazaki, T., Gouda, S., ... & Domae, N. (1998). Co-stimulation of T cells with CD2 augments TCR-CD3-mediated activation of protein tyrosine kinase p72syk, resulting in increased tyrosine phosphorylation of adapter proteins, Shc and Cbl. International immunology, 10(6), 833-845.
Vajdic, C. M., & Van Leeuwen, M. T. (2009). Cancer incidence and risk factors after solid organ transplantation. International journal of cancer, 125(8), 1747-1754.
Van Der Stegen, S. J., Hamieh, M., & Sadelain, M. (2015). The pharmacology of second-generation chimeric antigen receptors. *Nature reviews Drug discovery*, *14*(7), 499-509.
Villeneuve, P. J., & Bredeson, C. (2023). CAR-T Cells in Canada; Perspective on How to Ensure We Get Our Value's Worth. *Current Oncology*, *30*(4), 4033-4040.
Walsh, J. S., & Miwa, G. T. (2011). Bioactivation of drugs: risk and drug design. Annual review of pharmacology and toxicology, 51(1), 145-167.
Wang, E., Wang, L. C., Tsai, C. Y., Bhoj, V., Gershenson, Z., Moon, E., ... & Milone, M. C. (2015). Generation of potent T-cell immunotherapy for cancer using DAP12-based, multichain, chimeric immunoreceptors. *Cancer immunology research*, *3*(7), 815-826.
Wang, X. L., Zhao, G. H., Zhang, J., Shi, Q. Y., Guo, W. X., Tian, X. L., ... & Song, Y. (2011). Immunomodulatory effects of cinobufagin isolated from Chan Su on activation and cytokines secretion of immunocyte in vitro. *Journal of Asian natural products research*, *13*(05), 383-392.
Wang, X., Chuang, H. C., Li, J. P., & Tan, T. H. (2012). Regulation of PKC-θ function by phosphorylation in T cell receptor signaling. Frontiers in immunology, 3, 197.
Waring, P., & Müllbacher, A. (1999). Cell death induced by the Fas/Fas ligand pathway and its role in pathology. *Immunology and cell biology*, *77*(4), 312-317.
Weigelin, B., & Friedl, P. (2022). T cell-mediated additive cytotoxicity–death by multiple bullets. *Trends in cancer*, *8*(12), 980-987.
Weinberg, R. A. (1996). How cancer arises. *Scientific American*, *275*(3), 62-70.
Wiedemann, A., Depoil, D., Faroudi, M., & Valitutti, S. (2006). Cytotoxic T lymphocytes kill multiple targets simultaneously via spatiotemporal uncoupling of lytic and stimulatory synapses. *Proceedings of the National Academy of Sciences*, *103*(29), 10985-10990.

Woodward, P. W., Williams, C., Sewing, A., & Benson, N. (2006). Improving the design and analysis of high-throughput screening technology comparison experiments using statistical modeling. SLAS Discovery, 11(1), 5-12.
Xiong, Y., Taleb, M., Misawa, K., Hou, Z., Banerjee, S., Amador-Molina, A., ... & Adusumilli, P. S. (2023). c-Kit signaling potentiates CAR T cell efficacy in solid tumors by CD28-and IL-2-independent co-stimulation. Nature Cancer, 4(7), 1001-1015.
Xu, Z., Zhu, X., Su, L., Zou, C., Chen, X., Hou, Y., ... & Zhu, S. (2020). A high-throughput assay for screening natural products that boost NK cell-mediated killing of cancer cells. Pharmaceutical biology, 58(1), 357-366.
Yawata, M., & Yawata, N. (2010). NK cell KIR heterogeneity and evolution. In *Natural Killer Cells* (pp. 79-94). Academic Press.
Yonchev, D., & Bajorath, J. (2020). Inhibitor bias in luciferase-based luminescence assays. Future Science OA, 6(8), FSO594.
Zarour, H. M., DeLeo, A., Finn, O. J., & Storkus, W. J. (2003). Categories of tumor antigens. Holland-Frei Cancer Medicine. 6th edition. Hamilton (ON): BC Decker.
Zugazagoitia, J., Guedes, C., Ponce, S., Ferrer, I., Molina-Pinelo, S., & Paz-Ares, L. (2016). Current challenges in cancer treatment. Clinical therapeutics, 38(7), 1551-1566.

Appendix

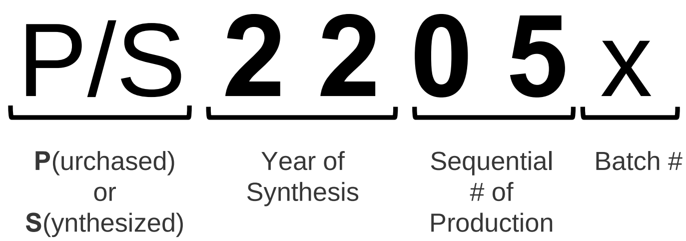

Figure 26. Analogue barcoding system.

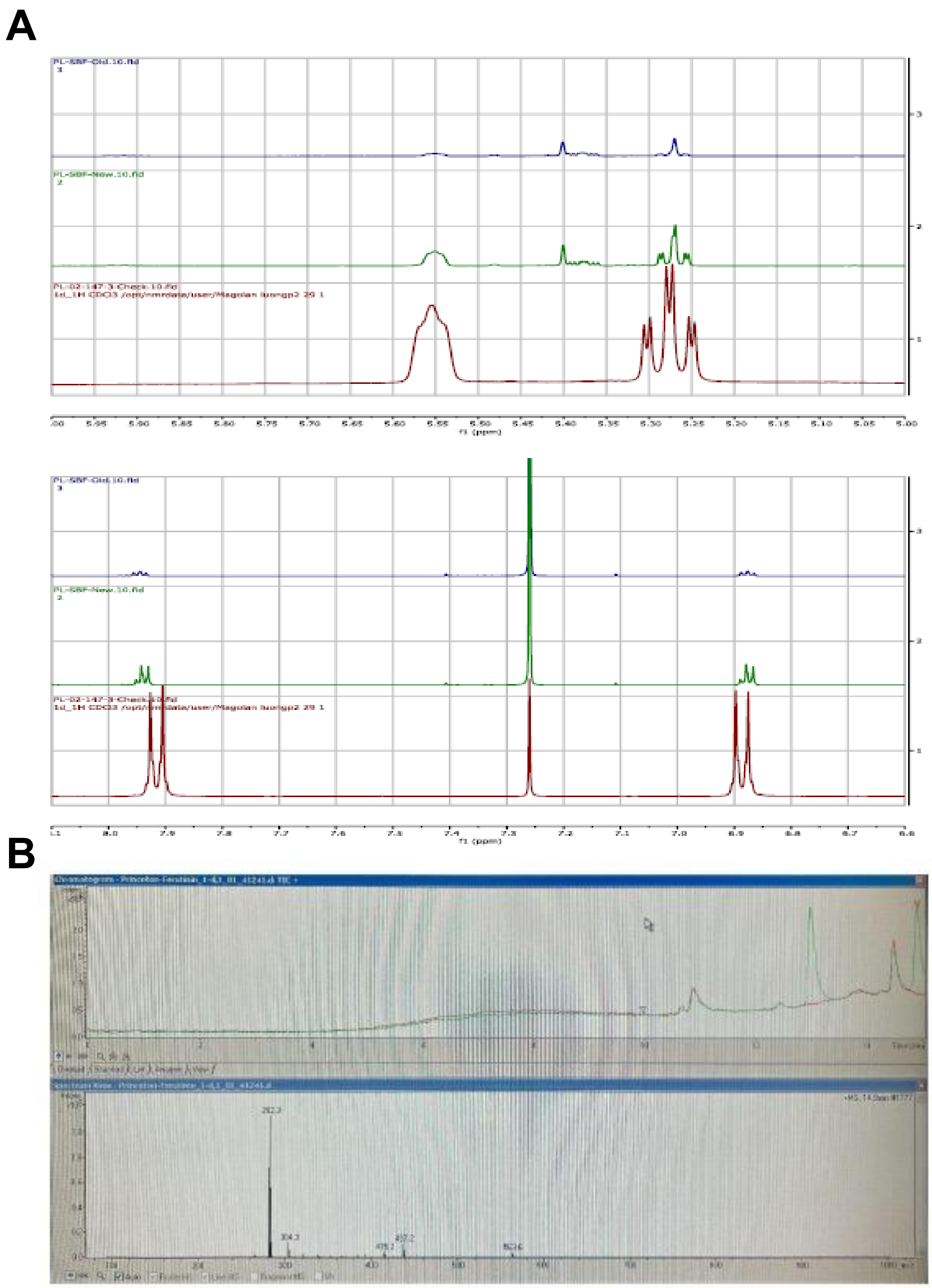

Figure 27. **A.** [1]H NMR Comparison of Different Ferutinin Batches. Comparing synthetic Ferutinin which was consistent with literature (red/bottom spectrum), both the repurchased (green/middle spectrum) and original store-bought (blue/top spectrum) samples were contaminated or had possibly degraded in some way. The appearance of an additional proton peak around 5.4 ppm, when only two signals were expected to be in that range (olefin proton and proton opposite the secondary alcohol). A separate set of aromatic signals were observed, giving rising to a pair of apparent triplets (or overlapping doublets) in place of the expected pair of doublets. **B.** High Resolution Mass Spectrometry of Original Ferutinin Sample. Observing two distinct peaks, the

sample appeared to be comprised of a 50-50 mixture of Ferutinin (initial peak) and an unknown compound (final peak) which corresponded to an exact mass of 282. Differing from the exact mass of Ferutinin (358) by 70 mass units, it is not clear what the structure of this unknown compound may be. Data generation and interpretation was completed by Princeton Luong.

Table A1: Complete list of Ferutinin analogues synthesized by Princeton Luong.

Compound ID	Descriptors	Structure
2101	Jaeschkeanadiol	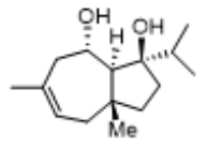
S-2102	Ferutinin	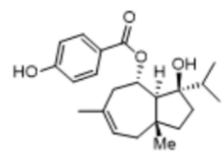
2103	Plain benzoic acid analogue	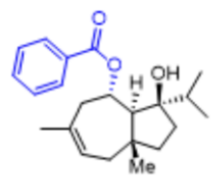
2104	Benzyl ether analogue	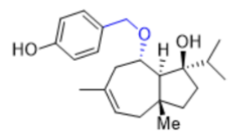
2105	1:1 mixture of dihydro-ferutinin (reduced double bond)	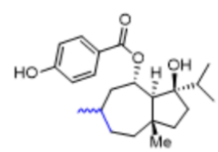
2106	Para-bromo analogue	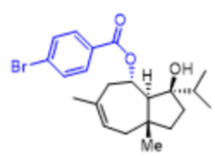
2107	Di-methoxy analogue	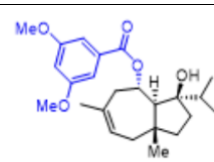

2108	Chloro-methoxy-methyl analogue	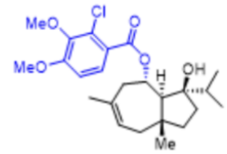
2109	Alkynyl analogue	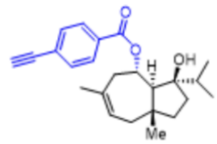
2110	Methoxy-methyl analogue	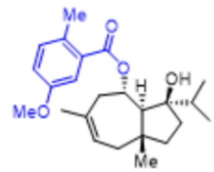
2111	Chloro-methyl analogue	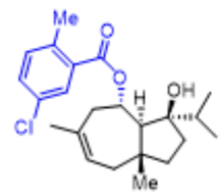
2112	Fluoro-methoxy analogue	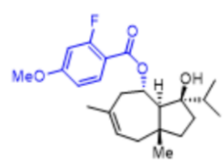
2113	Pivaloyl (Piv) - protected ferutinin	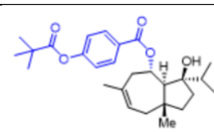
2114	Meta Piv-protected ferutinin analogue	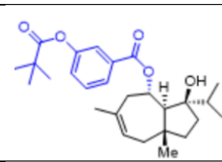
2115	Meta-hydroxyl ferutinin analogue	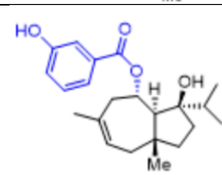
2201	Bi-pyridine analogue	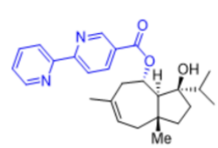

2202	Furan analogue	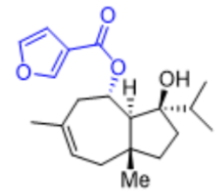
2203	Para-methoxy analogue	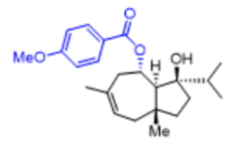
2206	Piv-protected cinnamic analogue	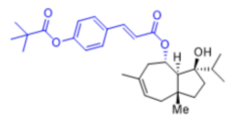
2207	Cinnamic analogue	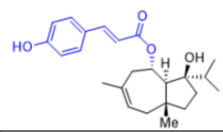
2208	Acetyl (Ac) - protected phenyl propanoic analogue	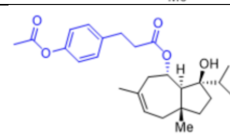
2209	Phenyl propanoic acid analogue	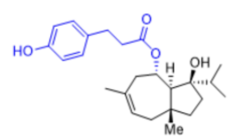
2210	Para-fluoro analogue	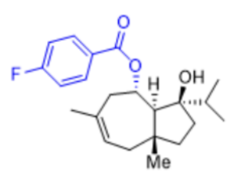
2211	Para-chloro analogue	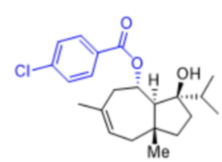
2301	Plain phenyl propanoic analogue	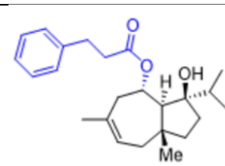

2302	Para-fluoro phenyl propanoic analogue	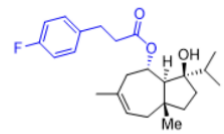
2303	Para-chloro phenyl propanoic analogue	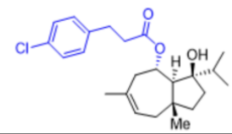
2304	Para-bromo phenyl propanoic analogue	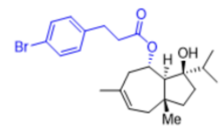
2305	Para-toluene phenyl propanoic analogue	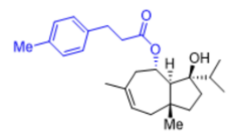
2306	Para-trifluoromethyl phenyl propanoic analogue	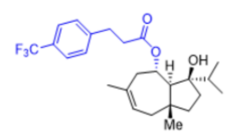
2307	Ac-protected meta-hydroxy phenyl propanoic analogue	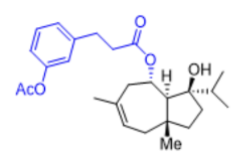
2308	Meta-hydroxy phenyl propanoic analogue	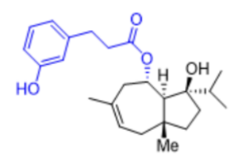
2309	Ac-protected ortho-hydroxy phenyl propanoic analogue	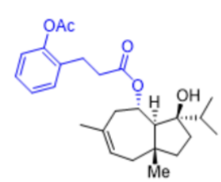
2310	Ortho-hydroxy phenyl propanoic analogue	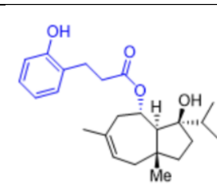

2311	Para-nitro ferutinin analogue	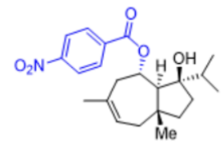
2312	Para-aniline ferutinin analogue	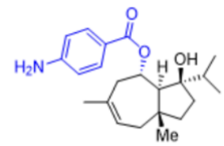
2313	Piv-protected des-hydroxyl ferutinin (elimination of tertiary alcohol)	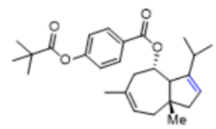
2314	Des-hydroxyl ferutinin (elimination of tertiary alcohol)	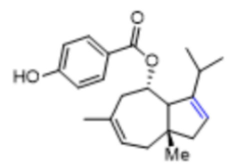

Table A2. Hits from the original and re-screen of the Bioactive A Library.

	Original hits	Rescreen hits
Overlap	5-(N,N-hexamethylene)amiloride	5-(N,N-hexamethylene)amiloride
	DEOXYPHORBOL 13-ACETATE, 12-	
	DEOXYPHORBOL 13-PHENYLACETATE 20-ACETATE, 12-	DEOXYPHORBOL 13-ACETATE, 12-
	Diacylglycerol kinase inhibitor I	DEOXYPHORBOL 13-PHENYLACETATE 20-ACETATE, 12-
	DIHYDROERGOCRISTINE	Diacylglycerol kinase inhibitor I
	E-64	DIHYDROERGOCRISTINE
	ERIOCITRIN	E-64
	FERUTININ	ERIOCITRIN
	GITOXIGENIN	FERUTININ
	HOMOORIENTIN	GITOXIGENIN
	INGENOL 3,20-DIBENZOATE	HOMOORIENTIN
	ISORHAMNETINE-3-GLUCOSIDE	INGENOL 3,20-DIBENZOATE
	KAHWEOL	ISORHAMNETINE-3-GLUCOSIDE
	MEZEREIN	KAHWEOL
	phloretin	MEZEREIN
	PHORBOL 12-MYRISTATE 13-ACETATE	PHLORETIN
	PICROTIN	PHORBOL 12-MYRISTATE 13-ACETATE
	STACHYDRINE	PICROTIN
	TSCHIMGANIDIN	STACHYDRINE
	VINCRISTINE	TSCHIMGANIDIN
	WEDELOLACTONE	VINCRISTINE
	DTNGBIGBPPPNNB-UHFFFAOYSA-N	WEDELOLACTONE
Unique	JNBOAUIJLDEICX-HOVIKNKYSA-N	
	JUQLTPCYUFPYKE-UHFFFAOYSA-N	
	PHORBOL 12,13-DIBUTYRATE	
	PVAMXWLZJKTXFW-YOUFMJPESA-N	
	QBILRDAMJUPXCX-RIBQKGKFSA-N	
	THAPSGARGIN	
	TROLEANDOMYCIN	
	5-(N,N-hexamethylene)amiloride	
		3,4'-DIHYDROXYFLAVONE
		3,7-DIHYDROXYFLAVONE
		4,4'-DIISOTHIOCYANOSTILBENE-2,2'-SUFONIC ACID SODIUM SALT
		5-(N,N-Dimethyl)amiloride hydrochloride
		7,4'-DIHYDROXYFLAVONE
		BROMOLAUDANOSINE, ()-6'-

		HETEROPEUCENIN, METHYL ETHER
		N,N-HEXAMETHYLENEAMILORIDE
		SCLAREOLIDE, (3aR)-(+)
		(S)-ENBA
		(Z)-Guggulsterone
		2-BENZOYL-5-METHOXYBENZOQUINONE
		2-METHYL-4-(PIPERIDIN-1-YLCARBOXY)-5-ISOPROPYLPHENYLTRIMETHYLAMMONIUM CHLORIDE
		3'-Azido-3'-deoxythymidine
		5-(N-Ethyl-N-isopropyl)amiloride
		5-(N-Methyl-N-isobutyl)amiloride
		5-Bromo-2'-deoxyuridine
		6-Methyl-2-(phenylethynyl)pyridine hydrochloride
		ACACETINE
		ACETOHYDROXAMIC ACID
		Actinonin
		ARTENIMOL
		Aurothioglucose
		AVOBENZONE
		BACCATIN III
		BAICALEIN
		Benztropine mesylate
		BERBERINE
		beta-SITOSTEROL
		BETAMIPRON
		BETULINIC ACID
		CAMYLOFINE DIHYDROCHLORIDE
		CAPSAICIN
		CBIQ
		CK2 Inhibitor 2
		CONDELPHINE
		COSMOSIIN
		COUMERMYCIN A1
		CYCLOPAMINE

		CYCLOPIAZONIC ACID
		DANTHRON
		DCEBIO
		DEGUELIN
		DEOXYANDIROBIN LACTONE
		Diacylglycerol Kinase Inhibitor II
		Domperidone
		Doxycycline hydrochloride
		DROFENINE HYDROCHLORIDE
		EDOXUDINE
		ESTRONE ACETATE
		ETHISTERONE
		FEROLINE
		Fiduxosin hydrochloride
		FISETIN
		FORSKOLIN
		FUMONISIN B2
		GITOXIGENIN
		GITOXIN
		GRAMINE
		HARMOL HYDROCHLORIDE
		Helveticoside
		HERNANDEZINE
		HETERATISINE
		HEXACHLOROPHENE
		Hydroxyurea
		Idoxuridine
		IODIPAMIDE
		IRIGENIN
		ISORHAMNETINE-3-GLUCOSIDE
		ISOSAFROLE
		ISOTETRANDRINE
		ITRACONAZOLE
		JERVINE

		KARANJIN
		Ketanserin tartrate
		LIQUIRITIGENIN DIMETHYL ETHER
		LYSERGOL
		Methoctramine tetrahydrochloride
		Minocycline hydrochloride
		MONOCROTALINE
		MYRIOCIN
		N-Acetyldopamine monohydrate
		N-Methyl-beta-carboline-3-carboxamide
		NARINGENIN
		OBLIQUIN
		OSTHOLE
		PANTHENOL
		PD 169316
		Pentamidine isethionate
		PEUCENIN
		PINOCEMBRIN
		PRATOL
		PRENYLETIN
		PROSTAGLANDIN A1
		Psora-4
		QUERCETIN
		QUERCITRIN
		Quinacrine dihydrochloride
		Quinacrine dihydrochloride dihydrate
		QUINIDINE GLUCONATE
		QUISQUALIC ACID
		RBI 257 maleate salt
		RESORCINOL MONOACETATE
		RHODINYL ACETATE
		Ro 90-7501
		S-(-)-Eticlopride hydrochloride
		S-(+)-Fluoxetine hydrochloride

		SB 202190
		SB 205384
		SB 224289 hydrochloride
		SB 242084 dihydrochloride hydrate
		SHIKONIN
		SPECTINOMYCIN
		SULFADIAZINE
		SULFAMETHOXAZOLE
		SULFAMONOMETHOXINE
		SWAINSONINE
		TAMARIXETINE
		TAXIFOLIN (+)
		TBBz
		Terconazole
		TETRAHYDROALSTONINE
		THEOBROMINE
		TILORONE
		TRIFLUMURON
		Tyrphostin AG 527
		UNGERINE
		XANTHOXYLIN